بسم الله الرحمن الرحيم

Optimal operating conditions determination of a SI engine with high CR; using biogas as main fuel with blends of methane or propane and hydrogen additions.

Submitted by:

Juan Pablo Gómez Montoya.

In partial fulfillment of the requirements for the Degree of Doctor of Philosophy.

University of Antioquia, Medellin –Colombia
September of 2017.

Doctoral Committee:
Advisor
Andrés Adolfo Amell Arrieta.
University of Antioquia.

Co-Advisor
Daniel B. Olsen.
Colorado State University.

Reviewers:
Jhon Ramiro Agudelo. University of Antioquia.
Leonel Cancino. Federal. University of Santa Catarina.
Helmer Acevedo. National University of Colombia.

Table of Contents

Chapter 1. Presentation of the research Project

1.1 Brief overview of original research project

Technologies that use biogas have significant direct and indirect benefits. As an effective way to treat and reuse different kind of waste including human, animal, agricultural, industrial, and urban residues, biogas production can improve the health of its users as a sustainable energy resource that is beneficial to the environment. In developing countries the expansion of biogas use has been based on small reactors designed for the digestion of the excreta of cattle, pigs, and poultry. In places such as landfills and water treatment plants, the anaerobic process naturally produces biogas. Normally the biogas is released into the atmosphere before or after a combustion process without effective utilization, while the biogas can be used for cooking, heating, illumination, and generation of electricity [1].

In the case of reciprocating internal combustion engines, the low energy utilization of biogas for the generation of electric energy is due to its low heating value and energy density. The Wobbe index is lower compared to natural gas, gasoline, and diesel. Also biogas has a low laminar burning velocity because of the high percentage of inert gases which decreased combustion stability, overall biogas has low capacity to produce effective work. Research and development of internal combustion engine technology for the exclusive use of gaseous fuels from renewable sources is in progress, seeking solutions to the above mentioned problems related to the stability of the combustion, pollutant emissions, and power derating with respect to the operation with conventional fuels [2-6].

This project aims to propose an alternative approach for biogas utilization in combustion engines, designed around its unique combustion properties. A technological trajectory that may be viable in the range of medium and low output powers, is the use of the comparative advantages of the diesel engine's, high compression ratio (CR) and consequently high generating efficiency, mitigating the negative effects of biogas' "non-ideal" combustion properties [7, 8]. Furthermore, a diesel engine modified with spark ignition (SI) allows 100% diesel substitution, resulting in greater fuel flexibility. Table 1 presents the general characteristics of four modes of operation, dual operation with diesel and gaseous fuels and spark ignition engine with alternative gaseous fuels. Lastly, the aim is to minimize carbon dioxide, carbon monoxide, and unburned hydrocarbons emissions that are generated from a fossil fuel such as diesel because of the use of biogas as alternative fuel. Thus, a diesel engine in SI mode is selected as the best strategy to implement in this project. In a diesel engine converted to SI mode there are two possibilities for supplying the gaseous fuel. In the first, the air and the fuel are mixed using a venturi before the throttle valve. In the second, the fuel is injected at high pressure close to the intake port after the throttle valve. In both cases the mixture, once admitted into the engine cylinder, is compressed during the compression stroke. To initiate ignition the engine is adapted with spark plugs in the place of the diesel injectors, controlled by a system that allows a variable spark timing (ST) to avoid knocking and optimize the combustion phasing for high generating efficiency [4, 7, 9-11].

SI configuration has the advantage of not depending on any diesel fuel fraction. This guarantees autonomy in the operation, better combustion stability at partial load given regulation of the air-fuel ratio, while achieving a more economic operation. However the comparative advantages of this configuration have been not been thoroughly studied, literature have a limited number of researches. Furthermore, there is no commercial offer of this technology [4, 6, 8, 17, 23-28]. In this context, the configuration and operation of a diesel engine in SI mode is proposed.

The low energy density and low Wobbe index of biogas compared to natural gas, are due to the fact that biogas is composed of 2/3 parts methane and 1/3 part CO_2, while natural gas achieves values of up to 95% methane. Due to the presence of CO_2, which is an inert gas, the laminar burning velocity and the adiabatic flame temperature are relatively low. On the other hand, the presence of CO_2 increases the autoignition temperature and the ignition delay time with respect to natural gas, allowing higher pressures at the end of

Table 1. Modes of operation in a diesel engine with alternative gaseous fuels (AGF)

Mode	Supply of AGF	Compression stroke	Ignition mode	Characteristics of Combustion	Advantage	Disadvantage	Ref.
Dual diesel + AGF	Through intake port mixed with the air.	Air and AGF	Autoignition of the pilot diesel.	Characteristics shared between premixed and non-premixed combustion.	- High level of effective thermal efficiency at full load	-Dependence on diesel fuel as pilot -High emissions of NOx, unburned hydrocarbons, and solid particles -Low thermal efficiency and increased cyclic dispersion at partial load - Possibility of ringing	[12-14]
Dual diesel + AGF	Injection of the AGF directly into the cylinder and injection of diesel.	Air	Autoignition of the pilot diesel.	Non-premixed combustion, similar to the conventional diesel engine	- High level of effective thermal efficiency at full load - High Pressure Fuel Injection	-Dependence on diesel fuel as pilot -High emissions of NOx, unburned hydrocarbons, and solid particles. -Low thermal efficiency and increased cyclic dispersion at partial load - High cost of dual injection system - Possibility of ringing	[15, 16]
Diesel in SI with 100% AGF	AGF by the intake port mixed with the air upstream in a venturi	AGF + air	Initiated by the spark.	Spherical flame front, turbulent premixed combustion	-100% diesel substitution -Presence of inert gases allows for high compression ratios -Decrease in pollution emissions -Similar generating efficiencies to dual diesel engine can be achieved.	- Knocking possibility. - Throttle is required to control the load. -Power derating due to the lower energy density and throttling of the charge. - High cyclic dispersion in lean mixtures.	[17-20]
Diesel in SI with 100% AGF	AGF injection into the intake port.	AGF + air	Initiated by the spark.	Spherical flame front, turbulent premixed combustion	-100% diesel substitution. -Presence of inert gases allows high compression ratio. -Decrease pollution emissions -Similar generating efficiencies to dual diesel engine can be achieved. - Higher output power.	- Knocking possibility. - Throttle valve is required to control the load. -Power derating due to the lower energy density and throttling of the charge - High cyclic dispersion in lean mixtures - Fuel is required at high pressure.	[6, 20-22]

the compression stroke. The use of biogas in a SI engine with high CR is allowed by the increased knocking resistance of biogas, biogas has the highest methane number (MN) among gaseous fuels. Use high CR leads to high generating efficiency, partly compensating low energy density, low turbulent flame speed, and power derating [4, 8, 29, 30]. Chemical composition variability of the gaseous fuel has a great influence on engine performance, in both operation modes: spark ignition and compression ignition. The MN gives an indication of knocking tendency to gaseous fuels in spark ignition engines, similarly to the octane number for liquid fuels [16]. Mixing biogas with methane or propane, and the addition of another alternative fuel (hydrogen), results in a fuel blend with higher energy density, higher adiabatic flame temperature, and higher flame speed, leading to higher engine output power and generating efficiency. These blends decrease the MN of the resulting fuel. Using high CR, the knock-free equivalence ratio range is narrow, straddled by knocking on one side and failure-to-ignite on the other side [4, 17, 31-33].
The addition of heavier fuels, such as propane and natural gas, decreases the ignition delay time, the trends between low and high pressures must be preserved since the phenomenon is governed by the processes branching the chemical kinetic chains between methane and major hydrocarbons. The CH_3 radical that dominates the ignition of methane is very difficult to oxidize, while the radical alkyl produced by fuels such as propane are consumed faster, leading to higher reaction rates [16]. Biogas used at high CR has a narrow knocking-free zone, with respect to the equivalence ratio, as the mixture is enriched the knocking possibility is increased, but also with an ultra-lean equivalence ratio it is quite possible that ignition fails. Under stoichiometric conditions the mixture has lower autoignition temperature than lean mixtures. NOx emissions under stoichiometric conditions are higher than the emissions of lean mixtures due to the higher flame temperature, which facilitates the dissociation of nitrogen. CO emissions are higher near stoichiometry than in lean mixtures [4, 17, 32, 33].

Increasing the turbulence intensity inside the cylinder by modifying the combustion chamber geometry increases the turbulent flame speed and the burn rate of the mixture, decreasing the combustion duration and the time required for the flame front to reach the walls, which leads higher generating efficiency [6]. In order to avoid the occurrence of autoignition points, the time required by the flame front to reach the farthest points away from the spark plug must be less than the ignition delay time of the end gas that is being compressed by the flame front and by the movement of the piston. Each fuel and equivalence ratio should be evaluated to determine the optimal ST, optimal combustion phasing, that deliver the highest level of generating efficiency and prevents knocking. Fuels with higher inert percentages have a lower flame speed requiring greater ST advances. In this case, the flame front will begin traversing the cylinder before the end of the compression stroke, leading to counter-pressures and decreasing generating efficiency. The addition of hydrogen increases the flame speed and decreases the ST required to obtain the highest performance. A small ST will cause the peak pressure to occur when the expansion stroke is very advanced, decreasing the ability to perform effective work [34].

The answers to the following questions are sought by this doctoral thesis:

- What is the best blend that can be used with biogas to increase the output power?
- What is the best equivalence ratio condition for optimal engine operation?
- Does increasing the turbulence intensity allow to increase the maximum output power to the biogas without knocking problems?
- What is the best combustion chamber geometry for biogas and natural gas?

To answer these questions, this research seeks to determine the optimal operating conditions of a SI engine with high CR, under conditions of stable combustion, with high generating efficiency, reduced emissions of pollutant, and minimization of power derating. The intervention variables identified are:

- Maintaining the compression ratio of the diesel engine at its maximum value to compensate the lower energy density of biogas.
- Blending biogas with methane or propane and hydrogen additions, with the purpose of increasing the energy density of the charge, the turbulent flame speed and fuel burn rate.

- Increase the turbulent flame speed at the end of the compression stroke and combustion, modifying the piston head to increase turbulence intensity and burn rate to avoid knocking.
- Operate the engine with two equivalences ratios, one close to stoichiometric and one lean, with the purpose to reduce specific emissions of pollutants such as NOx, HC, and CO.
- Running all tests at the maximum output power.
- Spark timing adjusted for the highest output power and generating efficiency.
- Test are performed close to the knocking threshold defined in this research to the SI engine.

It is expected that the combination of the interventions described allow to find the optimal operating conditions (high generating efficiency, stable combustion, and reduced pollutant emissions) of the SI engine with high CR using biogas and blends of biogas with methane or propane and hydrogen additions. .

1.2 General objective of the research

Determination of the optimal operational conditions of a spark ignition engine with high compression ratio, using biogas as main fuel, and biogas blended with methane or propane and hydrogen additions.

1.3 Specific objectives of the research

1. Identify the operating conditions that guarantee combustion stability, optimal output power and generating efficiency; performing a numerical analysis of fluid-dynamics and turbulence combustion phenomena, as well as a numerical estimation of the fuel properties, using in a SI engine with high CR with the different blends.

2. Guarantee the combustion stability, generating efficiency, and pollutant emissions to a SI engine with high CR; evaluating experimentally the intervention variables, using biogas and biogas blended with methane or propane, and hydrogen additions.

1.4 Impact and products

The development of this research project is expected to result in finding the best conditions to ensure optimum operation of an SI engine with high CR using biogas and biogas blended with methane or propane, and hydrogen additions. To get high generating efficiency with a correct combustion stability and low emissions. Using two equivalence ratios at the maximum output power and using two different combustion chamber geometries.

1.4.1 Scientific and Technological Impacts

The dissemination of these results to the scientific community encourages the formation of teams that take advantage of the energy content of alternative fuels such as biogas. This project contributes specifically to the combustion line of gaseous fuels with the theoretical and numerical simulation of kinetics and fluid-dynamics, which will be made for blends from the calculation of the combustion properties, as well as the evaluation of its applicability in a SI engine with high CR for electricity generation.

1.4.2 Impacts on the environment and society

The consolidation of the results hopes to encourage the use of alternative energies that have a positive effect on the environment, through the generation of electric energy, as well as the valuation and adequate utilization of the fuel reserves available in the country. The results obtained are expected to contribute to the reduction of greenhouse gases and pollutant emissions, as well as the assessment of solids and waste that can be used for the generation of biogas. The introduction of new combustion techniques promotes research and training of technical personnel for the development of new equipment and innovative technologies, which contributes to the generation of employment and knowledge.

1.5 Motivation

My motivation was to study biogas in an internal combustion engine; considered until now as a poor fuel. Resulting to the master study, which was focused in the same direction, some additional strategies were available to improve the previous work, a study of knocking in-line using the Kibox was possible. Lastly, a new engine was available to improve upon the first conversion to SI engine. The laboratory equipment provides a high quality infrastructure. A project presented to the University of Antioquia was approved.

Chapter 2 Properties of fuel at high pressure

2.1 Determination of fuel blends

This research has the precedent of the master's thesis by the author named "Theoretical and experimental study of the conversion of a diesel engine to spark ignition, using biogas blended with natural gas". From this research it was concluded that for a Lister Petter TR2 engine with a CR 15.5:1 the best blend was 50% biogas with 50% natural gas using an equivalence ratio of 0.9. The maximum output power was 7 kW @1800 rpm to electrical power generation. This fuel delivered the highest levels of generating efficiency in all evaluated loads without the knocking occurrence. This fuel blend is equivalent to a mixture of 80% CH_4 and 20% CO_2, similar to a purified biogas. This percentage of CO_2 allows using the fuel in an engine with high CR. The fuels blends selected for this research project were determined similar to this biogas.

Other five blends were proposed, having three similar characteristics to purified biogas:

- High concentration of CO_2. CO_2 as inert gas increase knocking resistance to the blends.
- Similar lower Wobbe index (LWI). Wobbe index is common used to fuel interchangeability.
- Similar energy density. Considered the best property for the operation to internal combustion engines, because of the interchangeability characteristics.

The aim is to study biogas blended with natural gas or propane, and hydrogen addition to determine the best operating conditions. According to the above, chemical compositions, wobbe index and energy density of the blends for this research are presented in Table 2.1. The Wobbe index for a gaseous fuel can be calculated using its low heating value and relative density. Energy density is the relation between low heating value and the stoichiometric air fuel ratio. For the basic fuel properties, the software "Calculo de propiedades de combustión para combustibles gaseosos" developed by the GASURE group, was used. The main fuel properties for this research are presented in Table 2, which are relative density, molecular weight, low heating value, and air fuel ratio.

Table 2.1 Volumetric composition of blends, low Wobbe index and energy density.

Designation	LWI (MJ/m^3_{fuel})	Energy density ($MJ/m^3_{air\ st}$)	CH_4 (% by vol.)	CO_2 (% by vol.)	H_2 (% by vol.)	C_3H_8 (% by vol.)
100GN	33.43	3.57	100			
100B	20.99	3.44	60	40		
50B50M	**31.40**	**3.57**	**80**	**20**		
57B38M5H	29.01	3.58	72	23	5	
54B36M10H	28.80	3.59	68	22	10	
83B17P	31.38	3.64	50	33		17
79B16P5H	31.04	3.65	47	32	5	16
75B15P10H	30.71	3.77	45	30	10	15
C3H8	16.66	3.56				100

2.2 Adiabatic Flame Temperature

Adiabatic Flame Temperature is a useful property to understand knocking tendency and is used to explain some results of the research. The Chemkin software with the EQUIL subroutine was used for the calculation of the adiabatic flame temperature for the equivalence ratios required for the blends studied. The equivalence ratios are over the range between 0.6 and 1. Grimech 3.0 reaction mechanism was used for calculations of the adiabatic flame temperature. Figure 2.1 shows the results of the adiabatic flame temperature, for the blends with the next input conditions: pressure 35 bar and temperature 850 K. Similar conditions are reached at the end of the compression stroke of the engine. The lowest adiabatic flame temperature for all equivalence ratios is for biogas due to the high percentage of CO_2 in the mixture. Biogas blends with propane have higher adiabatic flame temperatures than the biogas blends with methane

due to the higher low heating value of propane. The addition of hydrogen to the biogas blends with natural gas and propane increases the adiabatic flame temperature due to its high adiabatic flame temperature.

Table 2.2 Main fuel properties

Designation	Relative density	Molecular weight (kg/kmol)	Low heating value (MJ/kg)	Air fuel ratio (m^3_{air}/ m^3_{fuel})
100B	0.94	27.23	23.46	5.71
50B50M	0.75	21.63	33.30	7.61
57B38M5H	0.75	21.71	31.36	6.99
54B36M10H	0.71	20.68	31.81	6.75
83B17P	1.04	30.10	29.16	8.79
79B16P5H	0.99	28.70	29.50	8.48
75B15P10H	0.94	27.29	29.82	8.14

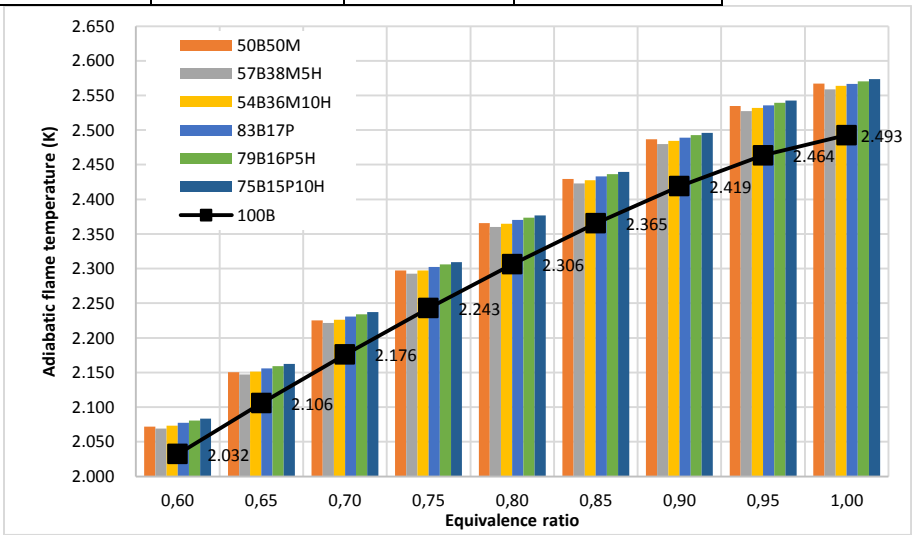

Figure 2.1 Adiabatic flame temperature, pressure 35 bar and 850 K

2.3 Laminar burning velocity

Chemkin software with the premix subroutine was used to calculate the laminar flame speed, using Grimech 3.0 reaction mechanism. Figure 2.2 presents the results of laminar flame speed with conditions of 35 bar and 850 K. Biogas has the lowest laminar flame speed due to its high CO_2 content. The blend 50B50M has a higher laminar flame speed than biogas because the CO_2 content is reduced by 20%. Blends of biogas with propane increase the laminar flame speed between 7-13% even more than biogas blended with methane, due to the higher energy content of propane. The addition of hydrogen to blends of biogas with methane or propane increases the laminar flame speed because of the high laminar flame speed of hydrogen. For all the blends, the highest laminar flame speed is given for an equivalence ratio equal to one, in the range simulated.

2.4 Ignition delay time and autoignition temperature

Ignition delay time is defined as the time take for a mixture of fuel and oxidant at an initial temperature and pressure to begin its combustion reaction. This reaction is characterized by rapid depletion of the reactants and the formation of transient intermediate species such as OH, CH_3, and H_2O_2. The calculation of the ignition delay time t is defined from the following expression derived from the Arrhenius equation, where P is pressure, T temperature, E activation energy, R gas constant, and A and n are constant values from the mechanism for each specific reaction.

$$t = A \times P^{-n} \exp\left(\frac{E}{RT}\right)$$ Equation 2.1

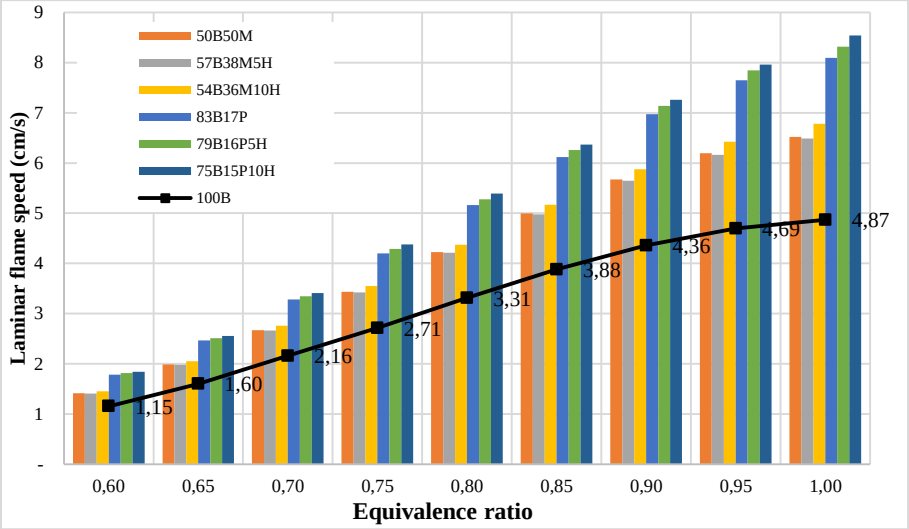

Figure 2.2 Laminar flame speed, at pressure 35 bars and 850 K

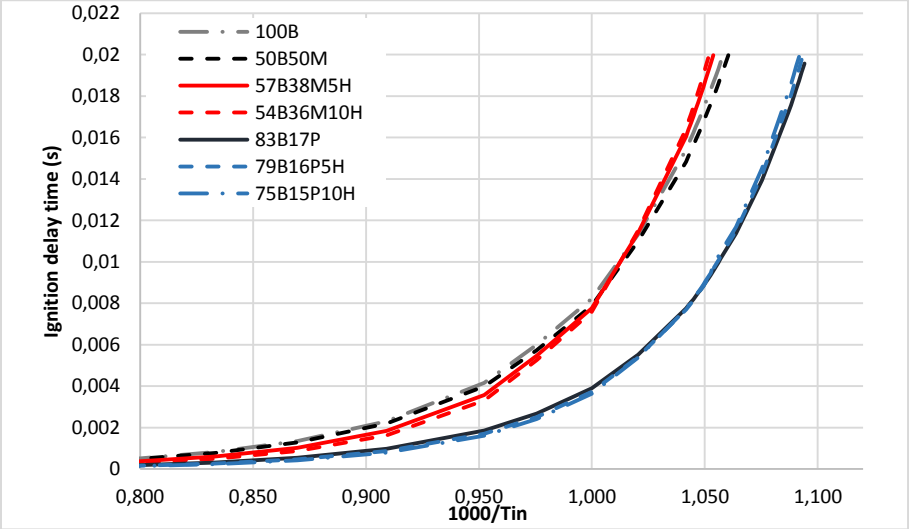

Figure 2.3. Ignition delay time and autoignition temperature at 35 bar and equivalence ratio of 0.9

Autoignition temperature defines the lowest temperature to which a mixture of fuel and oxidizer must be heated to achieve autoignition in the absence of an ignition source. This parameter is not a fixed value, as it depends on the concentration of the fuel, initial pressure, volume, and container geometry. The numerical calculation of these properties was made by the Chemkin software using the 0-D model homogeneous reactor. The detailed reaction mechanism of the University of San Diego was used. Figure 2.5 presents the results of the simulation for the ignition delay time and autoignition temperature at 35 bars and an equivalence ratio of 0.9. Blends of biogas with propane are more prone to autoignition, the addition of hydrogen slightly increasing the autoignition temperature. The addition of hydrogen to the biogas and methane mixture increases the autoignition temperature. The presence of CO_2 in biogas makes its autoignition temperature higher than other blends. Figure 2.6 presents the results of the simulation for the ignition delay time and autoignition temperature at 35 bars and an equivalence ratio of 0.6. The behavior is similar to that figure 2.5, with the difference that in this figure the autoignition temperature increases for all the blends, due to nitrogen excess in the air.

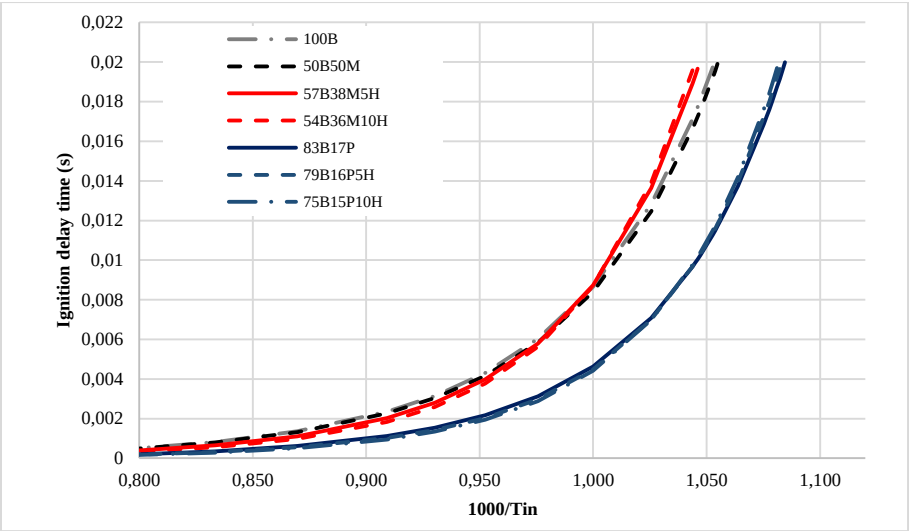

Figure 2.4. Ignition delay time and autoignition temperature at 35 bar and equivalence ratio 0.6

2.5 Quenching distance and minimum ignition energy

The mathematical model used in the calculation of the minimum ignition energy and the quenching distance is specific to conditions of low turbulence intensity (u') where it is considered as $u' \ll 2S_L$ [35]. The expression of the quenching distance is defined as a function of the laminar flame speed:

$$d_q = \frac{10k}{c_p \rho_0 S_L} \qquad \text{Equation 2.2}$$

Where, k: Conductivity of the premix, c_p: Heat capacity of the premix, ρ_0: Density of the premix, S_L: Laminar flame speed, The minimum ignition energy is a function of the quenching distance [35]:

$$E_{min} = c_p \rho_0 \Delta T_{ad} (\pi/6) d_q^3 \qquad \text{Equation 2.3}$$

Where ΔT_{ad} is the gradient between the initial temperature and the adiabatic flame temperature.

Figure 2.5 presents the results of the quenching distance calculations for a pressure of 35 bars and a temperature of 850K. The figure shows a comparison between the biogas and the blends. Due to the high CO_2 fraction in the biogas, because of it is an inert gas which reduced the reactivity of the mixture, biogas has the longest quenching distance compared with blends of biogas with methane, propane and hydrogen. In all the cases quenching distance decreases with the increase of the equivalence ratio because of the increase of the nitrogen fraction in the mixture, it is a typical tendency for hydrocarbons. Blends of biogas with propane have between 3% and 10% lower values than blends of biogas and methane. The addition of hydrogen in each case slightly decreases the quenching distance. For high pressure and temperature conditions the quenching distance decreases between 2.6 and 4.4 times with respect to low pressure and temperature conditions. The general trend is the same as at low pressure. The difference between the mixtures of biogas with propane and biogas with methane is between 38% and 41% lower values to the biogas and propane blends, for all the equivalence ratios.

Figure 2.6 shows the results of the minimum ignition energy calculations for a pressure of 35 bars and a temperature of 850K. Biogas requires the highest minimum ignition energy due to the high CO_2 fraction. For all the blends the minimum ignition energy decreases with increasing equivalence ratio, due to the decrease of nitrogen in the mixture. The addition of hydrogen in each case slightly decreases the minimum ignition energy

2.6 Flame front thickness

Flame front thickness is estimated using the results of numerical simulation to laminar flame speed. This property is an important parameter that affects hydrodynamic stability. A very thin flame front thickness will increase hydrodynamic instabilities [36, 37]. The flame front thickness is a characteristic length scale that is used to evaluate

hydrodynamic instabilities and to obtain the critical Peclet number, which sets the beginning of cellular instabilities. Figure 2.7 shows the calculation results for the flame front thickness for a pressure of 35 bar and a temperature of 850 K. In all cases, as the equivalence ratio increases towards the stoichiometric value, the thickness of the flame front is smaller. For each equivalence ratio, the flame front thickness is higher with the biogas. The addition of hydrogen, due to its low density, in all cases causes the flame front thickness to be smaller and thus the hydrodynamic instabilities increases**.**

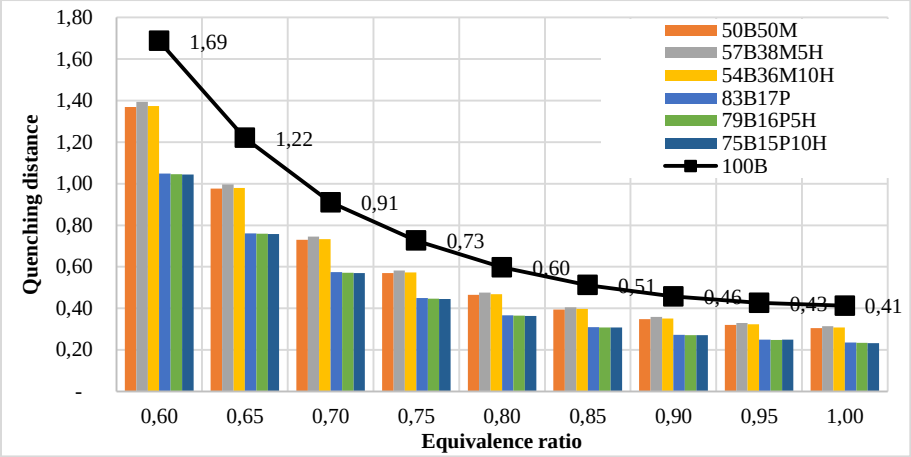

Figure 2.5. Quenching distance at a pressure of 35 bars and a temperature of 850K

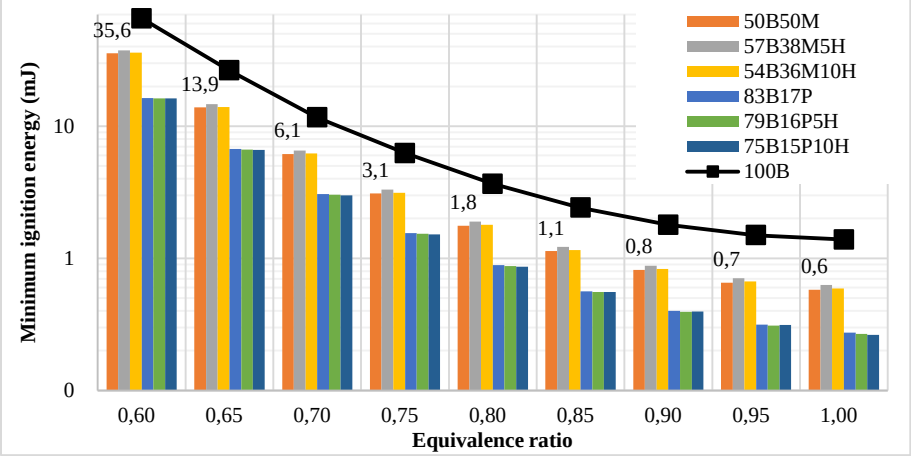

Figure 2.6. Minimum ignition energy at a pressure of 35 bars and a temperature of 850 K

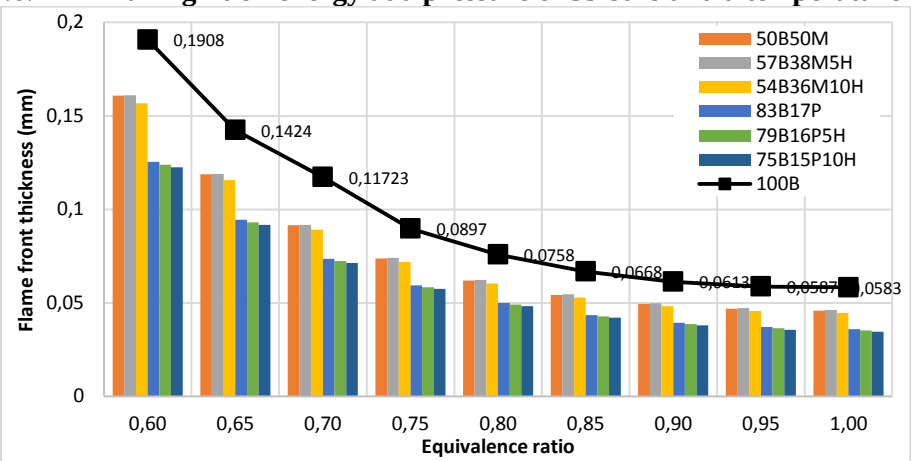

Figure 2.7. Flame front thickness at a pressure of 35 bars and a temperature of 850 K

Chapter 3 CFD simulations of fluid dynamics and turbulence phenomena.

3.1 CFD simulations in Fluent for SI engines

3.1.2 Most important aspects of CFD simulation

CFD simulations ran in Fluent 13.1, with 3D dynamic meshes, simulating piston movement at 1800 rpm, with actual cylinder and piston specifications, the cylinder head simplified by meshing effects. According to the suggestions of "Fluent user guide" the most relevant issues related with CFD simulation are presented. Convergence criteria for continuity, energy, and species respectively are 10e-4, 10e-7, and 10e-7. Calculations are made for the compression and expansion strokes, while the valves are closed, at intervals of 0.25 CAD degrees. The PISO (pressure implicit splitting of operators) model is used. Combustion is simulated in Fluent with spark ignition, simulating conditions of engine operation at each angle. Values of pressure, temperature, fuel composition, and equivalence ratio in the operation of the engine were measured. The combustion model is partially premixed combustion and the turbulence model is k-epsilon RNG (2 equations). The partial premix model defines by default a laminar flame speed to methane, a parameter dependent on the fuel and the equivalence ratio. A user defined function (UDF) is used to modify these values, depending on the fuel used, a correlation defined by Metghalchi and Keck [38]. The partially premixed combustion model is based on the "C equation model" [39]. The turbulent combustion model is based on the work of Zimont et al. [40], and involves the solution of the transport equation for the reaction progress variable, the closure of this equation based on the definition of the turbulent flame speed. The chemical reactions and the solution of the energy equation used is based on the solution of a simplified detailed mechanism[40].

The k-epsilon RNG model is similar to the standard k-epsilon model, with the following refinements:

- The RNG model has an additional term in the epsilon equation, which significantly improves accuracy for high velocity gradients.
- The effect of rotation on turbulence is included in the RNG model, improving accuracy for highly rotating flows.
- The RNG model provides an analytical formula for turbulent Prandtl numbers, while the standard model uses constant specific values.
- While the standard model is a model for high Reynolds numbers, the RNG theory provides an analytically derived differential formula for viscosity that improves the calculations in the low Reynolds number regime, improving the results close to the walls.

The transport equations for the k-epsilon RNG model are:

$$\frac{\partial}{\partial t}(\rho k)+\frac{\partial}{\partial x_i}(\rho k u_i)=\frac{\partial}{\partial x_j}(\alpha_k \mu_t \frac{\partial k}{\partial x_j})+G_k+G_b-\rho\varepsilon-Y_M+S_k \qquad \text{Equation 3.1}$$

$$\frac{\partial}{\partial t}(\rho \varepsilon)+\frac{\partial}{\partial x_i}(\rho \varepsilon u_i)=\frac{\partial}{\partial x_j}(\alpha_\varepsilon \mu_t \frac{\partial \varepsilon}{\partial x_j})+C_{1\varepsilon}\frac{\varepsilon}{k}(G_k+C_{3\varepsilon}G_b)-C_{2\varepsilon}\rho\frac{\varepsilon^2}{k}-R_\varepsilon+S_\varepsilon \qquad \text{Equation 3.2}$$

Gk represents the generation of turbulent kinetic energy due to the main velocity gradients. *Gb* is the generation of turbulent kinetic energy due to buoyancy. *Ym* represents the contribution of fluctuating expansion in compressible turbulent flows. α_k and α_ε are the inverse of Prandtl numbers for k and ε. S_k and S_ε are the source terms. The model for effective turbulent viscosity (μ_t) is

$$\mu_t=\rho C_\mu \frac{k^2}{\varepsilon} \qquad \text{Equation 3.3}$$

$$C_\mu = 0.0845$$

The main difference between the RNG model and the standard model, is that the RNG leads to an additional equation for epsilon given by:

$$R_\varepsilon = \frac{C_\mu \rho \eta^3 (1-\eta/\eta_0)}{1+\beta\eta^3}\frac{\varepsilon^2}{k}$$ Equation 3.4

$\eta \equiv S_k / \varepsilon$

$\eta_0 = 4.38, \beta = 0.012$

To flows with high velocity gradients, the k-epsilon RNG model leads to lower turbulent viscosities than the standard k-epsilon model, thus the RNG model is more adaptive to the effects of high changes in velocity gradients than the standard model. In the partially premixed model, the location of the flame front is identified using the reaction progress variable (*c)* defined as the sum of the mass fractions of the species of the products normalized by the sum mass fractions of the species solved with the detailed mechanism:

$$c = \frac{\sum_{k=1}^{n} Y_k}{\sum_{k=1}^{n} Y_k mr}$$ Equation 3.5

Where *n* is the number of products, *Yk* is the mass fraction of species *k,* and the subscript *mr* indicates solution conditions of the detailed reaction mechanism. At flame front *c* = 0, where the fuel and the oxidant are mixed without burning and behind the flame, *c* = 1, where the mixture is completely burned. As the flame front moves, combustion of unburned reactants occurs, converting the pre-blended reactants without combusting into burned products. The propagation of the flame front is given by the solution of the transport equation for the weighted average of the density for the reaction progress variable.

$$\frac{\partial(\rho \cdot c)}{\partial t} + \nabla \cdot (\rho \cdot u \cdot C) = \nabla \cdot \left(\frac{\mu_t}{S_{Ct}} \nabla c \right) + \rho \cdot S_c$$ Equation 3.6

Where ρ is the gas density, u is the gas velocity vector, μ_t is the turbulent viscosity, S_{Ct} is the turbulent Schmidt number, and S_c is the source term of the reaction of progress. The thermochemical properties are given as a function of the fraction of the mixture, based on typical premixed combustion. The smallest lengths of turbulent scales (Kolmogorov scales) are larger than the thickness of the laminar flame front, hence the effect of the turbulence is wrinkling the flame front, then an additional equation is required for the area density of the flame front $(\sum)$.

$$\frac{\partial \Sigma}{\partial t} + \nabla \cdot (u \cdot \Sigma) = \nabla \cdot \left(\frac{\mu_t}{S_{Ct}} \nabla \frac{\Sigma}{\rho} \right) + (P_1 + P_2 + P_3) \cdot \Sigma - D$$ Equation 3.7

Where P_1 is the source term due to the interaction of the turbulence, P_2 is the source term due to the flame front expansion, P_3 is the source term due to the unburned mixture expansion, and *D* is the flame area dissipation. The above equation requires a closing term for the terms of production and destruction for Σ.

$$\rho \cdot S_c = \rho_u \cdot \Sigma \cdot S_L .$$ Equation 3.8

Where ρ_u is the density of unburned gas and S_L is the laminar burning velocity. This equation suggests that for the calculation of the source term of the reaction rate, it is required that the laminar flame speed be evaluated for each fuel used in the CFD simulation. The premixed model requires the laminar flame speed, which depends on the composition of the fuel, equivalence ratio, temperature, and pressure. Although Fluent by default brings the laminar flame speed for air and methane mixtures, the polynomial for laminar flame speed for other fuels must be determined, either from the literature or with simulations using detailed OD mechanisms [39]. For the calculation of the laminar burning velocity at high pressure and high temperature, the Metghalchi and Keck model was used [38], which uses a known laminar burning velocity at a reference pressure and temperature for the different blends.

$$S_u = S_{u0}(T_u^{\ 0} / T_o)^\alpha (P/P_o)^\beta (1-2.1f)$$ Equation 3.9

$$S_{u0} = B_m + B_2(\phi - \phi_m)^2$$ Equation 3.10

$$\alpha = 2.18 - 0.8(\phi - 1)$$ Equation 3.11

$$\beta = -0.16 + 0.22(\phi - 1)$$ Equation 3.12

$T_o = 298K, P_o = 1atm.$ B_m, B_2, and ϕ_m are constants than must be estimated by the measurement and/or simulation of the laminar flame speed for each fuel. α, β are independent of the fuel. Figure 3.1 presents laminar flame speeds for the blends of this investigation to different equivalences ratios. Table 3.1 presents the values of the reference constants to laminar flame speed for a pressure of 1 atmosphere and a temperature of 298 K. These values are used in the UDF to make the correction of the calculation of the laminar flame speed at high pressure and high temperature, according to the model of Metghalchi and Keck [38]. The laminar flame speed was calculated with Chemkin, using Grimech 3.0 mechanism.

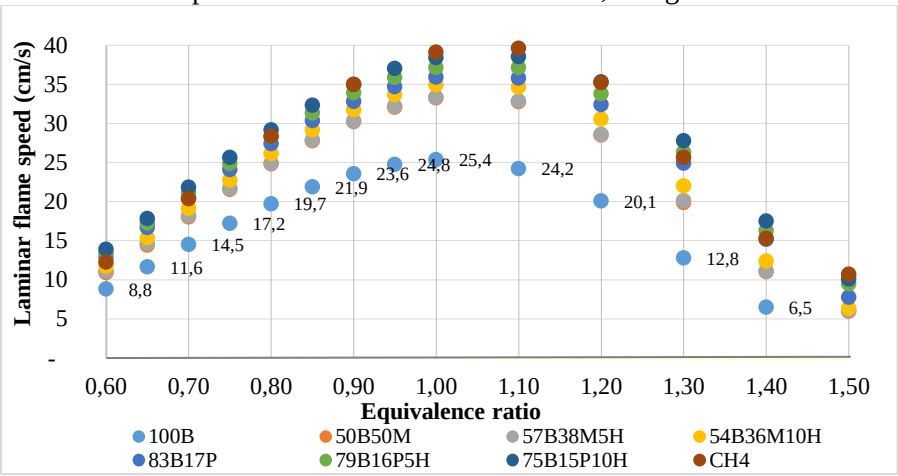

Figure 3.1 Laminar flame speed for all blends. Pressure of 1 atm and temperature of 298 K

Table 3.1 Reference constants to laminar flame speed at 1 atm and 298 K, for all blends

Blends	Bm	B2	Φm
100B	0.2559	-1.2098	1.0028
50B50M	0.3396	-1.5755	1.0183
95(60B40M)-5H	0.3396	-1.5592	1.0179
90(60B40M)-10H	0.3565	-1.6082	1.0198
83B17P	0.3658	-1.5102	1.0264
95M5-5H	0.3798	-1.5673	1.0272
90M5-10H	0.3926	-1.5837	1.0311

3.1.3 Mesh Independence

Table 3 presents the number of cells of the dynamic meshes for the original geometry of the engine, which were used to verify the independence of the mesh. The values are in the top dead center (TDC) and bottom dead center (BDC). In addition to the approximate time of each simulation, an analysis of the independence of meshing similar to that presented for the original geometry was performed for the rest of the geometries. Figure 3.2 shows the different 3D meshes used to find the best combustion chamber geometry that increases the turbulence intensity at the end of the compression stroke and during combustion. The ideas of these geometries were taken from previous researches that had the same purpose [6, 41-44]. Thirteen geometries were simulated: the original engine geometry and 12 alternative combustion chamber geometries. The volume of the chamber was held constant so as not to modify the CR of the engine. Figure 3.3 shows the in-cylinder pressure curves resulting from the CFD simulation of the original geometry, to validate mesh independence. Three different meshes were simulated: initial mesh, refined mesh, and another still more refined to evaluate the "yplus". 100% CH_4 was used as fuel for

the simulation. Atmospheric pressure was set at 1atm and temperature at 298 K, with a stoichiometric equivalence ratio. The solution was obtained using the San Diego detailed chemical mechanism. Figure 3.3 makes it possible to conclude that the refined mesh delivers sufficiently accurate values in terms of peak value and pressure location. Using an appropriate simulation time, this result was comparable to the more refined mesh "yplus", which requires significantly more time to the solution of the problem without notable improvements in simulation accuracy.

Table 3.3. Quantity hexahedral meshes for the original geometry for meshing.

Description	BDC	TDC	Simulation time
Initial mesh	208.484	13.223	13 hours
Refined mesh	473.861	41.044	28 hours
Refined to yplus	1.231.626	138.193	72 hours

Figure 3.4 presents the result of the CFD simulations, under the same conditions as presented for Figure 3.3, to validate the independence of the meshing for calculations in terms of temperature and mean velocity within the cylinder at different CAD degrees. TDC is located at 720 CAD degrees, ST is 715 CAD degrees. Again good agreement is observed for the simulations with the refined mesh and refined mesh "yplus". The decrease in the simulation time for the refined “yplus” mesh and the refined mesh is from 72 hours to 28 hours for each complete simulation. The meshing of all geometries has been generated using Gambit 2.4.6. Figure 3.5 presents an image taken of Fluent for the validation of the "yplus" mesh for the contour of the turbulence at the walls, close to TDC, where the turbulence intensity is high compared to the expansion stroke. The value of the “yplus” mesh should be between 30 and 300 at all the points near the walls, and in this case the values go up to 153. This parameter ensures a good calculation of the turbulence close to the walls. For different geometries yplus mesh was also validated to guarantee good numerical results of CFD simulations.

Figure 3.6 shows the simulation results using the MD19 mechanism and chemical equilibrium, compared to experimental data measured in the Lister Petter engine. The conditions of the experimental test were: Methane, equivalence ratio 0.6, output power 8.5 kW, atmospheric pressure of 0.849 bar, and 295 K. The simulation with the simplified detailed mechanism presents good precision throughout the compression and combustion strokes. What is most notable in this research is that at the end of the expansion stroke there are small differences in the in-cylinder pressure values. It is shown that the differences in peak pressure are less than 1% between simulation and experimentation. With this precision, it is justified that for the simulations only the refined mesh is used. The experimental curve is the average of 300 cycles.

Figure 3.2 Meshes used in Fluent 3-D CFD simulations.

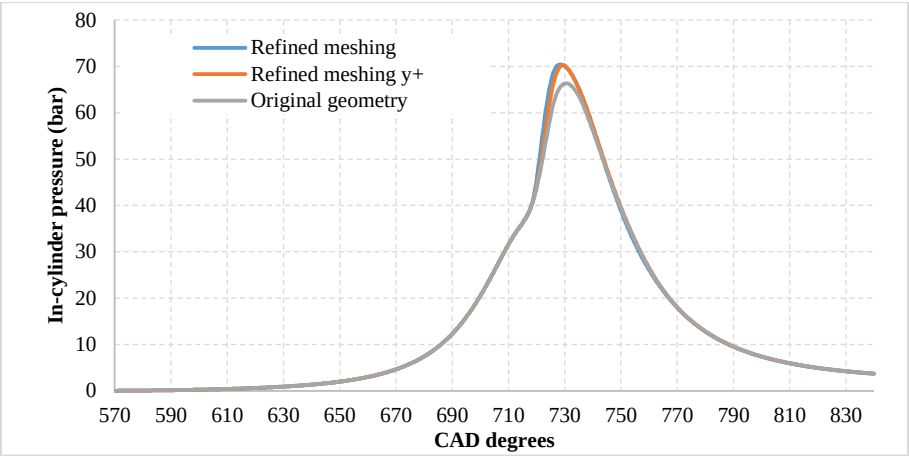

Figure 3.3 CFD result for the meshing independence, in-cylinder pressure, original geometry

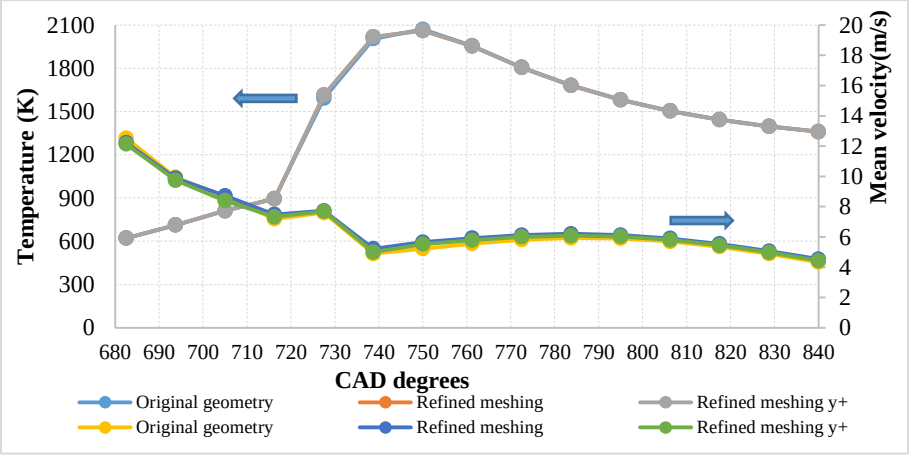

Figure 3.4 CFD result independence mesh, temperature, and mean velocity inside the cylinder

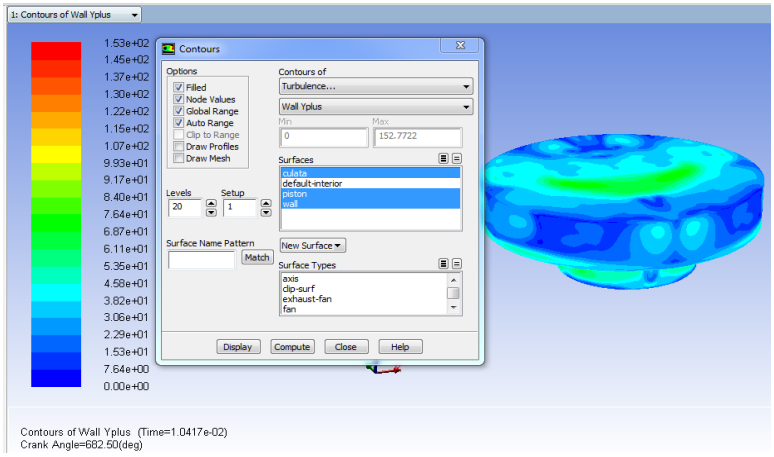

Figure 3.5 Validation of mesh for yplus for turbulence.

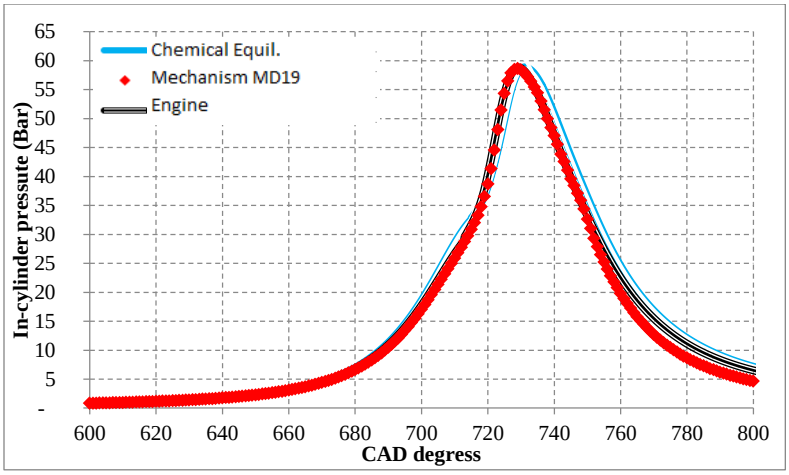

Figure 3.6 Comparison of in-cylinder pressure curves, engine operation validation, and CFD simulations.

Chapter 4 Statistical analysis of the research project

4.1 Introduction

The repeatability of measurement results is the proximity of concordance between the results of successive measurements of the same values under the same measurement conditions. These conditions are called repeatability conditions. Repeatability conditions include the same measurement procedure, the same observer, and the same measuring instrument, used under the same conditions, the same place, repetitively over a short period of time. Repeatability can be expressed quantitatively in terms of the characteristic dispersion of results [45]. The purpose of this chapter is to perform a repeatability analysis of the operation and performance of a SI engine with high CR using a blend of 50/50 biogas and natural gas. Experimental results of the repeatability tests are used to calculate the uncertainty in the measurement of location 5% mass burned, location 50% mass burned, location 90% mass burned, combustion duration, COV of IMEP, knock peak pressure, brake specific fuel consumption, thermal efficiency, CO, THC, and NOx emissions. The uncertainty of a measurement is usually associated with its quality, quantifying the doubt that exists regarding the result of that measurement. Research project experimental design is presented to calculate the number of replicates for the seven fuels and two equivalence ratio. In order for the experimental design methodology to be effective, it is essential that the experiment be well designed.

4.2 General procedure for testing

The general conditions of the test are presented in Table 4.1, where the effective output power, equivalence ratio, fuel blend, and engine speed were held fixed. The frequency for electric power generation is 60 Hz in Colombia. The fuel used is a mixture of 50 % biogas (60 % CH_4 and 40 % CO_2) with 50 % natural gas (98.05 % CH_4, 1.52 % N_2, 0.26 % C_2H_6, and 0.16 % CO_2) on a volumetric basis [18]. A similar conversion to SI was previously made on a Lister Petter TR2 (8.0 kW @ 1800 rpm) engine [19]. The new conversion of the engine led to an increase in the effective output power of 0.5 kW due to air and fuel supply improvements. With this power increase, the derating compared to the CI engine decreased from 12.50 % to 6.25 %. The rated power was set to 7.5 kW, which was close to the highest power reached at the running speed, equivalence ratio, and fuel blend. As one of the purposes of this research is to study the effect of knocking on the operation of a SI engine with high CR, the only parameter modified was ST. Three knocking intensities were evaluated: negligible, low, and high knock. For this evaluation, the engine was operated at three different ST: 12, 16, and 19 CA degrees before top dead center (BTDC). Figure 4.1a shows a plot of the measured pressure for these conditions, with one cycle for each ST. The largest knock peak pressure, calculated as the maximum value of the high-pass filtered pressure signal, for the spark timing (ST) 19 CA degrees BTDC, was 22.6 bar, which shows a high knock tendency that is dangerous for the operation and integrity of the engine. Large fluctuations in the pressure curve are also observed. For this reason, only one test was performed under these conditions. With an ST of 16 CA degrees BTDC, a low knock peak pressure of 2.2 bar was obtained. This level of low knock is barely audible; nevertheless, its occurrence is evident in the pressure curve. With an ST of 12 CA degrees BTDC, the knock peak pressure was 0.22 bar. This knock level is considered to be negligible, and the pressure curve appears smooth. Figure 4.1b shows the pressure variation dP/dTheta vs. crank angle for negligible, low, and high knock, the same behavior of the figure 4.1a is observed to knocking with the change in the spark timing.

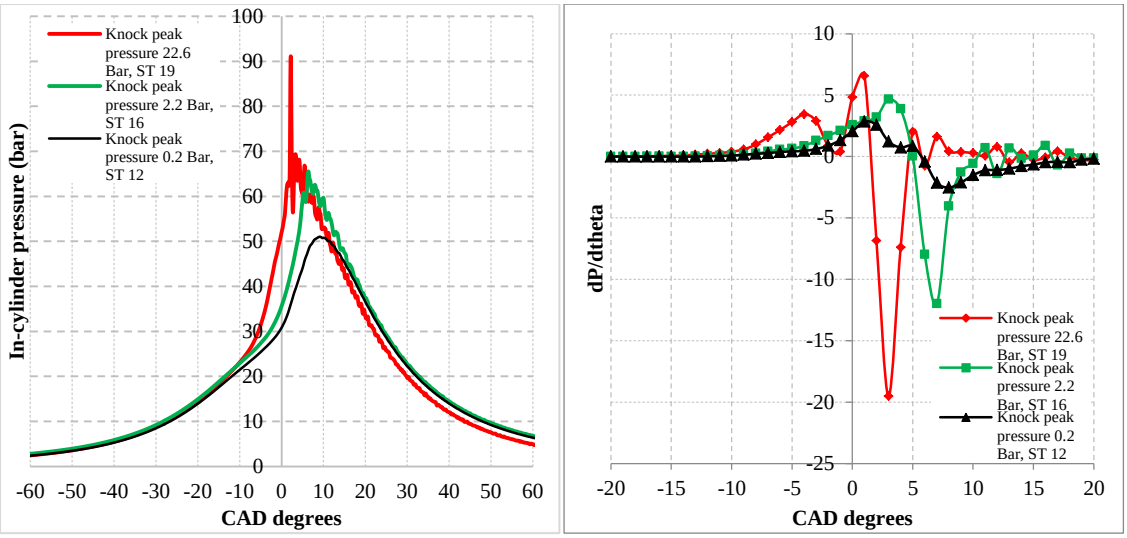

Figure 4.1 a) In-cylinder pressure and b) dP / dTheta for negligible, low, and high knock

4.2.1 Repeatability

Repeatability is a statistical measure of consistency between repeated measurements of the same characteristic in the same unit, essentially under the same conditions. This means samples taken by the same operator, in the same device, with environmental and other conditions as constant as possible. The following repeatability analysis will be carried out following the process of evaluation of test methods TAPPI [46, 47]. To calculate the repeatability it is necessary to have a clear concept of variance and standard deviation. Variance ($\mathbf{S^2}$) is a measure of the magnitude of the possible errors by dispersion and is equal to the sum of the squares of each deviation divided by the number of tests. The standard deviation (**S**) is the square root of the variance. The repeatability is equal to 2.77 multiplied by the standard deviation of the repeatability. The factor 2.77 comes from $\sqrt{2} \cdot 1.96$. The 1.96 is given by the assumption of a normal distribution and the choice of 95% confidence interval in the difference between 2 readings[48].

4.2.2 Experimental design

An experiment can be defined as a series of tests in which deliberate changes are made in the input variables of a system to observe and identify the reasons for the changes that are observed in the output response. In order to obtain valid and objective conclusions it is desired to design a robust experiment, that is, a process that is minimally affected by external sources of variability. This research project has two separate variable factors to evaluate, which are: seven fuels blends and two equivalence ratios, seven and two levels, respectively, according to table 4.1. For this we will use equation 5,17 of the book Design and Analysis of Experiment by Montgomery [49]

$$\Phi^2 = \frac{nb\Delta^2}{2as^2} \qquad \text{Equation 4.1}$$

Where Φ is the parameter of non-centrality (measure of degree of inequality) for characteristic operating curves in analysis of variance of the model with fixed effects, n is the number of replicas, Δ is the value of the selected reference variable with a high probability of rejecting the null hypothesis, a and b are the factor numbers to be modified and, s^2 is the known variance for the reference variable. Δ and s^2 are calculated from the experimental data presented in this chapter.

Table 4.1 Factors, Levels, and Output Variables of the experimental design to evaluate repeatability and standard deviation

Factors	Levels	Designation	Output Variables
Chemical compostion	50/50 biogas and natural gas	50B50M	Output power, location 5% mass burned, location 50% mass burned, location 90% mass burned, combustion duration, COV IMEP, knock peak pressure, brake specific fuel consumption, generating efficiency, CO, THC, and NOx emissions.
Equivalence ratio	0.9	ER	
Output power	7.5 kW	OP	
Spark timing	12, 16 and 19 CAD BTDC	ST	
Engine speed	1800 rpm	ES	

4.2.3 Calculation of uncertainty

The uncertainty is calculated differently depending on whether the value of the magnitude is directly observed in a measuring instrument or if it is obtained mathematically by manipulating one or several direct measures. Thermal efficiency (n_{ter}) is given by the formula:

$$n_{ter} = \frac{V*I*\sqrt[2]{3}}{\dot{V}*LHV} \qquad \text{Equation 4.2}$$

Where: V = voltage (volts), I = electric current (amps), LHV = Low heating value (MJ/kg), $\dot{V}$ = Volumetric flow of fuels (m^3/s). Once the uncertainty of the direct measures is obtained, the uncertainty of indirect measurements is calculated. Assuming that it is desired to measure the magnitude R=f(X, Y, Z), which is a function of other magnitudes X, Y, Z, which have been measured directly, together with their direct uncertainties, obtaining the values: $X = X \pm \Delta X$; $Y = Y \pm \Delta Y$; $Z = Z \pm \Delta Z$. The uncertainty of magnitude R is given by [50]:

$$\Delta R = \left|\frac{\partial R}{\partial X}\right|\Delta X + \left|\frac{\partial R}{\partial Y}\right|\Delta Y + \left|\frac{\partial R}{\partial Z}\right|\Delta Z \qquad \text{Equation 4.3}$$

With the constant low heating value equal to 27 MJ / m^3:

$$\Delta n_{ter} = \left(\frac{I*\sqrt[2]{3}}{\dot{V}*PCI}\Delta V\right) + \left(\frac{V*\sqrt[2]{3}}{\dot{V}*PCI}\Delta I\right) + \left(\frac{I*V*\sqrt[2]{3}}{\dot{V}^2*PCI}\Delta \dot{V}\right) \qquad \text{Equation 4.4}$$

4.3 Experimental results

4.3.1 Repeatability

Preliminary project data are presented, 18 tests performed on the Lister Petter TR2 engine, in which all parameters were constant, runs distributed in groups of 3 per day, as presented in Table 4.3. For each group, the mean, standard deviation, and variance are calculated as presented in Table 4.4.

Then the standard deviation of the repeatability is calculated, which is the square root of the sum of the standard deviation of each group divided by the number of groups, then the repeatability is calculated by multiplying the S of the repeatability by the factor 2.77. Finally, the percentage of repeatability is calculated by dividing the repeatability by the total average, see Table 5. To interpret these values of repeatability, given a reading of 29.96% for thermal efficiency and if several tests are performed, then 95 % of the calculations would be approximately plus or minus 0.58 units of thermal efficiency in percent (the value of r for the experiment). This result is permissible for the type of research being done. This is the methodology used with all the parameters of the experiment.

Table 4.3 Distribution of tests, thermal efficiency results

Day	1	2	3	4	5	6
Test 1	29,88	29,86	29,95	29,88	29,82	29,95
Test 2	30,18	29,96	29,91	30,31	29,88	30,01
Test 3	29,89	30,20	30,41	29,87	29,42	29,97

Table 4.4 Results of mean, standard deviation and variance by group

Day	1	2	3	4	5	6
Mean	30,0	30,0	30,1	30,0	29,7	30,0
S	0,17	0,17	0,28	0,25	0,25	0,03
S^2	0,03	0,03	0,08	0,06	0,06	0,00
Test number	3	3	3	3	3	3

Table 4.5 Repeatability analysis results

Total Average	29.96
S total	0,13
Number of groups	6
S of repeatability	0,21
Repeatability	0,58
Repeatability %	1.94 %

4.3.2 Experimental design

To solve Equation 4.1, the value of the reference variable is selected from the repeatability calculation (Δ), which is 0,58%. For thermal efficiency, this means that a difference of greater than 0.58 % of thermal efficiency between one test and another, with different equivalences ratio or blends, can be said to show that these input variables had an influence on the output variable. In order to calculate the known variance, the variance of the total of the tests for thermal efficiency is calculated, which is 0,046. For a and b, which are the numbers of factor levels selected, $a = 7$ for blends and $b = 2$ for equivalence ratios. With Δ and s^2 known, Φ is calculated for 2 and 3 replicates in order to find the false positive rate (β) lower. This is found in the characteristic operation curves for the analysis of variance of the model with fixed effects, appendix 5 of Montgomery [49], see Graph 4.1.

Where:

v_1 = Degrees of freedom of the numerator = (a-1)

v_2 = Grados de libertad del denominador = $(n-1)_x(a.b)$

α = Criterion of relevance, assumed to be 0,05

For two replicas β is about 0.05 and the power of the experiment that has β-1 equal to 0.95, a possibility of 95 % to reject the null hypothesis if the difference in thermal efficiency between 2 samples is over 0.58%, which is completely acceptable for this experiment. For three replicates, the data comes from the graph but it can be said that β is less than 0.01 and the power of the experiment is greater than 0.99, a greater possibility of 99% to reject the null hypothesis if the difference in thermal efficiency between 2 samples is over 0.58%. It is considered that two replicates obtaining a power of 0.95 is an adequate condition for the development of the research project.

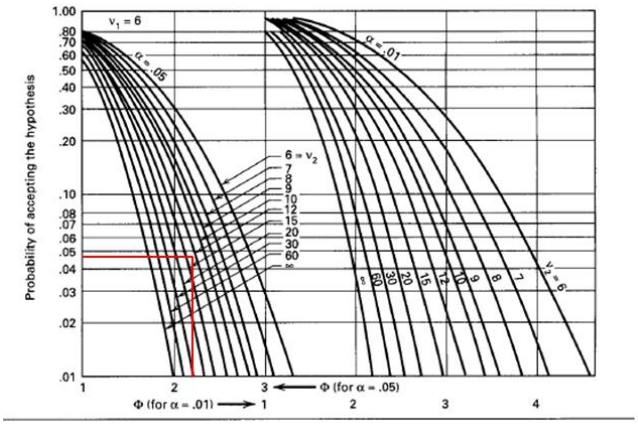

Graph 4.1 Analysis of variance of the model with fixed effects, Montgomery [49]

Table 4.4 a) Value of Φ to 2 replicas. b) Value of Φ to 3 replicas.

Factor	Blends (a)	Equivalence ratio (b)
Levels	7	2
No. replicas	2	
Variance	0,046	
Δ	0,58	
Φ	2,18	
v1	6	
v2	14	

Factor	Ble ds (a)	Equivalence ratio (b)
Levels	7	2
No. replicas	3	
Variance	0,046	
Δ	0,58	
Φ	2,77	
v1	6	
v2	28	

4.3.3 Calculation of uncertainty

Table 4.5 shows the values of the minimum resolution of the measurement equipment used in this research project, followed by the solution of equation 6.4 for the calculation of uncertainty, which is 0.034%, indicating that for the average of the thermal efficiency that is 29.96%, the values of the efficiency by uncertainty in the measurement of the equipment can be located between 29.99% and 29.93%. Table 4.6 presents the values for the calculation of the total error of the thermal efficiency measurement.

Table 4.5 Uncertainty values of measuring equipment

Parameters	Equipment	Resolution	Unity
Voltage	Multimeter	0,0001	KV
Electric current	Amperimetric Tweezers	0,01	A
Volumetric flow	Rotameter	1,67E-07	M^3/S

$$\Delta n_{ter} = \left(\frac{(19.46)\ \sqrt{3}}{(0{,}000925)(27000)}(0{,}0001)\right) + \left(\frac{(0.22)\ \sqrt{3}}{(0{,}000925)(27000)}(0.01)\right) + \left(\frac{(0.22)(19.46)\ \sqrt{3}}{(0{,}000925)^2(27000)} * 1{,}666 * 10^{-7}\right)$$

Δn_{ter}= 0.034%

Table 4.6 Values for calculating the total error of the thermal efficiency measurement

	Values	Unity
Electric current	19,46	A
Voltage	0,22	kV
R Amperimeter	0,01	A
R Multimeter	0,0001	kV
Output power error	0,005	kW
Output power	7, 2	kW
Volumetric flow	0,000925	M^3/S
R Volumetric flow	1,67E-07	M^3/S
Uncertainty thermal efficiency	0,034	%
Thermal efficiency	29,96	%
Total error (Uncertainty + repeatability)	**0.61**	**%**

References

1. Bond, T. and M.R. Templeton, *History and future of domestic biogas plants in the developing world.* Energy for Sustainable Development, 2011. **15**(4): p. 347-354.
2. Davis, S.G., et al., *An optimized kinetic model of H2/CO combustion.* Proceedings of the Combustion Institute, 2005. **30**(1): p. 1283-1292.
3. *A. Roubaud, r.r., d. Favrat,, Lean-Burn Cogeneration Biogas Engine with Unscavenged Combustion Prechamber: Comparison with Natural Gas. Applied Thermodynamics, 2002. 5(4): p. 169-175.*
4. Porpatham, E., A. Ramesh, and B. Nagalingam, *Investigation on the effect of concentration of methane in biogas when used as a fuel for a spark ignition engine.* Fuel, 2008. **87**(8–9): p. 1651-1659.
5. Vu, T.M., et al., *Effects of diluents on cellular instabilities in outwardly propagating spherical syngas–air premixed flames.* International Journal of Hydrogen Energy, 2010. **35**(8): p. 3868-3880.
6. Mehrzad Kaiadi, P.T., Ashish Shah, *Extending the performance, fuel efficiency and stability of stoichiometricspark ignition natural gas engines – Gas engine research at KCFP 2007-2012,* S.G.C. AB, Editor. 2013.
7. T.Korakianitis, A.M.N., R.J.Crookes, , *Natural-gas fueled spark-ignition (SI) and compression-ignition (CI) engine performance and emissions.* . Progressin Energy and Combustion Science,. , 2010. **1**: p. 1-24.
8. Porpatham, E., A. Ramesh, and B. Nagalingam, *Effect of compression ratio on the performance and combustion of a biogas fuelled spark ignition engine.* Fuel, 2012. **95**(0): p. 247-256.
9. *Juan Pablo Gómez Montoya, Andrés Adolfo Amell Arrieta. Tesis de Maestría. Estudio teórico y experimental de la conversión de un motor diesel a encendido provocado, utilizando como combustible mezclas de biogás y metano. Universidad de Antioquia. Junio de 2012.*
10. *S. Dasappa, On The Estimation Of Power From A Diesel Engine Converted For Gas Operation – A Simple Analysis, Astra, Editor, Indian Institute of Science: Bangalore, India. p. 1S. Dasappa, On The Estimation Of Power From A Diesel Engine Converted For Gas Operation – A Simple Analysis, Astra, Editor, Indian Institute of Science: Bangalore, India. p. 1.*
11. **Heywood, J.B.**, ***Internal Combustion Engines Fundamentals***, ed. M.G. Hill. 1988.
12. *Bari, S., "Effect of carbon dioxide on the performance of biogas/diesel dual-fuel engine". Renewable Energy,1996. Vol-9: p. 1007-1010.*
13. Henham, A. and M.K. Makkar, *Combustion of simulated biogas in a dual-fuel diesel engine.* Energy Conversion and Management, 1998. **39**(16–18): p. 2001-2009.
14. *Bedoya., I., Thesis: Study of the influence of the mixing system and pilot fuel quality on the performance of a dual engineFacultad de Ingeniería. Universidad de Antioquia. 2007.*
15. Douville, P.H.a.B., *Analysis of Combustion in Diesel Engines Fueled by Directly Injected Natural Gas* Journal of Engineering for Gas Turbines and Power, 2000. **Vol. 122**: p. 141-449.
16. J.D. Naber, D.L.S., S.S. Di Julio, C.K. Westbrook. *Effects of Natural Gas Composition on Ignition Delay Under Diesel Conditions. Twenty-Fifth International Symposium on CurnbustionUC Irvine, Irvine CA July 31-Aug 5, 1994*. 1994.

17. Porpatham, E., A. Ramesh, and B. Nagalingam, *Effect of hydrogen addition on the performance of a biogas fuelled spark ignition engine.* International Journal of Hydrogen Energy, 2007. **32**(12): p. 2057-2065.
18. Park, C., et al., *Effect of mixing CO2 with natural gas–hydrogen blends on combustion in heavy-duty spark ignition engine.* Fuel, 2012. **102**(0): p. 299-304.
19. Bade Shrestha, S.O. and G. Narayanan, *Landfill gas with hydrogen addition – A fuel for SI engines.* Fuel, 2008. **87**(17–18): p. 3616-3626.
20. Cho, H.M. and B.-Q. He, *Spark ignition natural gas engines—A review.* Energy Conversion and Management, 2007. **48**(2): p. 608-618.
21. Demuynck, J., et al., *Investigation of the influence of engine settings on the heat flux in a hydrogen- and methane-fueled spark ignition engine.* Applied Thermal Engineering, 2011. **31**(6–7): p. 1220-1228.
22. Moreno, F., et al., *Efficiency and emissions in a vehicle spark ignition engine fueled with hydrogen and methane blends.* International Journal of Hydrogen Energy, 2012. **37**(15): p. 11495-11503.
23. *Combustion Gasification Propulsion Laboratory, Final Report on Strategic Development of Bio-Energy (SDB) Project. 2006, Indian Institute of Science: Bangalore. p. 85-115, 186-193.*
24. José Carrera, J.R., Simón Martínez , Fausto Sánchez,Armando Gallegos, *NUMERICAL STUDY ON THE COMBUSTION PROCESS OF A BIOGAS SPARK-IGNITION ENGINE.* THERMAL SCIENCE, 2013. **17**(1): p. 241.
25. Huang, J. and R.J. Crookes, *Assessment of simulated biogas as a fuel for the spark ignition engine.* Fuel, 1998. **77**(15): p. 1793-1801.
26. Xin, Z., et al., *The experimental study on cyclic variation in a spark ignited engine fueled with biogas and hydrogen blends.* International Journal of Hydrogen Energy, 2013. **38**(25): p. 11164-11168.
27. Jeong, C., et al., *Generating efficiency and emissions of a spark-ignition gas engine generator fuelled with biogas–hydrogen blends.* International Journal of Hydrogen Energy, 2009. **34**(23): p. 9620-9627.
28. Arroyo, J., et al., *Efficiency and emissions of a spark ignition engine fueled with synthetic gases obtained from catalytic decomposition of biogas.* International Journal of Hydrogen Energy, 2013. **38**(9): p. 3784-3792.
29. Malenshek, M. and D.B. Olsen, *Methane number testing of alternative gaseous fuels.* Fuel, 2009. **88**(4): p. 650-656.
30. Ma, F., et al., *Effect of compression ratio and spark timing on the power performance and combustion characteristics of an HCNG engine.* International Journal of Hydrogen Energy, 2012. **37**(23): p. 18486-18491.
31. Lee, S., et al., *Effect of n-Butane and propane on performance and emission characteristics of an SI engine operated with DME-blended LPG fuel.* Fuel, 2011. **90**(4): p. 1674-1680.
32. Karim, G.A., ***The onset of knock in gas fueled spark ignition engines prediction and experiment*** Journal of KONES Powertrain and Transport, Vol.14, No. 4, 2007.
33. Karim, G.A., *Autoignition and Knock in Engines Fueled with Hydrogen and Hydrogen Supplemented Gaseous Fuel Mixtures*, U.o.C. Mechanical Engineering, Editor. 1997.
34. Magín Lapuerta, J.J.H., *Thermochemical behaviour of producer gas from gasification of lignocellulosic biomass in SI engines*, S.P.s. 2001-01-3586, Editor. 2001, University of Castilla-La Mancha.
35. R. Tabaczynski, C.F.a.K.R., *A Turbulent Entrainment Model for Spark-Ignition Engines. SAE 770647, pp. 2414-2433.* 1977.
36. Vu, T.M., et al., *Effects of hydrocarbon addition on cellular instabilities in expanding syngas–air spherical premixed flames.* International Journal of Hydrogen Energy, 2009. **34**(16): p. 6961-6969.
37. Vu, T.M., et al., *Experimental study on cellular instabilities in hydrocarbon/hydrogen/carbon monoxide–air premixed flames.* International Journal of Hydrogen Energy, 2011. **36**(11): p. 6914-6924.
38. M. Metghalchi, J.K., *Burning velocities of mixtures of air with methanol, isooctane, and indolene at high pressure and temperature.* COMBUSTION AND FLAME 48:191-210 (1982).
39. 2006, F.U.s.G.S., F. Inc, Editor.
40. *V. Zimont. Gas Premixed Combustion at High Turbulence. Turbulent Flame Closure Model Combustion Model. Experimental Thermal and Fluid Science, 21:179-186, 2000.* .
41. YU, X., et al., *OPTIMIZE COMBUSTION OF COMPRESSED NATURAL GAS ENGINE BY IMPROVING IN-CYLINDER FLOWS* International Journal of Automotive Technology, 2013. **Vol. 14, No. 4, pp. 539−549**.
42. *Zefaan, H. 2012, "Combustion chamber geometry effects in spark ignitionengine exhaust emissions", Australian Journal of Mechanical Engineering, Vol. 10, No. 1, pp.29-40, http://dx.doi.org/10.7158/M11-799.2012.10.1.*
43. Mawle, C.D., *The effects of turbulence and combustion chamber geometry on combustion in a spark ignition engine*, in *University of British Columbia*. 1989.
44. Papagiannakis, R.G., et al., *Study of the performance and exhaust emissions of a spark-ignited engine operating on syngas fuel.* International Journal of Alternative Propulsion, 2007. **1**(2): p. 190-215.
45. Asociados, M.M. *Aplicación metrológica de los estudios R&R (Repetibilidad y Reproducibilidad)*. 2003.
46. TAPPI, *Steering Committee of the Process and Product Quality Division, Precision statement for test methods, 1991 Florida.*
47. *Technical Association of the Pulp and Paper Industry, All about TAPP, 2015 Atlanta, Georgia USA.*
48. Ullman, N. *Dean Neubauer. ¿Qué son la repetibilidad y la reproducibilidad? ASTM International.* 2014.
49. Douglas, M., *Diseño y Análisis de Experimentos, 2da edición, Limusa Wiley, 2004, P 1, 189-192*. Vol. *1. P189-192. 2004*.
50. UCM. *Cálculo de incertidumbres y expresión de los resultados de las práctica. http://pendientedemigracion.ucm.es/info/Geofis/practicas/errores. U. Complutense de Madrid*.

5.1 Prediction and measurement of the critical compression ratio and methane number for blends of biogas with methane, propane and hydrogen.

Abstract

Methane number (MN) and the critical compression ratio (CCR) measurements for twelve blends of biogas with methane or propane and hydrogen additions were taken in a Cooperative Fuel Research (CFR) F2 model engine according to the standard. In addition, CHEMKIN simulations of MN and the CCR were performed on these blends at similar conditions to the CFR F2 engine operation. Eight chemical kinetics mechanisms were used; it was concluded that the best mechanism to simulate the CCR is USCII, and the best mechanism to simulate MN is San Diego. In almost all blends that include propane, the best mechanism to predict the CCR and MN is Butane. It was not possible to find an optimal mechanism for all gaseous blends to simulate the CCR and MN. Experimentally, three blends of biogas were found with methane or propane and hydrogen additions with an MN of 100, with the intention to find blends of alternative and conventional fuels to interchange with methane from the viewpoint of knock resistance. For two blends, tests were carried out while changing the equivalence ratio and inlet pressure to evaluate their effect on knocking, measured with the CCR. A correlation between MN and the CCR is presented utilizing data from current and past tests performed at Colorado State University. The MN and CCR characterize the knocking tendency for each blend and indicate the maximal compression ratio to spark ignition engines; a higher CCR will lead to higher thermal efficiencies. These proposed blends use mostly biogas with a high percentage of inert gas, with favorable combustion properties including relatively large energy densities, low heating values, laminar flame speeds and low adiabatic flame temperatures. Blends of biogas with conventional fuels allow desirable combustion characteristics and high resistance to knocking.

5.1.1 Introduction

Knocking is an abnormal combustion phenomenon that adversely affects the performance, emissions, and service life of spark-ignited (SI) internal combustion (IC) engines. The normal combustion event in an SI engine can be described as a turbulent flame front, originating at the spark plug and moving through the fuel–air mixture in a controlled fashion dictated by the chemical kinetics of the oxidation. The unburned portion of the fuel–air mixture ahead of the flame front is termed ‘‘end gas”[1]. During normal engine operation, the flame propagates through the end gas, consuming the fuel–air mixture in a controlled way. In contrast, the term ‘‘knock” describes an abnormal combustion phenomenon that produces an audible sound. During knocking, the end gas autoignite and combusts before the arrival of the flame front and produces a rapid pressure rise and extremely high localized temperatures. The combination of high temperature and high pressure degrades the materials, and erosion can occur[2; 3]. For these reasons, engine manufactures strive to design engines that operate knock-free. The occurrence of knocking is dependent on many variables, including combustion chamber design, equivalence ratio, intake air temperature and pressure, and fuel properties[1]. Examples of engine parameters that are available to the engine designer for adjustment include the compression ratio (CR), spark timing (ST), intake boost pressure, intake temperature, exhaust backpressure, spark plug placement, valve configuration, and combustion chamber geometry[4; 5].

The MN is a metric that indicates the resistance to knocking of gaseous fuels. It was introduced in 1972 by Dr. Max Leiker and associates. Octane number measurement uses a mixture of isooctane and n-heptane as the reference fuel, The octane rating of gasoline is measured in a test engine and is defined by comparison with a mixture of 2,2,4-trimethylpentane (iso-octane) and n-heptane that would have the same knock resistance SI engines

The reference fuel for the MN method is a mixture of methane (CH_4) and hydrogen (H_2). The method is analogous to octane number in that the knock characteristics for a test fuel matched by 100% methane are considered to have an MN of 100 and 100% hydrogen has an MN of 0. A mixture of 80% methane and 20% hydrogen, for example, has an MN of 80. Methane and hydrogen were chosen as reference fuel constituents because methane has the highest resistance to knocking of any gaseous hydrocarbon and is the principal constituent in natural gas, whereas hydrogen is a principal constituent of reformed natural

gas, wood gas and coal gas, which are notorious for their knocking tendencies[1]. By definition, to assign a MN greater than 100 carbon dioxide (CO_2) is added to pure methane. The MN is defined as 100 plus the percentage of CO_2 added to the blend (e.g. a blend of 80%CH_4 and 20% CO_2 has a MN of 120) [6; 7]. The use of in-cylinder pressure data in a fast Fourier transform (FFT) methodology is an effective means for quantifying knocking, establishing a repeatable metric for MN measurement. This method allows knock detection well in advance of audible knock indication and provides an objective and quantitative means to establish a level of overall knocking among different fuel blends[8].

The MN and CCR are valuable tools for the diagnosis of alternative fuels that can help select the optimal engine operating conditions. Thermal efficiency in internal combustion engines is fundamentally dependent on the CR. To achieve the highest possible efficiency, an engine should be operated at the highest possible CR without risk of knocking or degradation of mechanical efficiency. The chemical composition of alternative fuels, such as biogas and producer gas, depend on how they are generated. The chemical composition of a gaseous fuel determines the MN and CCR. In addition, it is not yet clear regarding what specific engines for these fuels should be used to obtain the best possible thermal efficiencies. Moreover, to improve the properties of combustion such as flame speed, low heating value or knock resistance, alternative fuels can be blended with conventional fuels such as compressed natural gas (CNG) or liquefied petroleum gas (LPG). These desired mixtures must be characterized in terms of resistance to knocking and maximum CR to select an engine to deliver the best thermal efficiency. For biogas, it is reported that the MN is between 130 and 140, indicating that an engine operating on biogas can operate at higher CRs [1]. The mixture of biogas with CH_4 or propane (C_3H_8) and the addition of H_2 results in fuels with higher energy density, higher adiabatic flame temperature, faster flame speed, greater capacity to produce engine power and higher thermal efficiency. These mixtures also reduce the MN of the resultant blend, so the tendency to knock is greater because the autoignition temperature and the ignition delay time are decreased [9; 4; 10; 11; 12]. Producer gas is normally composed of mixtures of H_2, CO, CH_4, CO_2 and N_2; in this case, the MN can range from 54 to 125, depending on the type of gasifier and the organic material used, which yield different chemical compositions. Mixtures with high values of H_2 and CO dramatically reduce the MN, whereas the presence CO_2 or N_2 increase knock resistance and thus increase the MN [13; 14]. Biogas is mainly composed of CH_4 and CO_2. CH_4 is a gaseous fuel with high resistance to knocking, and CO_2 is inert gas that further increases the knock resistance and results in high MN of common biogas [12; 15]. Reformed natural gas, which is constituted mainly of H_2 and CH_4, has an MN near 60 owing to the presence of H_2. Coal gas produced by coal gasification in a fixed bed reactor, which is mainly composed of CO and H_2, has a low MN of less than 30, indicating a high tendency to knock, which suggests that it should be used in SI engines with low CR, close to 8 [1].

A fuel with a shorter flame initiation period will have a lower MN and knock more readily. Conversely, a fuel with a longer flame initiation period will have a higher MN and be less likely to knock. Early flame development is strongly related to laminar flame speed; consequently, MN is expected to be correlated to laminar flame speed. The location of 50% burn mass is a measure of overall combustion rate, which is related to the laminar flame speed and turbulence level. In the CFR engine the turbulence level for all cases is similar because engine operating parameters that influence turbulence such as speed and combustion chamber geometry do not change. This indicates that the laminar flame speed is related to the MN and the knock tendency of a fuel. There is a clear trend indicating that lower adiabatic flame temperatures correlate to higher MN[5]. Characteristics of lean-burn engines are low adiabatic flame temperatures, low NOx output (prior to treatment) over a wider range of air/fuel ratios, high brake mean effective pressures (bmep) due to the high charging capability, high thermal efficiencies, and sensitivity to combustion stability. At low MN, operators cannot benefit from higher efficiencies at a high CR owing to the extreme retardation of ignition required to avoid unacceptable knocking behavior. The correlation between lower heating value and MN is nonexistent. This pattern strongly suggests that this is because the percentage of pro-knock species ($CO+H_2$) is more critical than the fuel energy content[5].

An experimental test matrix was designed for quantifying the effects of blends of ethane, propane, butane, and CO_2; a statistically designed test matrix of 31 different gas mixtures was used to develop relationships

for the MN at conditions that represent typical conditions in both lean burn and stoichiometric engines[16].
Gas composition has a definite effect on the octane number of natural gas blends used as fuel for internal combustion engines; motor octane tests were conducted, and relationships developed for motor octane number and MN are presented. If the gas composition is known, the octane number can be calculated by two methods. A correlation for motor octane number versus the reactive hydrogen–carbon ratio was developed, and octane weighting factors, which used the molar composition of the fuel to predict motor octane number, were also found. These correlations provide practical methods for determining octane number and significant insight into the effects of heavy hydrocarbons on the octane number of the fuel[17].
The design of stoichiometric and lean-burn SI engines was optimized by selective modifications to the design and operating parameters to accommodate changing MN (LPG addition to CNG). Based upon the results obtained, concepts for the control of SI gas engines to accept changing MN were developed. The test results show that dedicated SI gas engines can meet the most stringent emission limits for commercial vehicles while maintaining high efficiencies. MN as a function of propane/butane concentration in different CNG blends with respect to CO_2/N_2 concentration in methane was evaluated[5].
One study detailed a method for predicting the MN requirement of a natural gas spark ignition engine. The prediction relies on a specific thermodynamic model. Engine design and operating parameter specification are normally determined so as to provide maximum efficiency while meeting emissions limits. When the engine is operating under its nominal conditions, a low MN fuel gas can lead to engine knock. An indicator was evaluated for different blended gases (CH_4, C_2H_6, C_3H_8, C_4H_{10}, C_5H_{12}, N_2 and CO_2) and engine settings. Simulations were made on three different engines. The objective of the paper was to predict MN as a function of engine settings for three engines. Simulation results show that the critical value of the considered knock criterion varies from one engine to another. A normalized knock indicator based on the energy ratio is proposed to enable this comparison. [18].
Research related to MN has historically focused on measuring MN of conventional gaseous fuels such as CH_4, C_2H_6, C_3H_8, C_4H_{10}, C_5H_{12} and mixtures thereof with additions of N_2 and CO_2. In recent years, evaluations have been performed of alternative gaseous fuels such as landfill gas, digester gas, reformed natural gas, producer gas and wood gas. Still, MN evaluations have not been carried out for mixtures of conventional fuels with alternative fuels. This paper is part of an investigation that focuses on the use of biogas (60% CH4 and 40% CO2) and blends with methane/propane and hydrogen additions in a high compression ratio (15.5:1) engine. The blends are generated to have similar Wobbe index and energy density with the intention to improve combustion properties like lower heating value, flame speed and flame temperature. It is desired to utilize biogas with high efficiency and no power loss compared with natural gas engine operation. The resistance to knock, as indicated by the methane number, is an important metric. The knock-limited, or critical, compression ratio fixes the maximum output power for each blend. The methane number of the blends is measured in a CFR engine to determine which blends are more prone to knock. A methane number simulation method is examined that could permit the analytical determination of methane number. An analytical method could reduce the cost of methane number determination.

5.1.2 Methane number estimation

5.1.2.1 Experimental apparatus

This research project requires the availability of a test cell capable of conducting engine operations with almost any gaseous gas fuel blend desired, with engine operational parameters that are controllable with regard to compression ratio, indicated mean effective pressure (IMEP), intake boost pressure, intake temperature, exhaust back-pressure, air–fuel ratio and ignition timing with instrumentation and controls capable of establishing stable engine operation and data recording to enable the analysis of the experiment results. The overall test cell design is depicted schematically in detail in Figure 1. The type of engine used in this project is a Cooperative Fuel Research (CFR) F-2 model. It is a stationary, constant speed (~940 rpm), un-throttled, single-cylinder, 4-stroke engine with a cylinder bore of 8.26 cm and piston stroke of

11.43 cm. The displacement volume of the engine is 611.7 cm^3. To enable operation at a range of CR from 4:1 to 18:1, the engine is constructed with a can-type casting forming the cylinder and cylinder head as a single part. The exterior of the cylinder is configured with a jack-screw type threaded race, allowing an engaged worm-gear to raise and lower the cylinder relative to the piston/connecting rod assembly, held laterally stable in a clamping sleeve. By raising or lowering the cylinder, the clearance volume is increased or decreased, respectively, resulting in the adjustment of the CR. The engine is operated through a belt-driven connection with a 5 horsepower synchronous motor. On start-up and while operating without producing power, the engine is rotated by the motor; when fueled and producing power, the synchronous motor operates as a generator feeding power to the electrical grid. Engine speed is limited by the set constant motor speed during motoring operation and corresponding electric grid frequency during powered operation. The knock measurement system begins with a water-cooled, piezoelectric transducer (Kistler model 6061A) mounted through the cylinder head to provide unobstructed access to the in-cylinder gases for accurate pressure measurement. The signal from the transducer is fed to a charge amplifier, which relays the pressure signal input to the controlling software. A rotary 0.1° incremental optical engine encoder (BEI model L25) provides positive crank angle position indication, enabling real-time display of cylinder pressures as a function of crank rotation.

An inline mass flowmeter (calorimetric type electronic mass flowmeter, Model FMA 1700 Series, 0-500 SLM, from Omega Engineering, Inc.) is installed to provide direct measurement of combustion air mass flow to the engine used to control the air–fuel mixture. A pressure transducer mounted in the buffer volume of the intake system provides the signal to the controlling program used to trigger the positioning of the intake air admission valve. A buffer volume approximately ten times the displacement volume of the engine is installed to dampen the pressure fluctuation upstream of the engine intake. An inline tumble mixer is installed immediately downstream of the fuel admission port to promote uniform distribution of the fuel gas in the combustion airstream. The fuel blending system is designed to allow proportioning of any combination of constituent gas desired to create specific fuel gas blends. The system consists of a number of compressed gas cylinders with regulators discharging flow first into mass flowmeters, then into a buffer volume, and then to the inlet of a pulse width modulated (PWM) injector for each gas. The PWM injectors introduce respective gases to a common manifold, and the blended gas mixture is then allowed to flow through a combination flash arrestor/check valve and finally mix with combustion air prior to entering the engine intake. The gases available for blending include CH_4, H_2, propane (C_3H_8) and CO_2. Inline mass flowmeters (calorimetric type electronic, Model FMA 1700 Series, 0-15 SLM, 0-100 SLM, and 0-200 SLM, from Omega Engineering, Inc.) are installed for each constituent gas to provide direct measurement of net fuel gas flow to the engine. The rotameters installed in the low-flow loop serve two purposes; (1) they provide a visual indication to the operator of gas flowrate and (2) the rotameter valves allow precise manual control of the gas flow to be achieved. The research initially proposed seven fuels, mixtures of biogas with methane or propane and hydrogen additions. These mixtures have similar Wobbe indices and energy density. In the tests performed at Colorado State University (CSU), three additional mixtures were evaluated. These mixtures of biogas with methane or propane and hydrogen additions have a knock resistance equal to CH_4, evaluated with MN=100 at CR=15. Additionally, pure fuels are evaluated such as CH_4 and C_3H_8. Table 1 presents the experimental fuel schedule used in this research. The biogas composition is 60% CH_4 and 40% CO_2. The blend designations are illustrated with the following two examples: 54B36M10H is composed of 54% **B**iogas, 36% **M**ethane and 10% **H**ydrogen by volume, and 75B15P10H is composed of 75% **B**iogas, 15% **P**ropane and 10% **H**ydrogen by volume. Other blends are specified using the same designation convention. The blends are calculated to have a Wobbe index similar to the blend 50B50M, which is composed of 50% biogas and 50% methane; this blend has a good balance between energy density and MN, high reactivity and high knock resistance.

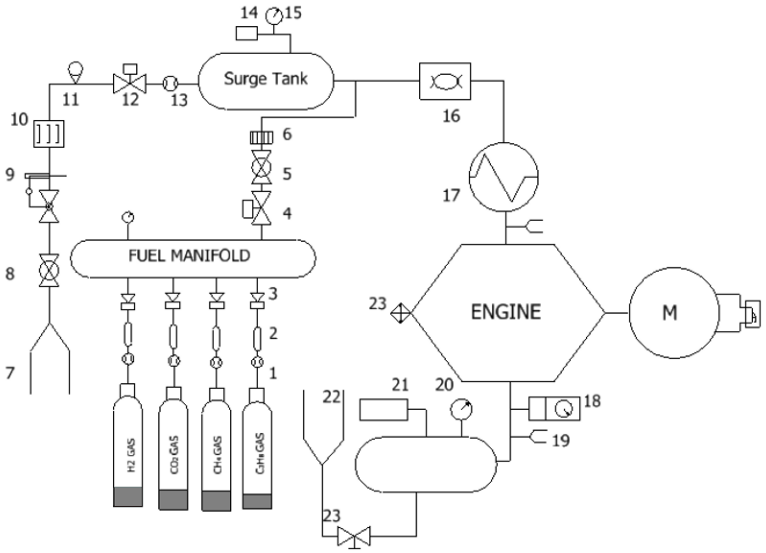

NUMBER	DESCRIPTION	NUMBER	DESCRIPTION
1	Mass flow meters	13	Flow meter
2	Surge volumes	14	Pressure sensor
3	PWM Injectors	15	Pressure Gauge
4	Control valve	16	Tumble Mixer
5	Manual ball valve	17	Intake Heater
6	Flash arrester/Check	18	O2 sensor
7	Compressed air	19	Thermocouple
8	Isolation valve	20	Pressure Gauge
9	Remote shut-off	21	Pressure sensor
10	Desiccant air drier	22	Exhaust
11	Rotameter	23	Piezoelectric Transducer
12	Intake air control valve		

Figure 1 detail of cell design schematically

5.1.2.2 Methodology to find the methane number in a CFR engine

It this work the methane number test procedure described in reference[7] is used. This method is similar to the original methane number test method proposed by Leiker *et.al.* [6]. The authors recognize that currently there is no standard methane number test method that defines standard test engine hardware and parameters such as engine speed, knock intensity, charge equivalence ratio, fuel energy flow, intake pressure, temperature, and humidity, ignition timing, and coolant temperature. A key measurement is the quantification of knock intensity. The knock intensity is quantified using the knock integral (KI), which is a measure of knock intensity. The KI is the sum of the FFT power spectrum maximum amplitude over 200 cycles. This method is described in detail in the original development by Wise [7]. The summarized methodology to find the MN is as follows:

Run the CFR engine on natural gas under stable operating conditions: inlet pressure 100 kPa, inlet temperature 40ºC, stoichiometric equivalence ratio and ignition timing 25ºBTDC. Change the engine fuel supply to blended gas, maintaining the same operational conditions. Increase the CR until light knocking (KI 10, integrated over 200 cycles) occurs. Sweep the equivalence ratio to maximize knocking, but do not change the blend composition or quantity; only increase the air quantity slightly to maximize knocking. Increase the CR until medium knocking (KI 25–30 integrated over 200 cycles) occurs, and set the CR at this point. Record the engine and blend composition data. Change the fuel supply to the reference fuel, a blend of CH_4 and H_2. Observe KI and the change reference fuel blend to achieve a similar KI (25–30 to 200 cycles). If KI is lower, add hydrogen. If KI is higher, add methane. If KI does not decrease with a mole fraction of 100% methane, use a blend of CO_2 and methane. The required MN is the mole fraction of methane in the reference blend if methane and hydrogen are used. If the reference blend is methane and CO_2, then the methane number is 100 plus the mole fraction % CO_2 [13]. If it is desired to evaluate the CCR at conditions other than the standard procedure, the procedure is as follows to obtain the equivalent MN using the correlation developed in the next section: Retain the desired mixture (blended gas evaluated under standard conditions and standard procedure) and the CR at the point where the MN was evaluated. Change the desired condition: inlet temperature, inlet pressure, spark timing or equivalence ratio. Increase or decrease the CR until the KI is equal to 25–30. Record the CR.
The uncertainty of the MN measurement method is difficult to determine. There are many measurements with individual uncertainties that can contribute to systematic (bias) error. However, the same instruments and sensors are used for both the test and reference fuels at the same engine operating conditions. Thus,

systematic errors are normalized and do not contribute to MN measurement uncertainty. The primary source of uncertainty is repeatability (random error) between MN measurements. To determine the repeatability of the measurement method, a check case methane number measurement was conducted by Wise [7]. The check case blend chosen was 90% methane (CH_4) and 10% ethane (C_2H_6). The methane number for the check case was measured on each test day, resulting in 21 individual measurements over the course of that work. The average methane number value for the check blend was 77.9, the mean value was 78.0, and the standard deviation was 1.85. The data showed that the methane number measurement method used in this work is repeatable to within ± 2%.

Table 1 Experimental fuel schedule

Designation	%CH4	%CO2	%C3H8	%H2
100C3H8	0	0	100	0
50B50M	80	20	0	0
54B36M10H	68	22	0	10
100B	60	40	0	0
100CH4	100	0	0	0
83B17P	50	33	17	0
79B16P5H	47	32	16	5
75B15P10H	45	30	15	10
57B38M5H	72	23	0	5
54.5B36.5M9H	69.2	21.8	0	9
90B10P	54	36	10	0
88B12H	53	35	0	12

5.1.2.3 Methodology for methane number numerical prediction

The evaluation of a chemical kinetics model is enabled by the use of the software CHEMKIN using the IC engine module. The point of autoignition of an alternative gaseous fuel is modeled and then compared to the modeled autoignition point of a blend of CH_4 and H_2, wherein the percentages of CH_4 and H_2 are adjusted until the modeled results closely match that of the original gaseous blend. The resulting percentage of CH_4 in the mixture is defined to be the MN. CHEMKIN is a chemical kinetics simulation program originally developed at Sandia National Laboratory. The software includes an IC engine module that provides a zero-dimensional model simulating the autoignition of air–fuel mixtures. Input parameters to the program include specific engine geometries, operating speed, fuel composition, stoichiometric conditions, and heat transfer models [19]. Engine geometries include displacement volume, connecting rod to crank radius ratio, starting crank angle and CR. Fuel composition is entered into the program by individual constituents, and stoichiometric conditions are specified to define the airflow to the engine. The program allows heat transfer characteristics through the cylinder wall to be selected from adiabatic assumptions, constant heat rejection, heat rejection based on an input time-dependent profile, or use of the Woschni heat transfer correlation [20].

Table 2. Chemkin IC Engine model input parameters

Displacement Volume	611.7 cm^3
Connecting Rod to Crank	4.44
Engine Speed	940 rpm
Starting crank angle	-180°

For the purpose of this work, the engine geometries and operating speed of the CFR F2 engine are input to the program, and the Woschni Correlation is used because it allows a more accurate estimation of the average cylinder gas speed used in the definition of the Reynold's number for the heat transfer correlation. The rationale for use of CHEMKIN IC engine module and the heat transfer mechanism is that the MN determination is based on a comparison of the gas fuel blend to a mixture of methane and hydrogen for an autoignition event, similar to the CFR engine test method. The comparison should be valid provided that

the same heat transfer mechanism is employed in both cases, described in detailed by Wise in reference[7]. The input parameters describing the engine characteristics used in this model are provided in Table 2.

Arunachalam incorporated the CHEMKIN IC engine model to predict the MN for selected producer gases[13]. Several chemical kinetic mechanisms were evaluated, and it was concluded that the modeled results for the "Güssing" producer gas blend most nearly matched the experimental results for MN when utilizing the USCII mechanism [21]. In CHEMKIN as a model, it is desired to closely replicate the experimental procedure used to measure MN. The model is executed using input values for the blended gas in question, under stoichiometric conditions, with all input conditions constant less CR, which is stepped in appropriate increments. The actual CFR F2 engine has the capability to vary the compression ratio from 4:1 to 18:1; however, this model simulates autoignition in the cylinder and not autoignition in an end gas concentration after spark initiation. The point of simulated autoignition is determined by the peak change in pressure per unit change in crank angle, a form of in-cylinder $dP/d\theta$ that has been used previously as a metric to define the initiation of engine knocking [22]. The simulation is then repeated with all input values held constant, including CCR, for a mixture of CH_4 and H_2 under stoichiometric conditions. The percentage of H_2 in the mixture is varied until the point of autoignition (θcrit) very nearly matches that determined for the associated gaseous gas blend. In the event that 100% methane autoignite too early for a given value of CCR, the procedure is to add CO_2 to CH_4 until autoignition occurs at θcrit. The MN is determined by adding the percentage of CO_2 in the blend to 100. For example, an MN of 110 would result if the matching gas blend consisted of 90% methane and 10% CO_2. Table 3 presents the different chemical reaction mechanisms used to simulate the MN and CCR. In each case, the number of species and reactions of each mechanism are presented. The curves of simulated pressure and temperature from the validation method are similar to the those achieved by Dr. Wise, using a CFR F2 geometry with a CR of 12 for the " Güssing" producer gas blend using the USCII mechanism, presented in his doctoral thesis[7].

Table 3 Chemical Kinetics Mechanism details

Mechanism	Species	Reactions	Ref.	Mechanism	Species	Reactions	Ref.
USC-Mech II	109	784	[23]	DRM-19	19	84	[24]
San Diego	46	350	[25]	DM19	19	89	[26]
GRI-Mech 3.0	51	325	[27]	Natural gas III	230	1328	[28]
DRM-22	22	104	[24]	Butane	230	1328	[28]

5.1.3. Results and analysis

5.1.3.1 Measure and prediction of critical compression ratio and methane number

Figure 2 shows the variation of MN with the critical compression ratio (CCR) for different alternative fuels tested at Colorado State University [13; 1; 8]. These data are identified as solid circles, and new experimental data from the present research (Table 1) are identified as solid squares. A regression fit of all points is presented in Equation 3.1, which allows the calculation of the MN from the CCR. The coefficient of determination R^2 is equal to 0.90 and the number of experimental data points was 64 in total. The MN can also be calculated using this equation at conditions other than the standard method (e.g., inlet pressure, inlet temperature, equivalence ratio, spark timing) to study the knocking tendency.

$$MN = 0.1792 \times CCR^3 - 6.9152 \times CCR^2 + 96.236 \times CCR - 398.16 \qquad \text{Equation 3.1}$$

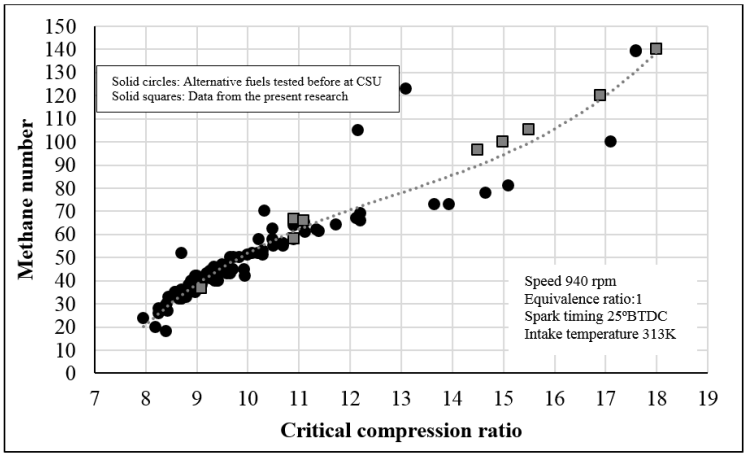

Figure 2 Variation of MN with the CCR for alternative fuels [13; 1; 8] and blends of the present research

Figure 3 presents the MN results of the tests for blends of biogas with methane, propane, and/or hydrogen additions. 100B, 50B50M and 100CH4 have an MN given by the definition. Mixtures of biogas with methane and hydrogen have relatively high MN, close to 100. Mixtures of biogas with propane and hydrogen have an MN near 65. As a result of the tests, three additional mixtures were defined: 54.5% biogas, 36.5% methane and 9% hydrogen; 90% biogas and 10% propane; and 88% biogas and 12% hydrogen. All of these have an MN equal to 100. To determine the composition of the fuel, a CR was set as 15:1, and the chemical composition of the blend was varied to achieve the same KI. The volumetric addition of propane to biogas is more prone to knocking compared with hydrogen addition in the CFR engine, requiring 10% propane to achieve an MN of 100, whereas when hydrogen is added, 12% is required. Hydrogen is the gas with the highest tendency to knock as a pure fuel, but in these engine conditions (high pressure and temperature) and in the presence of biogas, propane has a greater tendency to knock than hydrogen when blended with biogas.

Figure 4 shows the CCR for the fuels tested in this research. The overall trend is as described previously; fuels with higher MN also have a higher CCR. For the three fuels with an MN of 100, the same CR 15:1 was set, which was the value found for pure methane. For the blends 100B, 50B50M and 100CH4, it is more important to find the CCR than MN because the MN is given by the definition. Figure 5 shows the results of the CCR measurements in the CFR F2 engine and the results of simulations in CHEMKIN in the IC engine module, with the chemical kinetics mechanism named in the figure, for 100% biogas. MN is 140, equal in all cases by definition, which is equal to 100 plus 40% CO_2. In this case, it is more important to know the mechanism that more reliably predicts the CCR. For biogas, the best mechanism that predicts the end gas autoignition is DM19. The DM19 mechanism was developed at CSU[26]. AVL Methane 3.0 is a computer program developed at AVL to predict the methane number of a given gaseous fuel blend, using chemical composition. The AVL Methane software application predicts only MN and does not calculate CCR. The AVL Methane software, similar to other MN models, predicts MN based on empirical data. The MN result is more appropriately termed a methane index (MI) because a methane number measurement is not performed. Figure 6 shows the results for CCR and MN measurements in the CFR F2 engine and the results of simulations in CHEMKIN mixing 54% biogas, 36% methane and 10% hydrogen. Regarding the prediction of CCR, the most accurate mechanism is USCII [28]. However, for MN, the best mechanism was San Diego[25]. In each case, the MN is simulated with the CCR that was calculated with the respective mechanism.

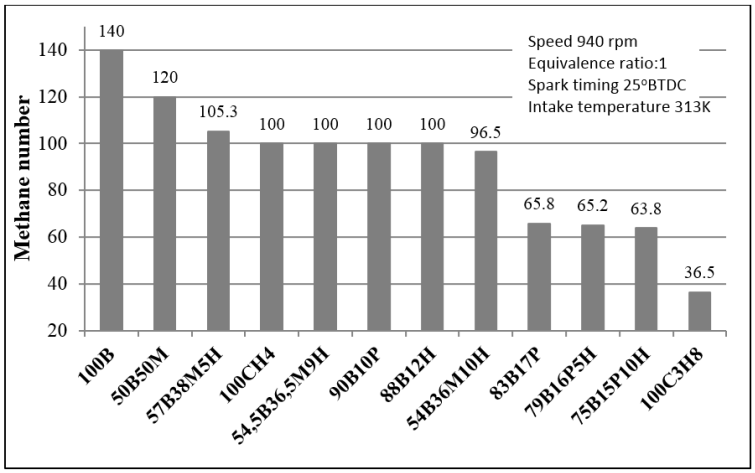

Figure 3 Methane Number for researched fuels

Figure 7 shows the comparison between MN and the CCR for the CHEMKIN simulations and measurements in the CFR F2 engine for the mixture of 75% biogas, 15% propane and 10% hydrogen. Regarding the prediction of MN and CCR, the calculated values closest to the experimental values were obtained using the Butane mechanism[28]. Simulations were carried out to determine the CCR and MN for all fuels with the different mechanisms. Simulations with added CH_4 and H_2 to biogas have better predictions of the CCR than the simulations with added propane. For the evaluation of MN in both cases, the results are very close to the measured values. Table 4 presents a summary of the mechanisms found with the CCR and MN predictions closest to the experimental results for various fuels evaluated. Overall, the USCII mechanism predicted the CCR most accurately, and the San Diego mechanism gave the most accurate evaluations of MN. The USCII mechanism has more species and reactions than the San Diego mechanism and can simulate better autoignition and CCR for blends than include hydrogen, methane, propane and CO_2. To simulate MN for blends comprising only methane and CO_2, San Diego is generally considered to be the best natural gas mechanism. In almost all blends that included propane, the best mechanism to predict CCR and MN was the Butane mechanism, which includes a large quantity of species and reactions optimized to heavier hydrocarbon, although the results of the San Diego mechanism were very close to the simulated MN in all cases. There is not a mechanism that closely predicts the MN and CCR in all cases because the mechanisms are optimized for specific fuels. It was not possible to find an optimal mechanism to be used for all blends of CH_4, CO_2, C_3H_8 and H_2.

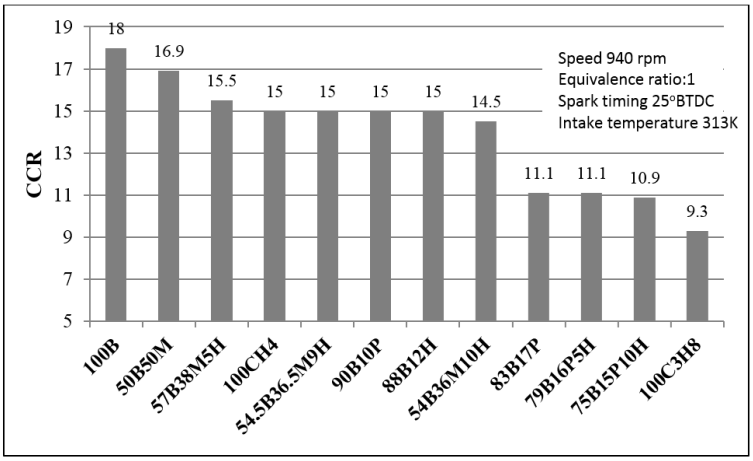

Figure 4 Measured critical compression ratio

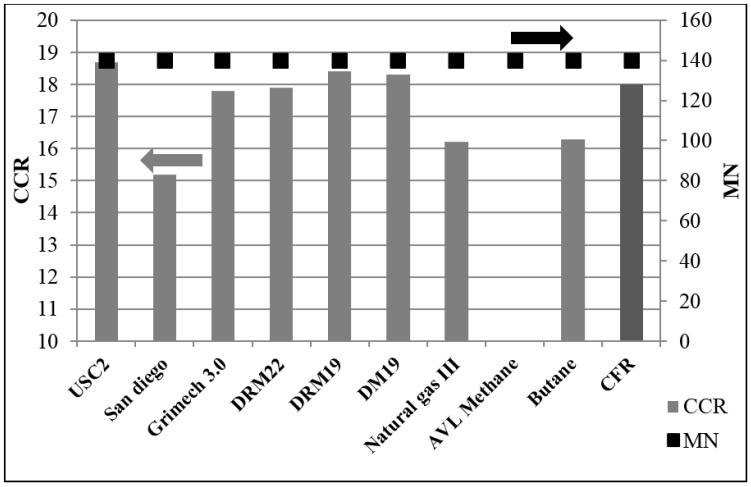

Figure 5 CCR and MN comparison between simulations and measurements of 100B

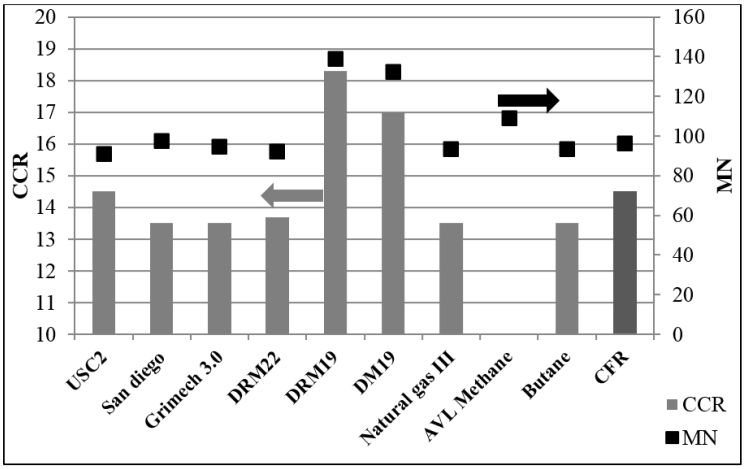

Figure 6 CCR and MN comparison between simulations and measurements of 54B36M10H

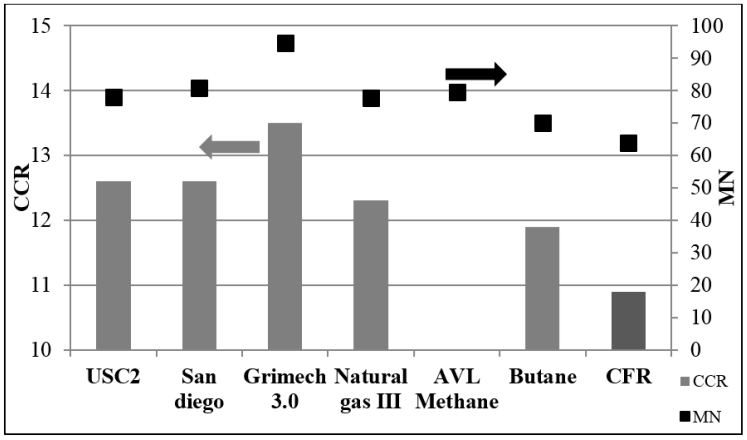

Figure 7 CCR and MN comparison between simulations and measurements of 75B15P10H

Table 4. Summary of best mechanisms encountered compared with measurements made in the CFR engine

DESIGNATION	Best mechanism CCR	Relative error CCR	Best mechanism MN	Relative error MN
100B	DM19	1.7 %	* MN by definition	-
50B50M	DRM22	0.0 %	* MN by definition	-
57B38M5H	USC2	-1.3 %	San Diego	-1.9 %
100CH4	DM19	2.7%	* MN by definition	-
54,5B36,5M9H	USC2	1.5 %	San Diego	-2.5 %
90B10P	USC2	8.8 %	San Diego	-5.5 %
88B12H	USC2	3.9 %	San Diego	1.5 %
54B36M10H	USC2	0.0 %	San Diego	1.2 %
83B17P	San Diego	11.1 %	USC2	12.9 %
79B16P5H	Butane	8.1 %	Butane	10.3 %
75B15P10H	Butane	9.2 %	Butane	9.6 %
100C3H8	Butane	13.3 %	Butane	11.5%

5.1.3.2 Effect of equivalence ratio and inlet pressure on critical compression ratio

Figure 8 shows the variation of CCR with the equivalence ratio. The blends have similar Wobbe indices 54B36M10H (28.8 MJ/m^3) and 75B15P10H (30.7 MJ/m^3), and both blends have 10% of hydrogen, but 54B36M10H has a concentration of 36% methane, whereas 75B15P10H is 15% propane. Reducing the equivalence ratio is equivalent to increasing the air supply to the engine, resulting in a charge with more nitrogen, an inert gas that reduces the knock tendency in the fuel owing to the lower reactivity and flame speeds. Higher resistance to knock permits operation at a higher engine CR, leading to higher thermal efficiency. The blend of biogas with methane and hydrogen has a higher CCR value than the blend of biogas with propane and hydrogen at stoichiometric conditions, but for lean combustion, the blend of biogas with propane and hydrogen has a higher CCR values. At the same time, lean combustion has advantages in terms of lower emissions of carbon monoxide (CO), nitrogen oxides (NOx) and total hydrocarbon (THC) resulting from excess oxygen (CO and THC) and the reduction in the flame temperature (NOx).

Figure 9 shows the variation of the CCR with the intake manifold pressure, or boost pressure. The intake manifold pressure is controlled with an automated control valve with air supplied from an air compressor system that allows the intake pressure to be controlled from the local atmospheric pressure in Fort Collins (85 kPa) to boosted conditions. The exhaust manifold pressure, or backpressure, is controlled with a backpressure valve to match the intake manifold pressure. Higher pressures cause higher mixture density and trapped mass in the engine cylinder. During compression, pressure will be greater, which increases the tendency to knock. Additionally, the brake power increases with increasing intake manifold pressure at a constant equivalence ratio, resulting in increased power density. The CCR is smaller with increasing intake pressure owing to the increased charge density. Locations at high altitudes above sea level will have lower atmospheric pressures, leading to SI engines that can operate knock-free at higher compression ratios. There are two phenomena resulting from the decrease in cylinder pressure: 1. Reduced pressure leads to increased ignition delay time in the end gas, which reduces the tendency to knock and allows higher compression ratios. 2. Reduced pressure decreases the turbulent flame speed in the cylinder, increasing the probability that the end gas will autoignite because the flame front is less likely to consume the end gas. Based on the data, the first phenomenon prevails because the pressure reduction results in a decreased knock tendency. The altitude affects the equivalence ratio even more than the boost pressure.

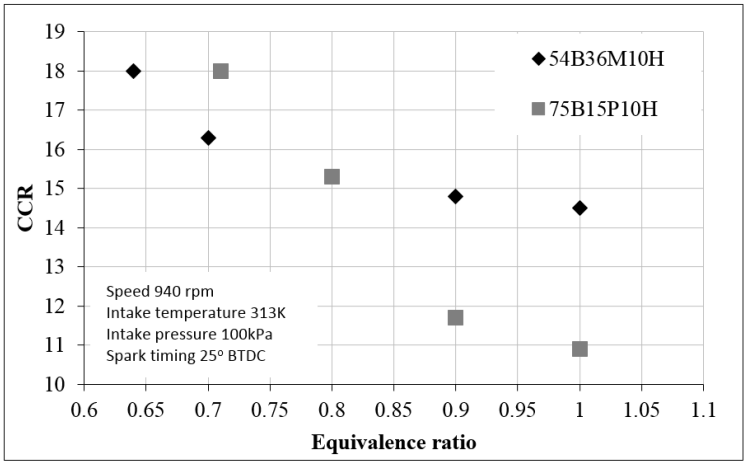

Figure 8 CCR vs. equivalence ratio for 54B36M10H and 75B15P10H

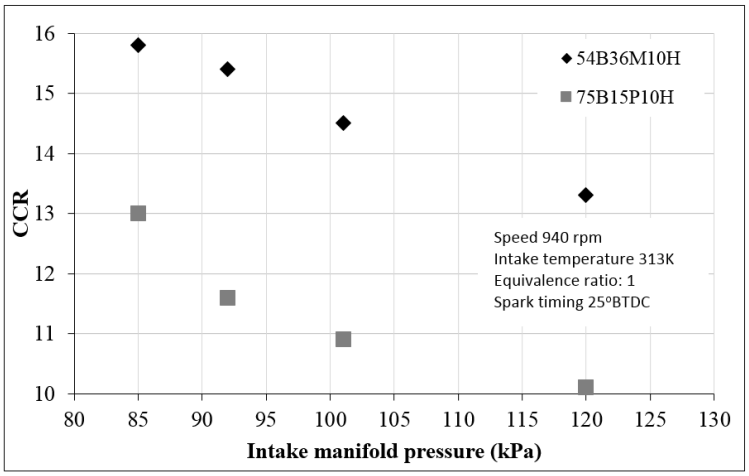

Figure 9 CCR vs. intake manifold pressure for 54B36M10H and 75B15P10H

5.1.4. Summary and conclusions

- MN and the CCR were measured for twelve blends of biogas with $CH_4/C_3H_8/H_2$ in a CFR engine. Mixtures of biogas with methane and hydrogen have relatively high MN, close to 100. Mixtures of biogas with propane and hydrogen have an MN near 65. A correlation between the MN and CCR is presented utilizing data from current and past tests. The blend 50B50M has high MN (120) and CCR; and achieved a high thermal efficiency in the CFR F2 engine operation.
- As a result of simulations in CHEMKIN of the IC engine module and the measurements of the CFR F2 engine constructed at CSU, it is concluded that to simulate the CCR, the best mechanism is USCII and to simulate the MN, the best mechanism is San Diego. In almost all blends that include propane, the best mechanism to predict the CCR and MN is the Butane mechanism. It was not possible to find an optimal mechanism for all gaseous blends to simulate the CCR and MN.
- To achieve interchangeability from the viewpoint of knock resistance, 3 blends of biogas with $CH_4/C_3H_8/H_2$ with MN 100 were found, using the same compression ratio as methane. Adding propane to biogas results in a greater tendency to knock than when hydrogen is added. To achieve an MN of 100, 10% propane must be added to biogas, whereas 12% hydrogen is required.
- Reducing the equivalence ratio of the mixture increases resistance to knocking, allowing the CR to be increased for lean mixtures. For fuel blends 54B36M10H and 75B15P10H, it was possible to obtain a CR up to 18:1 using lean combustion; this could allow higher thermal efficiency to be achieved with the same blends.

- Increased intake manifold pressure leads to increased tendency to knock. With a reduction of intake manifold pressure from 100 kPa to 85 kPa, it is possible to increase the compression ratio by 9% for 54B36M10H and 19.3% for 75B15P10H, which increases the thermal efficiency.

References

[1] Malenshek M., Olsen D.B. Methane number testing of alternative gaseous fuels. Fuel 88; 2009; 650-656.
[2] Heywood J.B. Internal Combustion Engines Fundamentals; 1988.
[3] Heywood J.B. Tagalian J. Flame Initiation in a Spark-Ignition Engine. Combustion and Flame 64:243-246; 1986.
[4] Karim G.A. The onset of knock in gas fueled spark ignition engines prediction and experiment. Journal of Powertrain and Transport, Vol.14, No. 4; 2007.
[5] Schiffgens H.J., Endres H., Wackertapp H., Schrey E. Concepts for the Adaptation of SI Gas Engines to Changing Methane Number. Journal of Engineering for Gas Turbines and Power; 1994; Vol. 116.
[6] Leiker M., Christoph K. Evaluation of Antiknocking Property of Gaseous Fuels by Means of Methane Number and its Practical Application to Gas Engines. ASME paper 72-DGP-4;1972.
[7] Wise D.M. Producer Gas Utilization in High Performance Natural Gas Engines. Mechanical Engineering, Colorado State University, Phd Thesis; 2013.
http://dspace.library.colostate.edu/webclient/DeliveryManager/digitool_items/csu01_storage/2013/06/20/file_1/207674.
[8] Wise D.M., Olsen D.B., Kim M. Development of a Lean Burn Methane Number Measurement Technique for Alternative Gaseous Fuel Evaluation. Proceedings of the ASME 2013 Internal Combustion Engine Division Fall Technical Conference.
[9] Karim G.A. Autoignition and Knock in Engines Fueled with Hydrogen and Hydrogen Supplemented Gaseous Fuel Mixtures, Mechanical Engineering; 1997.
[10] Lee S., Oh S., Choi Y., Kang K. Effect of n-Butane and propane on performance and emission characteristics of an SI engine operated with DME-blended LPG fuel. Fuel 90;2011; 1674-1680.
[11] Porpatham E., Ramesh A., Nagalingam B. Effect of hydrogen addition on the performance of a biogas fuelled spark ignition engine. International Journal of Hydrogen Energy 32 (2007) 2057-2065.
[12] Porpatham E., Ramesh A., Nagalingam B. Investigation on the effect of concentration of methane in biogas when used as a fuel for a spark ignition engine. Fuel 87 (2008) 1651-1659.
[13] Arunachalam A., Olsen D.B. Experimental evaluation of knock characteristics of producer gas. Biomass and Bioenergy 37 (2012) 169-176.
[14] Shrestha S., Karim G.A. Predicting the effects of the presence of diluents with methane on spark ignition engine performance. Applied Thermal Engineering 21 (2001) 331-342.
[15] Porpatham E, Ramesh A, Nagalingam B. Effect of compression ratio on the performance and combustion of a biogas fuelled spark ignition engine. Fuel 95; 2012; 247-256.
[16] Ryan W., King S.R. Engine Knock Rating of Natural Gases. M.N. Journal of Engineering for Gas Turbines and Power 115;1993.
[17] Kubesh J., Liss W. Effect of Gas Composition on Octane Number of Natural Gas Fuels. SAE Technical Paper Series 922359;1992.
[18] Saikaly K. et al, Normalized knock indicator for natural gas SI engines: methane number requirements Prediction Proceedings of the ASME 2009. Internal Combustion Engine Division of ASME. Conference. September 27-30, Lucerne, Switzerland.
[19] Kee R.J., Meeks E., Miller J. Chemkin III: A fortran chemical kinetics package for the analysis of gas-phase chemical and plasma kinetics; 1996.
[20] Chang J., Güralp O., Filipi Z., Assanis D.. New Heat Transfer Correlation for an HCCI Engine Derived from Measurements of Instantaneous Surface Heat Flux. SAE International; 2004;01-2996.
[21] Wang H., Ameya V., Scott G., Davis A., Egolfopoulos F., Chung K. USC Mech Version II. High-Temperature Combustion Reaction Model of H2/CO/C1-C4 Compounds. http://ignis.usc.edu/USC_Mech_II.htm; 2007.
[22] Barton R.K, Lestz S.S., Duke L.C. Knock Intensity as a Function of Engine Rate of Pressure Change, New York: Society of Automotive Engineers; 1970.
[23]Combustion-Kinetics Laboratory. http://ignis.usc.edu/Mechanisms/USCMech%20II/USC_Mech%20II.htm. University of Southern California, Aerospace and Mechanical Engineering. Web page was accessed in March, 2015.
[24] Frenklach AK, University of California at Berkeley. http://combustion.berkeley.edu/drm/. Web page was accessed in March, 2015.
[25] Combustion Research Group. http://web.eng.ucsd.edu/mae/groups/combustion/mechanism.html. UC San Diego. Web page was accessed in March, 2015.
[26] Martinez D., Tozzi L., Marchese A. A reduced chemical kinetic mechanism for CFD simulations of high BMEP lean-burn natural gas engines. Proceedings of the ASME. Internal Combustion Engine Division Spring Technical Conference; 2012.
[27] Gregory D.M., Smith P. Berkeley University. http://www.me.berkeley.edu/gri_mech/. Web page was accessed in March, 2015.
[28] Combustion Chemistry Centre. National University Ireland, Galway. http://c3.nuigalway.ie/mechanisms.html. Web page was accessed in March, 2015.

5.2 Engine operation just above and below the knocking threshold, using a blend of biogas and natural gas.

Abstract

This research involves a knocking effect analysis of the operation and performance of a spark ignition engine with high compression ratio using a blend of 50% biogas (60% CH_4 and 40% CO_2) with 50% natural gas on a volumetric basis. A diesel engine was converted to spark ignition mode. The compression ratio (15.5:1) was kept constant. The output power was increased by 5.8% compared with previous research. During testing, the output power, equivalence ratio, fuel blend composition and engine speed were kept constant while the spark timing was modified. Three knock intensities were evaluated (negligible, low, and high) using three different spark timing values of 12, 16, and 19 degrees before top dead center to evaluate the combustion parameters and engine performance. Eighteen tests were developed for repeatability analysis. A knocking analysis compare the engine performance with negligible and low knocking intensities. The knocking effect was analyzed with respect to instantaneous pressure in the combustion chamber, heat release rate, crank angle location for 5%, 50%, and 90% of mass burned, combustion duration, coefficient of variation of indicated mean effective pressure, knock peak pressure, specific fuel consumption, thermal efficiency, and emissions of carbon monoxide and total hydrocarbon. The thermal efficiency reached was 28.76% with an output power of 7.5 kW. High values of efficiency result from high CR and high output power, close to the knocking threshold. The repeatability was 1.96% for the data collected with negligible knock. For this research, a knock peak pressure in the range between 0.3 and 0.5 bar averaged over 200 cycles is established as the knocking threshold.

5.2.1 Introduction.

Knocking is an abnormal combustion phenomenon, which adversely affects the performance, emissions, and service life of spark ignition (SI) engines. The normal combustion event of a SI engine can be described as a turbulent flame front originating from the spark plug that moves through the air fuel mixture in a controlled fashion, mainly governed by the chemical kinetics of the oxidation process. The portion of the unburned mixture ahead of the flame front is called "end gas" [1]. During normal engine operation, the flame front propagates through the end gas, consuming the fuel in a controlled way. In contrast, knocking describes a phenomenon of abnormal combustion that produces an audible sound due to the autoignition of the end gas before it is consumed by the flame front, leading to a rapid increase of the in-cylinder pressure and extremely localized temperatures. The mixture burns quickly and releases energy between 5 and 25 times faster than the normal combustion, causing large pressure waves with an amplitude of several bars [2]. These pressure waves cause high-frequency oscillations of the in-cylinder pressure, thus producing a sharp sound. Even after top dead center, when the piston moves down, the end gas is compressed between 10-15 degrees by the flame front. The presence or absence of knocking reflects the outcome of a competition between the flame front and the pre-combustion reactions of the end gas. Knocking will not occur if the flame front consumes the whole mixture before pre-combustion reactions reach the end gas auto-ignition [3; 4].

Autoignition may occur in some places within the unburned mixture in the cylinder, causing a significant increase in the chamber pressure; this increased pressure excites an acoustic resonance between the gas in the cylinder and the engine block. The knock causes excessive exothermic oxidation, with the temperature exceeding 1000 K. The combination of high temperatures and high pressures degrades the materials, leading to erosion of the piston head and the cylinder head, even piston ring failure [3-5]. As a result, engine manufacturers strive to design engines that operate free of knocking. The knocking occurrence depends on many variables, such as the design of the combustion chamber, the equivalence ratio, the fuel chemical composition, the intake pressure, and the intake temperature [8]. Knocking can be avoided by adjusting some parameters, such as compression ratio (CR), spark timing (ST), spark plug location, valves configuration, combustion chamber geometry, intake pressure, and intake temperature [6; 7]. The effective thermal efficiency of engines increases with CR; however, an upper limit of the CR exists due to the occurrence of knocking of the end gas; when the CR is high, the pressure and the temperature will be higher at the end of compression stroke, which facilitates the occurrence of autoignition of the end gas. A

control of the end gas autoignition is the ST; this controls the compression of the flame front over the end gas. The knocking can be prevented by delaying the ST, which delays the main combustion phase. Each fuel has a different knock resistance, as measured by the methane number (MN) for gaseous fuels. The MN restricts the maximum CR that the engine can have for a specific fuel: the maximum CR for methane is 14,4:1, and the maximum CR for biogas is 17,6:1 [1]. The phenomenon of knocking is attractive from a chemical perspective for two reasons: First, because small differences in the chemical fuel structure could have a large change in knock behavior, and second, because knocking is one of the few situations in which the chemical kinetic of the gas could dominate the physical behavior of a system [4].

The amplitude of the pressure oscillations associated with each resonance mode immediately after knocking occurs depend on the boundary conditions, the size and shape of the combustion chamber, the autoignition location, the average local sound speed, the combustion temperature, the equivalence ratio, and the percentage of recirculated gases. The pressure inside the cylinder is the most direct method of measurement of knocking in SI engines using piezoelectric sensor [8]. By increasing the engine speed, the time to begin knocking is gradually retarded, and the knock intensity decreases; in addition, faster propagation of the flame front prevents the occurrence of autoignition of the end gas. To achieve higher brake output torque with low fuel consumption, the CR should be increased or turbocharging should be used to increase thermal efficiency. The great challenge for the SI engines is addressing the fatal problem related with knocking; the main technical bottleneck of SI engines is to increase the power by volume while inhibiting knocking. Operation of an engine under knocking conditions leads to an increase in undesirable emissions, heat and power losses, and reduction of the thermal efficiency. Autoignition at low engine speeds occurs earlier because 1) there is adequate time for chemical reactions to occur at low temperature and 2) a large amount of unburned mass exists in the zone of the end gas; these factors lead to a strong knock. By increasing the engine speed, the turbulence intensity of the mixture within the cylinder drastically increases, thereby increasing the propagation speed of the flame front, reducing the duration of combustion, and decreasing the possibility of occurrence of knocking[9].

Autoignition is rarely homogeneous because propagation reactions depend on the composition and thermal stratification of the end gas. Autoignition usually occurs at random points. When autoignition occurs, pressure waves are generated, which can cause the formation of knock waves and could result in a resounding metallic sound, which is different from the normal combustion sound. Sometimes autoignition will not lead to knock. There are three basic modes of propagation of the autoignition, depending on temperature gradients and end gas temperature, as described below. (1) When the end-gas has low temperature and high temperature gradients. This condition leads to the production of weak pressure waves that propagate and are attenuated. The combustion could experience a gradual transition to knocking. The cold flame travels with a speed between 50-200 m/s. At this stage, knocking does not occur. (2) When the end gas has high-temperature and low-temperature gradients, it generates simultaneous chemical reactions followed by autoignition. With the start of the main heat release, the average flame speed can reach to 500 m/s. (3) When the end gas has intermediate temperatures and temperature gradients. When the gradient is smaller than a critical value, it generates sufficient intensity to initiate chemical reactions, resulting in the creation of strong shock waves. The pressure waves are generated by the rapid propagation of the reaction front. When the pressure is strong and the end gas is sufficiently reactive, an intense flame front is generated that travels in the opposite direction to the high temperature, leading to flame speeds of 2000 m/s. At this time, the combustion presents knocking [2].

The development of methods to suppress knocking has been a major challenge in the development of SI engines. Knocking can be effectively suppressed by various methods; however, each one has advantages and disadvantages. Some of these methods are described below. (1) Increase the turbulence intensity. At the start of combustion, high turbulence intensities require high energy sparks to initiate the combustion process; this requirement can delay the start of combustion. However, once the flame front is formed, the high turbulence increases the flame speed, thus decreasing the burning time and the knock tendency. (2) Reduction of the combustion time can be achieved by increasing turbulence or reducing the distance of propagation of the flame front, through optimal design of the combustion chamber and the location of the spark plug. (3) Reduction of the temperature of the end gas. This reduction can be achieved by delaying

the ST; however, this may reduce engine performance. In addition, it is possible to reduce the temperature of the end gas without significantly diminishing the efficiency by reducing the temperature of the cylinder walls. Reducing the intake temperature is possibly the most useful and effective method to reduce knocking. (4) Reducing CR leads to lower pressure and temperature at the end of the compression stroke; however, the thermal efficiency is diminished. (5) Developing specific engines for each type of fuel: natural gas, biogas, synthesis gas, propane, producer gas, and others. The problem with this approach is that the use of any different blend than the specified blend will be outside of the optimal operating point for each engine. (6) Increasing the MN of the fuel can be achieved by adding inert gas, anti-knock additives, or fuels with high MN, such as biogas. (7) Using cooled external exhaust gas recirculation. The addition of combustion product gases to intake charge has substantial effects to suppress knocking due to the high concentration of CO_2, N_2, and H_2O. However, the high temperature of these gases can increase the temperature of the charge, consequently leading to the tendency to knock. The recirculated gases must be cooled before admission. (8) Using direct injection technology. Because fuel is not present during the compression stroke, it is not at a high temperature for as long a period, and there is a cooling effect associated with the expansion of the fuel as it is injected into the combustion chamber. Consequently, the tendency to knock is reduced [10-15]. The knock limit is defined in terms of the equivalence ratio as the line on which the knock is initiated at specific operating conditions. The engine is operated from a poor to stoichiometric mixture to detect the equivalence ratio in which knocking begins. The use of high CR can result in a narrow operational range between the knock and misfire limits. Increasing the intake temperature narrows the knock-free region [16, 17].

Studies relating to the knocking phenomenon are discussed above. Even so knocking is a phenomenon that needs more study. The first step is to quantify the phenomenon. No related research was found that compares engine operation just above and below the knocking threshold using alternative fuels.

The need to quantify the knock intensity and determine the exact point of knock onset has been investigated. The main methods to measure the knock tendency of gaseous fuels are [19]:

- Methane number is a metric to quantify the anti-knock characteristics.
- Knock intensity metric based on the rate of pressure change in the combustion chamber, using a Fourier series. A knock level defined by a threshold of 0.12 magnitude, occurring at least 5 times in every 50 combustion cycles.
- The ratio of pressure magnitude at the knocking frequency to the magnitude occurring at engine speed.
- Knock peak pressure define as the maximum positive value of the knock frequency pressure component.
- Use of ignition timing to quantify knock margin, which is the difference between a given spark advance and that corresponding to knock onset.
- The first index, termed the integral of modulus of pressure oscillations (IMPO) and the second index is maximum amplitude of pressure oscillations (MAPO).
- The knock onset crank angle (KOCA) then coincides with ignition delay associated with reactive species building up in the end gas.

Even though there are several ways to measure knocking, it is not clear how to best measure the knocking threshold and how to quantify the knock threshold. One approach is the knock intensity metric [18], which is a measure of knock threshold and is the basis for the measurement used in this research using the knock peak pressure. Several authors have conducted studies using the IMPO and MAPO indices at different threshold levels with mixed results. The consensus opinion appears to be that an appropriate threshold level determination will depend on the individual engine and operating conditions of equivalence ratio, volumetric efficiency, and ignition timing. The first objective of this research is to define the knock threshold using the knock peak pressure measure for a Lister Petter TR2 SI engine with high compression ratio. Then primary objective is to use this metric to make a comparison between the engine operation just above and below the knocking threshold, using a blend of biogas and natural gas, at a fixed output power of 7.5 kW@1800 rpm. The engine operation is evaluated to determine the impact of knocking on performance metrics, combustion parameters, and pollutant emissions.

5.2.2 Experimental setup and general procedure for testing.

5.2.2.1 Experimental setup

Table 5.2.1. Engine specifications

Engine model	Lister Petter TR2
Engine Cycle	4 stroke
Total displacement	1550 cm^3
Compression ratio	15.1:1
Diameter x Stroke	98 mm × 101 mm
Max. power	20 kW @ 3000 rpm in CI mode
Max. Torque	76 N-m @ 2500 rpm in CI mode

A Lister Petter TR2 compression ignition (CI) engine is used for the research. The engine was converted to SI mode for use with 100% gaseous fuels. The engine has a high CR, with the intention to achieve high effective thermal efficiency levels. The engine is connected to an asynchronous electric generator, which is connected to a grid of electrical resistances to simulate the engine load, in this manner the performance of the engine can be evaluated at different load levels. The most important original specifications of the engine are shown in Table 5.2.1. To measurement of the fuel flow, two rotameters of variable area were used to measure the volumetric flow of methane and carbon dioxide. The ABB rotameters have a maximum capacity of 110 standard liters per minute, with an average supply pressure of 2000 mbar. The minimum resolution is approximately 1%. The measurement of the airflow was performed using an orifice plate. The orifice differential pressure is measured with a U-tube manometer, and static pressure is measured with a Siemens pressure transducer. The total fuel mass flow is measured with a Piezo-Metrics Coriolis meter. A Sick Maihak S710 gas analyzer is used to determine the values of the combustion emissions, such as CO, CO_2, CH_4, and O_2. This instrument uses a non-dispersive infrared method for measuring CO_2, CH_4, and CO and a paramagnetic technique for measuring O_2. A Thermo Scientific Model 42i-HL gas analyzer is used for NOx (NO and NO_2) emissions, which employs a chemiluminescence technique. The minimal resolution of the equipment are given for each gas and is defined as follows in volumetric basis: 0.01% CO_2, 0.1% CH_4, 1 ppm CO, 0.1% O_2, 1 ppm NO, and 1 ppm NO_2. The instantaneous in-cylinder pressure measurement is performed by adapting a piezoelectric pressure sensor (Kistler Type 6125C). The intake pressure is measured through a Kistler piezoresistive absolute pressure sensor (4005A) located in the intake port.

The crank angle is measured via an angular encoder, Kistler 2614B4, with a resolution of 0.1 crank angle (CA) degrees. A Kistler measurement system called "KiBox To Go" type 2893A was designed specifically to measure and analyze the combustion in real time for internal combustion engines. The measurements of combustion chamber pressure, intake pressure and crank angle allow a full analysis of the combustion process in the Lister Petter TR2 engine. The measurements of knock peak pressure, indicated mean effective pressure (IMEP), coefficient of variation (COV) of IMEP, maximal pressure, engine speed, combustion duration, heat release rate, among others, are performed simultaneously cycle to cycle. Figure 1 shows the experimental setup of the test cell used in this research.

5.2.2.2 General procedure for testing

The general conditions of the test are presented in Table 2, where the effective output power, equivalence ratio, fuel blend, and engine speed were fixed. The fuel used is a blend of 50% biogas with 50% natural gas on a volumetric basis. The blend composition is presented in Table 2 [20]. This blend is selected because it is similar to a purified biogas; this was the best fuel blend in an earlier research project on a similar engine [21]. Also, the main goal of the research is to find the best operating conditions for biogas. As part of this evaluation, different blends of biogas with methane or propane and hydrogen additions are used [22]. The output power was set to 7.5 kW, which was close to the highest output power reached at constant speed, equivalence ratio, and fuel blend listed in Table 3. Because the purpose of this research is to study the effect of knocking on the operation of a SI engine with high CR, the only parameter modified was ST.

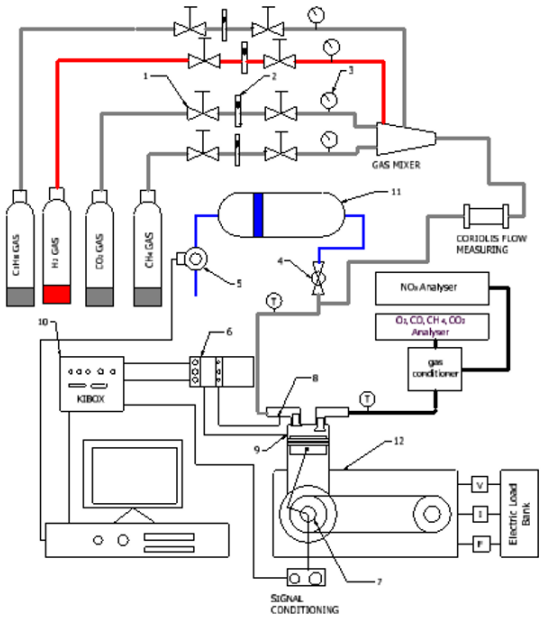

NUMBER	DESCRIPTION
1	Control Valve
2	Variable Area Flowmeters
3	Manometer
4	Proportional Valve
5	Orifice Plate Measurement
6	Signal Amplifier
7	Angle Encoder
8	Piezoresistive Pressure Sensor
9	Piezoelectric Pressure Sensor
10	Kibox
11	Damping Tank
12	Motor, 4 Strokes, 2 Cylinders

Figure 5.2.1. Experimental setup.

Table 2 Blend composition

	% CH_4	% CO_2	% C_2H_6	% N_2
Blend composition	79,03	20,16	0,26	0,55

Table 3. General test conditions

Engine speed	1800 rpm +/- 20 rpm
Output power	7.5 kW +/-0.05 kW
Equivalence ratio	0.9 +/- 0.01
Fuel Blend	50% Biogas and 50% natural gas +/- 0.2% by volume

5.2.3 Experimental results.

5.2.3.1 Knocking threshold

Three levels of knocking were evaluated: negligible, low, and high knock. For this evaluation, the engine was operated at three different ST: 12, 16, and 19 CAD degrees before top dead center (BTDC). Figure 2a shows a plot of the measured in-cylinder pressure for these conditions, one cycle for each ST. Knock peak pressure is calculated as the maximum value of the high-pass filtered pressure signal, the largest value of the knock peak pressure was 22.6 bar with a spark timing (ST) of 19 CAD degrees BTDC, which shows a high knock tendency that is dangerous for the operation and integrity of the engine. Large fluctuations in the pressure curve are also observed. For this reason, only one test was performed under these conditions. With ST of 16 CAD degrees BTDC, a low knock peak pressure of 2.2 bar was obtained. This level of low knock is a bit audible; nevertheless, its occurrence is evident in the pressure curve. With ST of 12 CAD degrees BTDC, the knock peak pressure was 0.22 bar. This knock level is considered negligible, and the pressure curve appears smooth. Figure 2b shows the heat release rate curves vs. crank angle for negligible, low and high knock. The greatest knock intensity results in a faster and larger heat release rate, reaching a peak of almost twice the value of negligible knock. The fast heat release occurs because the end gas is burned by autoignition in different points. Knocking occurs at a very high speed, higher than the turbulent flame speed of the flame front. Knocking produces a rapid increase in pressure and highly localized temperatures, leading to faster release of the fuel energy.

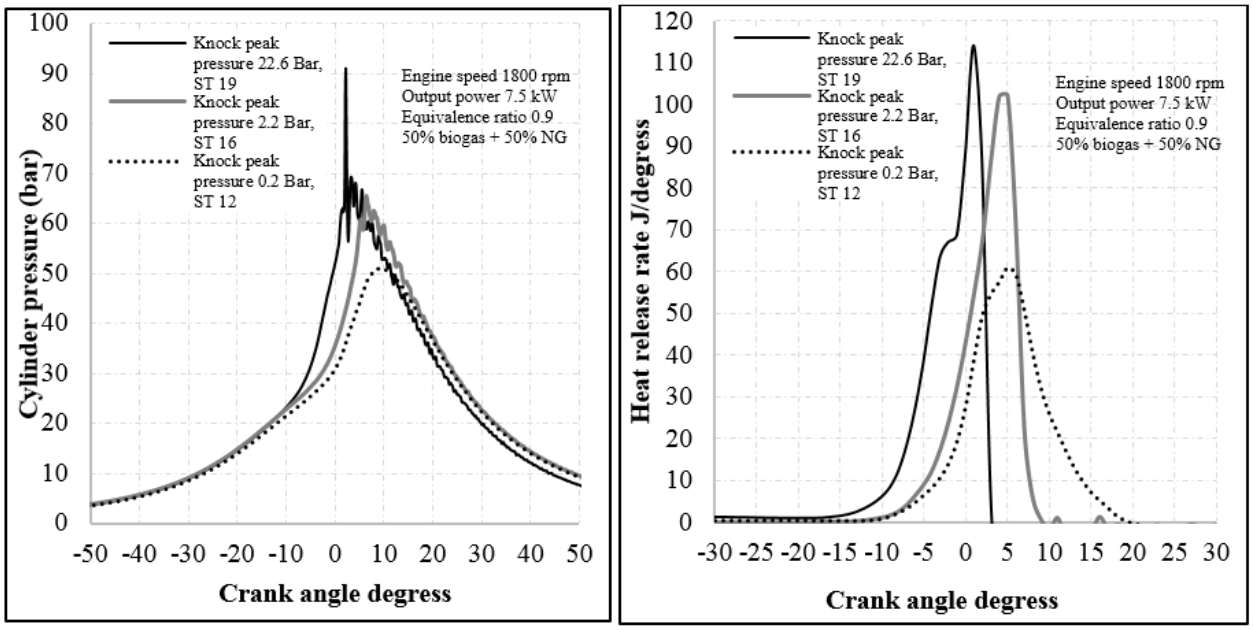

Figure 2. a) Instantaneous pressure chamber and b) heat release rate for negligible, low, and high knock.

Figure 3 shows the result of the measurement of the knock peak pressure for 200 consecutive cycles at three knock intensity levels for the three selected spark timing values. Due to high cycle-to-cycle knock variation, is required to average many cycles. For example, with ST 19 CAD degrees BTDC, in cycle 797, the value of the knock peak pressure is 22.64 bar, and in cycle 798, the value is 5.91 bar, at the same output power and engine speed. The average knock peak pressure value is 7.29 bar. Due to the random nature of the knocking phenomenon, the amplitude of the knock peak pressure is different for each cycle [18]. The quantification of knock peak pressure throughout this work is an averaged over 200 cycles. Testing with a ST of 16 CAD degrees BTDC resulted in low knock conditions with a knock peak pressure of 3.26 bar. Testing with a ST of 12 CAD degrees BTDC resulted in stable, knock free operation. Knock peak pressure was 0.42 bar. Very stable engine operation resulted, knock peak pressure between 0-0.2, when using late ST values. At knock peak pressure values higher than 0.3 bar the pressure curve begins to increase due to knocking. At knock peak pressures above 0.5 bar the pressure curve increase begins to be significant. The value chosen as the knock threshold is subjective; it is difficult to assign and utilize one specific value. Based on the tests conducted, a knock peak pressure in the range between 0.3-0.5 bar is designated as knock-free engine operation. Therefore, the engine is operated with knock peak pressures in the range between 0.3 and 0.5 bar to measure maximum output power. Knock peak pressure values higher than 0.5 bar indicate knocking.

5.2.3.2 Comparison between the engine operation just above and below the knocking threshold

Eighteen tests were performed with each setting of ST 12 and 16 CA degrees BTDC (negligible and low knocking), to validate the effect and repeatability of knocking in the operation and performance of a SI engine with high CR. Figure 4a and Figure 4b show the pressure curves for tests with ST 12 CA degrees BTDC and ST 16 CA degrees BTDC. In each test, the stored data corresponded to 200 cycles; each curve of these plots is the average for 200 cycles. For each ST. In this case, all curves are not presented for clarity. In the tests with ST 12 CA degrees BTDC, a negligible knock is observed, and little variation is found in the value and location of the peak pressure. The peak pressure variation is less than 2 bars, indicating high combustion stability. These small variations are characteristic of SI engines operation, in which the values should not exceed 10% of COV IMEP [10]. Figure 4b shows the pressure curves of the tests with ST 16 CA degrees BTDC. A large variation of the value and location of peak pressure is observed, approximately 10 bars of difference between the maximum and the minimum values, indicating

a high coefficient of variation due to the presence of knocking. Each one of the curves of Figure 4b are the average of 200 cycles; even so, large global differences are evident. In Figure 3, cycle-to-cycle variations in the knock peak pressure are also observed.

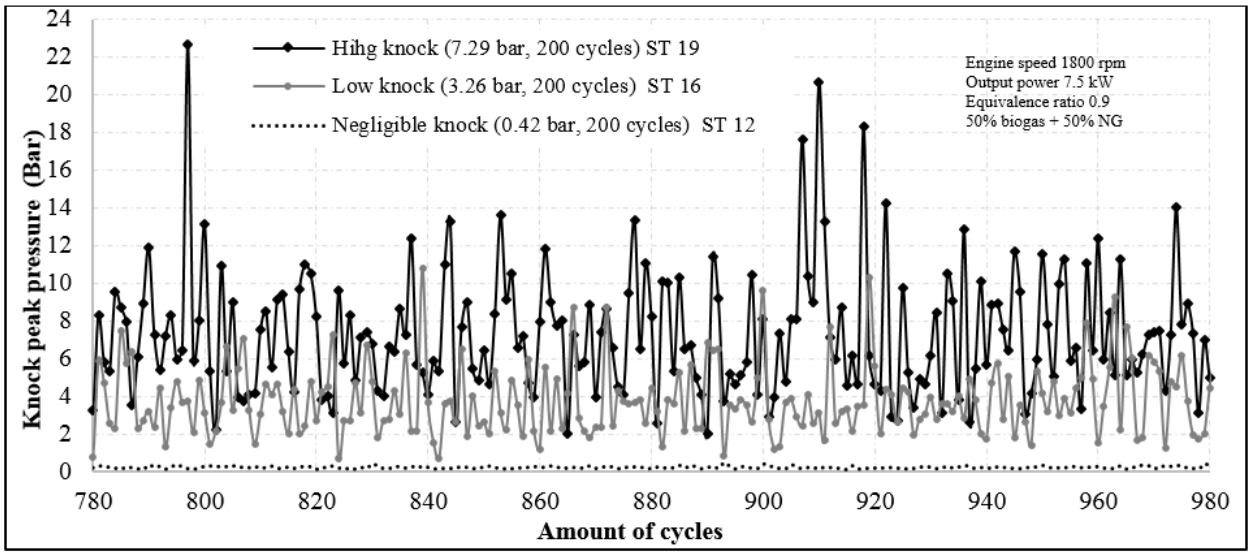

Figure 3. Knock peak pressure for 200 consecutive cycles for negligible, low, and high knock.

Figure 5 shows the curves for heat release rate versus crank angle, where the crank angle of zero corresponds to top dead center (TDC). Figure 5a shows little variability due to knock-free operation. Small normal differences characteristic of SI engines operation are observed. Figure 5b shows large differences, over 30 J/CA, due to the high cycle-to-cycle variability in combustion. The autoignition of the end gas leads to a higher heat release rate in the global combustion process. In contrast, under normal operating conditions, the end of the heat release occurs near 20 CA degrees ATDC, and the presence of the autoignition causes the end of the heat release to occur before of 8 CA degrees ATDC. This process leads to higher heat release peaks for the same energy released in the mixture. When the engine operates under knock conditions, it is difficult to control. The engine is highly unstable and can overheat if it is operated under these conditions for a long time.

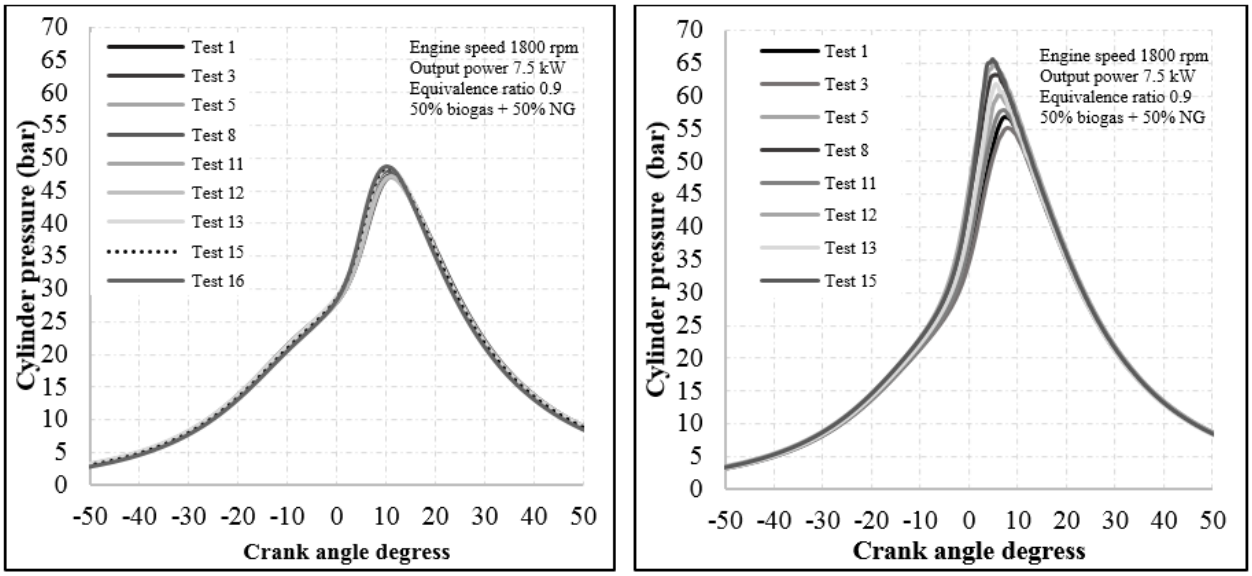

Figure 4. a) Cylinder pressure ST 12 and b) Cylinder pressure ST 16 vs. Crank angle.

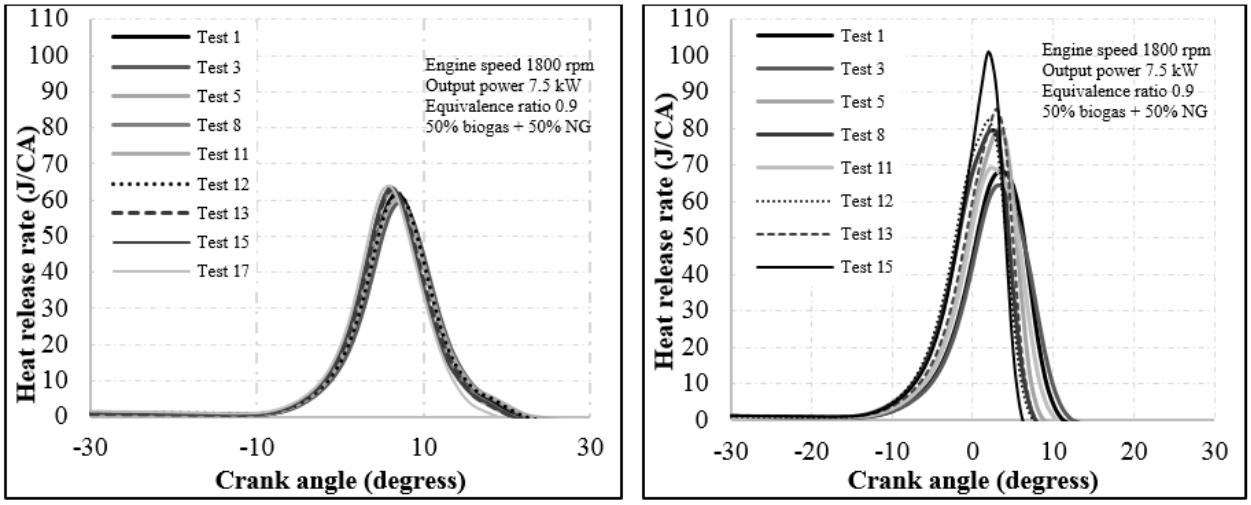

Figure 5. a) Heat release rate ST 12 vs. Crank angle. b) Heat release rate ST 16 vs. Crank angle.

Calculations of the repeatability are similar to those in TAPPI standard T 1200, "Interlaboratory Evaluation of Test Methods to Determine TAPPI Repeatability and Reproducibility" [23]. Figure 6 presents the repeatability tests results for two ST values, 12 and 16 CA degrees BTDC (negligible and low knock). For each ST value, 18 tests were conducted. The difference between the two ST values is four degrees under the same operating conditions, equivalence ratio, effective output power and fuel blend. Each data point is the average of 200 cycles. Figure 6a shows the location of 5% fuel mass burned. The average difference between the two tests is 3.95 CA degrees; this value is almost equal to the difference of the ST of the tests, indicating that there are no significant differences in the two tests due to knocking phenomenon for the location of 5% fuel mass burned. This result occurs because, in each test, for this point, the flame front has not been developed completely, and there are no autoignition points. The start of combustion occurs as a kernel of burned fuel at the spark plug. In Figure 6b, the difference in the average for the location of 50% fuel mass burned for the tests with and without knocking is 4.67 CA degrees, demonstrating that there is a higher burned rate due to autoignition that occurs when increasing the ST. In this case, as the flame front is developed, the end gas becomes compressed and heated. Consequently, some points of autoignition are formed. The autoignition points accelerate the fuel consumption at the angle where it is located, and the 50% fuel mass burned is advanced 0.67 CA degrees.

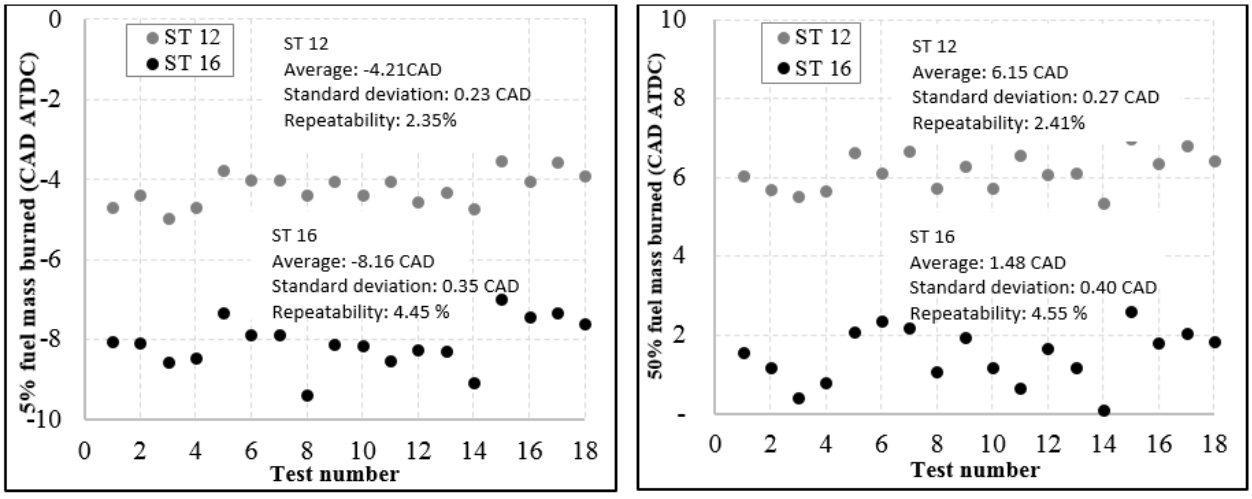

Figure 6. a) Location angle of 5% fuel mass burned. b) Location angle of 50% fuel mass burned.

Figure 7a shows that the difference in the location of the 90% fuel mass burned for the tests with and without knock is 6.58 CA degrees. The location of 90% fuel mass burned is 2.58 CA degrees earlier for the tests with knocking, after accounting for the difference in spark timing. At the moment when 90% fuel mass burned, the flame front is arriving at the end points within the cylinder, and autoignition has already occurred. Part of the mixture burns by autoignition. The knock intensity depends on the fraction of fuel mass burned by autoignition. Finally, Figure 7b shows the results of combustion duration. On average, the knocking phenomenon reduced the combustion duration by 2.66 CA degrees. When knocking is presented, a pressure shock wave is generated with high amplitude at supersonic speed, which propagates from the end gas through the combustion chamber [10]. Figures 6 and 7 show that the duration and location of fuel mass burned is more repeatable for the tests without knocking compared to the tests with knocking because the tests that present knocking increased the value of the COV IMEP, as discussed below.

Figure 8a shows the results of COV IMEP for tests, each point of the plots is the average of 200 consecutive cycles. Each ST was repeated 18 times. As observed in Figure 3, the knocking phenomenon is highly random, where two consecutive cycles can have very different knock peak pressure values. Combustion in each cycle is different and consecutive cycles may have different heat release rates and maximum pressure. This leads to IMEP that varies drastically cycle to cycle. The 200 cycle average also varies. In addition, the knock increases the COV IMEP relative knock-free combustion. The COV of IMEP was 1.98% for knock-free combustion and 3.10% for combustion with knock occurrence. The repeatability of the tests without knocking is better than the tests with knocking. Figure 8b presents the average values for knock peak pressure (each point are 200 data averaged). The difference for the tests is 2.30 Bar using ST 16 CA degrees BTDC (low knock) and 12 CA degrees BTDC (negligible knock), validating the aims comparisons of this research to the tests with and without knock using the same fuel blend, equivalence ratio, and effective output power. It is expected that COV IMEP would be less than 5% in normal operation conditions for SI engines. The engine used in this research, although operated with an average knock peak pressure of 2.53 Bar over 200 cycles, had an average of 3.10% COV of the IMEP, indicating a very stable operation after the conversion from CI to SI. The normal operation of the engine without knock (knock peak pressure 0.23Bar) leads to a low COV of the IMEP of 1.98%. The repeatability of the knock peak pressure average in both cases is difficult to achieve, even when knocking increases, due to the random nature of knocking.

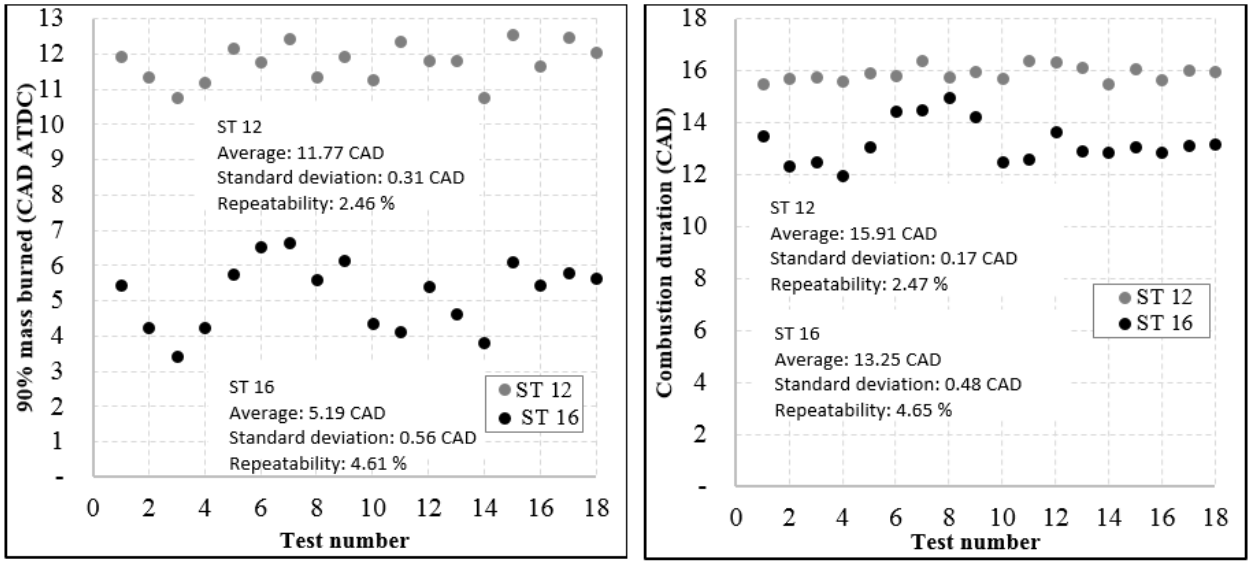

Figure 7. a) Angle of 90% fuel burned mass. b) Combustion duration.

Figure 9 shows results of calculations for a) Brake specific fuel consumption (BSFC) and b) Brake thermal efficiency BTE. Because of more stable combustion and low COV IMEP levels with negligible knocking, better engine performance is achieved with 0.97% higher BTE and 14 g/kWh lower BSFC compared with low knocking because the knock produces higher temperatures inside of the cylinder with greater heat losses to the engine walls that ultimately causes overheating of the engine. Further, as presented in Figures 10a and 10b, CO and CH_4 emissions are higher when the engine is knocking. This causes an increase in unburned fuel in the exhaust gases, without being used in the engine to produce energy, reducing the BTE and increasing the BSFC. With knock, CO emissions are increased on average 4.54 g/kWh, more than double on average of the emissions in knock-free operation. Total hydrocarbon (THC) emissions are increased to 0.93 g/kWh by the presence of the knocking phenomenon. The knock increases the COV IMEP, resulting in changes in the cycle-to-cycle burning rate the movement of the mixture inside the cylinder, air quantity, fuel and exhaust gas recirculation. This implies that, in each cycle, the air-fuel mixture and fluid-dynamic conditions change, causing variations in knock peak pressure, CO, and THC emissions. Regarding the CO and THC emissions, repeatability is not easily achieved when combustion is free of knocking, with values of 9.93 and 4.38%, respectively, and increasing more with knocking operation, 14.88% and 16.74% of CO and THC emissions, respectively.

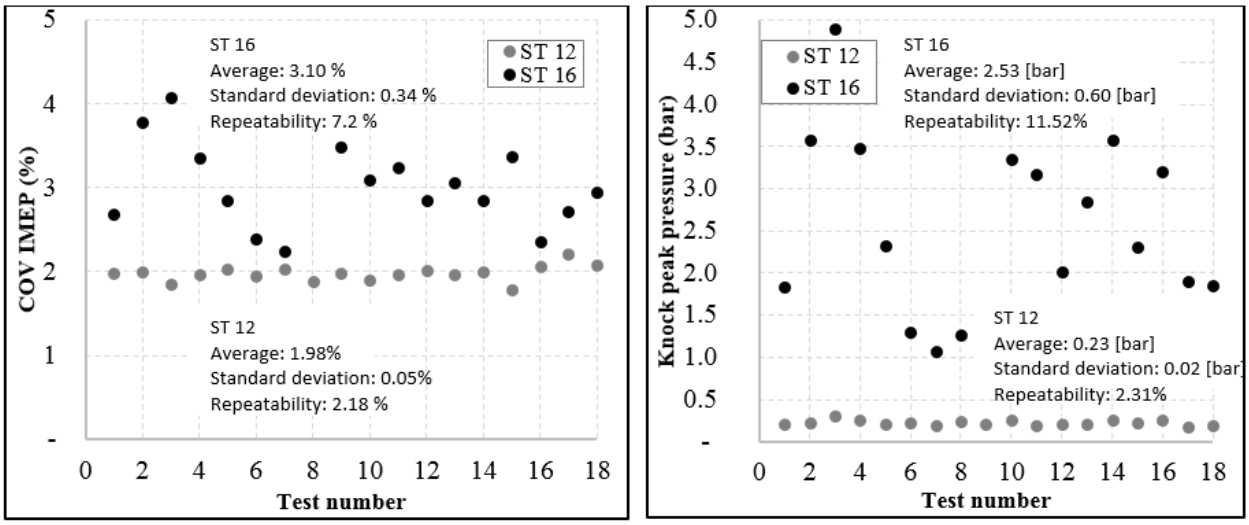

Figure 8. a) COV of IMEP (%), b) Knock peak pressure.

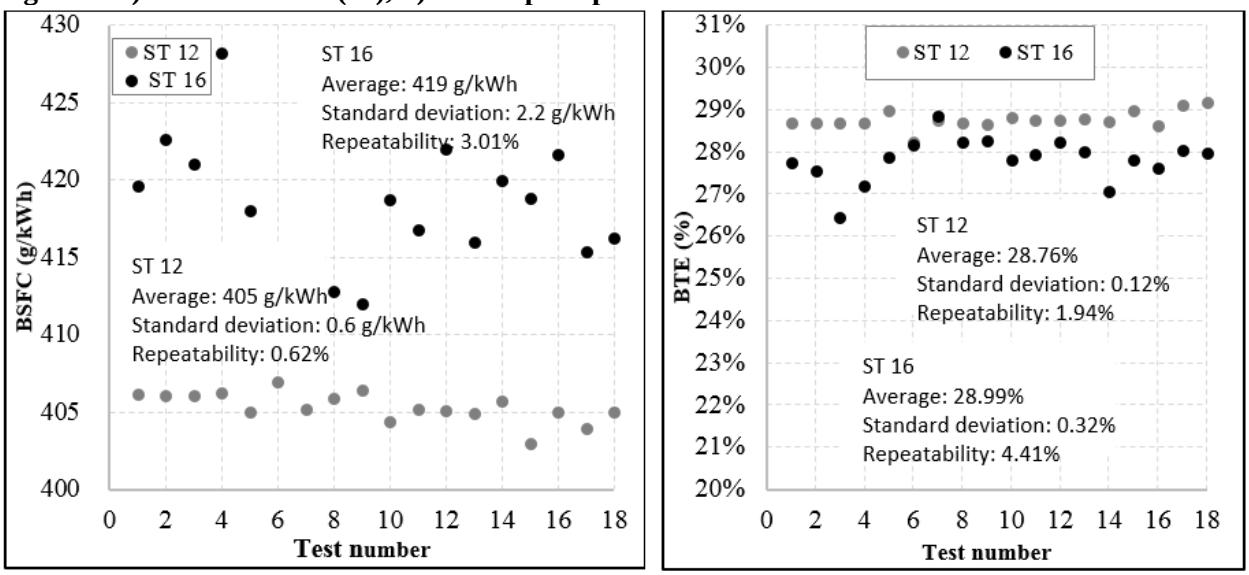

Figure 9. a) Brake specific fuel consumption. b) Brake thermal efficiency.

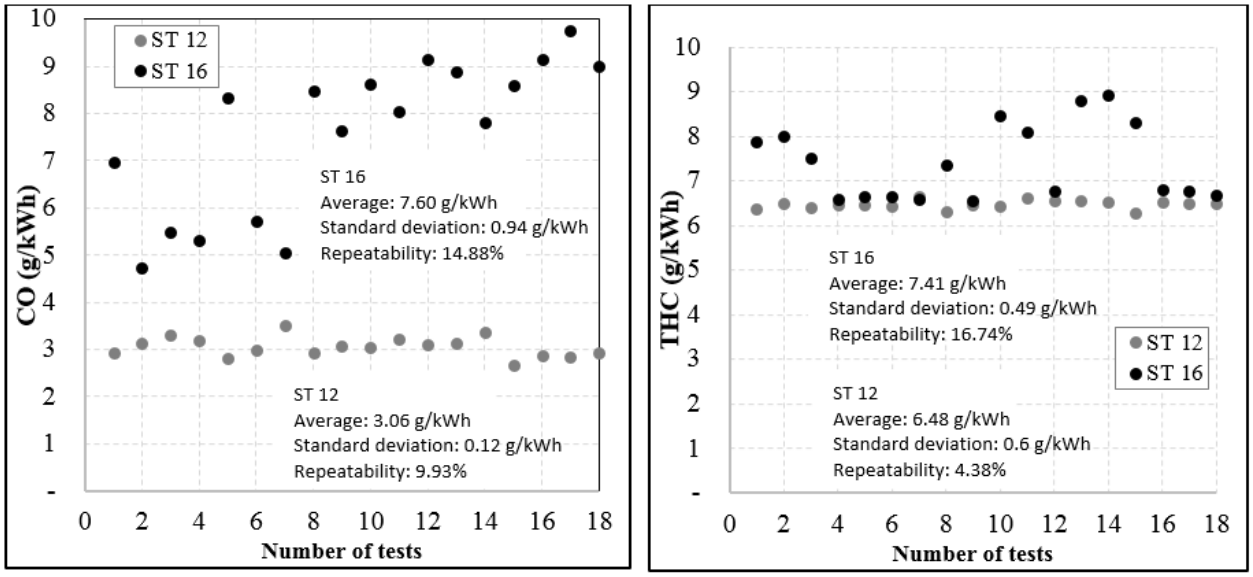

Figure 10. a) CO emissions. b) THC emissions.

5.2.4 Conclusions.

This research work involved a repeatability analysis of the knocking effect on the operation and performance of a SI engine with high CR using a mixture of biogas and natural gas. The output power, equivalence ratio, fuel blend used and engine speed were constant. Only the ST was varied to evaluate different knock intensities. The knock threshold was established to be 0.5 bar and knock-free measurements for maximum power were performed with knock peak pressure between 0.3-0.5 bar. The main conclusions from this work are as follows:

- For the tests with negligible knocking, there is a little variation in the value and location of the peak pressure. The peak pressure varies less than 2 bars, indicating high combustion stability. Tests with low knocking show a high variation of the peak pressure, approximately 10 Bar.
- For the tests with a negligible knocking, there are small differences in the normal heat release rate, characteristic of SI engine operation. Operation with low knocking leads to large differences, over 30 J/CA, due to the high cycle-to-cycle variability in the combustion process.
- Engine operation with low knocking does not affect the location of 5% mass burned but decreases the combustion duration and the location of 50% and 90 % mass burned because the heat release rate is accelerated by autoignition.
- Engine operation with a negligible knocking has better engine performance, 0.97% higher in BTE and 14 g/kWh less BSFC compared with low knock engine operation.
- The engine operation with low knocking increases the COV of the IMEP due to changes in cycle-to-cycle burning rate. In each cycle the air-fuel mixture and fluid-dynamic conditions change, causing variations in knock peak pressure, CO, THC, and NOx emissions.
- For tests with a negligible knocking the BTE, BSFC, duration and phasing of combustion are more repeatable compared with the tests with low knocking. There is a direct relationship between the COV IMEP and repeatability. The repeatability of knock peak pressure, CO and THC emissions is difficult to achieve because of the random nature of knocking.

References.

[1] M. Malenshek, D.B. Olsen. Methane number testing of alternative gaseous fuels. Fuel, 88 (2009) 650-656.
[2] X. Zhen, Y. Wang, S. Xu, Y. Zhu, C. Tao, T. Xu, M. Song, The engine knock analysis – An overview. Applied Energy, 92 (2012) 628-636.
[3] J.B. Heywood, Internal Combustion Engines Fundamentals, 1988.
[4] D. Bradley and C. Morley, Autoignition in Spark-Ignition Engines. Comprehensive Chemical Kinetics Volume 35, 1997, Pages 661–760
[5] J.B. Heywood and J. Tagalian. Flame Initiation in a SI Engine. Combustion and Flame 64:243-246 (1986).

[6] G.A. Karim. The onset of knock in gas fueled spark ignition engines prediction and experiment Journal of KONES Powertrain and Transport, Vol.14, No. 4 (2007).
[7] H.J. Schiffgens, H. Endres, H. Wackertapp, E. Schrey. Concepts for the Adaptation of SI Gas Engines to Changing Methane Number Journal of Engineering for Gas Turbines and Power. October 1994,Vol. 116.
[8] G. Shu, J. Pan, H. Wei. Analysis of onset and severity of knock in SI engine based on in-cylinder pressure oscillations. Applied Thermal Engineering 51 (2013) 1297-1306.
[9] G.A. Karim, Autoignition and Knock in Engines Fueled with Hydrogen and Hydrogen Supplemented Gaseous Fuel Mixtures, in: U.O.C. Mechanical Engineering (Ed.).
[10] S. Shrestha, G.A. Karim G.A. Predicting the effects of the presence of diluents with methane on spark ignition engine performance. Applied Thermal Engineering 21 (2001) 331-342
[11] W. Ryan, S.R. King. Engine Knock Rating of Natural Gases. M.N. Journal of Engineering for Gas Turbines and Power 115;1993.
[12] J. Kubesh, W. Liss. Effect of Gas Composition on Octane Number of Natural Gas Fuels. SAE Technical Paper Series 922359;1992.
[13] K. Saikaly. et al, Normalized knock indicator for natural gas SI engines: methane number requirements Prediction Proceedings of the ASME 2009. Internal Combustion Engine Division of ASME. Conference. September 27-30, Lucerne, Switzerland.
[14] A. Arunachalam, D.B. Olsen. Experimental evaluation of knock characteristics of producer gas. Biomass and Bioenergy 37 (2012) 169-176.
[15] E. Porpatham, A. Ramesh, B. Nagalingam. Effect of compression ratio on the performance and combustion of a biogas fuelled spark ignition engine. Fuel 95; 2012; 247-256.
[16] L. Hailin, et al. An experimental and numerical investigation of spark ignition engine operation on H2, CO, CH4, and their mixtures. Journal of Engineering for Gas Turbines and Power Vol. 132 (2010) 032804.
[17] H. Li, G.A. Karim, Knock in spark ignition hydrogen engines. International Journal of Hydrogen Energy 29 (2004) 859-865.
[18] D.M. Wise, Producer Gas Utilization in High Performance Natural Gas Engines. Mechanical Engineering, Colorado State University, 2013.
[19] D.M. Wise. Doctoral thesis. investigation into producer gas utilization in high performance natural gas engines. Colorado State University. 2013.
[20] Promigas. http://www.promigas.com. Consulted in December 2015.
[21] Juan Pablo GÓMEZ MONTOYA, Andres AMELL y Jaime ZAPATA, Experimental study of spark ignition engine performance and emissions in a high compression ratio engine using biogas and methane mixtures without knock occurrence. Thermal Science. Vol. 19, No. 6, pp. 1919-1930.
[22] Gómez Montoya J.P., Amell A.A. and Olsen D.B. Prediction and measurement of the critical compression ratio and methane number for blends of biogas with methane, propane and hydrogen. Fuel, 2016. 186: p. 168-175.
[23] Interlaboratory evaluation of test methods to determine TAPPI repeatability and reproducibility, Test Method TAPPI/ANSI T 1200 sp-14. http://imisrise.tappi.org/TAPPI/Products/01/T/0104T1200.aspx. Consulted: March 14, 2016.

5.3 Strategies to improve performance of a SI engine with high compression ratio.

Abstract

The main focus of this work is to transform a diesel engine with high compression ratio to a spark ignition engine, for exclusive use with gaseous fuels. Biogas is used as the main fuel to increase knocking resistance of the blends. Biogas is blended with natural gas or propane and hydrogen to improve the properties of the fuel. Spark timing is adjusted for optimum generating efficiencies, close to the knocking threshold. The engine is operated on each blend at the maximum output power, under stable combustion conditions. The maximum load is measured at partial open throttle limited by knocking. The engine is operated with a lean equivalence ratio. The fuel blends are injected at a pressure close 2 bar to increase the output power. The use of biogas in the engine results in a power derating of 6.25% compared with the original diesel engine (8 kW @ 1800rpm). Purified biogas (80% CH_4 and 20% CO_2), which was the blend with the highest output power (8.66 kW @1800 rpm) and highest generating efficiency (29.8%). Tests conditions were selected to achieve an average knock peak pressure between 0.3 and 0.5 bars and COV IMEP lower than 4%, both for 200 consecutive cycles. With the blends of biogas, propane and hydrogen, the output power obtained was just over 8 kW, while with the blends of biogas, natural gas and hydrogen, the output power was close to 8.6 kW.

5.3.1 Introduction

Biogas is a product of anaerobic digestion of organic matter. Biogas can be formed spontaneously in landfills or in a controlled manner in digesters. Biogas is now viewed as an important energy resource because of current efforts to reduce the use and dependence of fossil fuels [1]. The biogas production technology provides a unique collection of benefits. The use of biogas is able to improve the environment of users merely by reusing organic waste. It is a sustainable energy resource, which builds a more secure energy future. The digestion of biogas produces fuel from human, animal, agriculture, industrial and municipal waste. In developing countries, the increase of biogas production has been based on small scale reactors that use animal waste and landfill plants with anaerobic production processes; however, biogas is commonly burned without any productive use. Biogas could be used for cooking, heating, lighting, or electricity generation. The use of digesters has steadily increased since the 1970´s; currently, there are 4 million biogas plants in India and 27 million in China [2]. Despite increased research on digesters, biogas use in internal combustion engines for power generation is not increasing significantly because of the problems that biogas presents, such as low heating value, low flame speed, high content of inert gases, and the presence of hydrogen sulfide [3-7].

Knocking is an abnormal combustion phenomenon, which adversely affects the performance, emissions, and service life of SI engines. The normal combustion event of a spark ignition (SI) engine can be described as a turbulent flame front originated from the spark plug that moves through the air and fuel mixture in a controlled fashion, mainly governed by the chemical kinetics of the oxidation process. The portion of the unburned mixture ahead of the flame front is called "end gas"[8]. During normal engine operation, the flame front propagates through the end gas, consuming the mixture in a controlled way. In contrast, knocking describes a phenomenon of abnormal combustion that produces an audible sound due to the autoignition of the end gas before it is consumed by the flame front, leading to a rapid increase of the in-cylinder pressure and extremely high localized temperatures. The mixture burns quickly and releases energy between 5 and 25 times faster than normal combustion, causing large pressure waves with amplitudes of several bar and speeds up to ~2000 m/s. These pressure waves cause high-frequency oscillations of the in-cylinder pressure, thus producing a sharp sound. Even after top dead center (TDC), when the piston moves down, the end gas is compressed between 10-15 degrees by the flame front[9].

The presence or absence of knocking reflects the outcome of a competition between the flame front and the pre-combustion reactions of the end gas. Knocking will not occur if the flame front consumes the whole mixture before pre-combustion reactions reach the end gas autoignition [10, 11]. Autoignition may occur in some places in the cylinder, causing a significant increase in the chamber pressure; this increased pressure excites an acoustic resonance between the gas in the cylinder and the engine block. The knock causes excessive exothermic oxidation, with the temperature exceeding 1000 K. The combination of high

temperatures and high pressures degrades the materials, leading to erosion of the piston head and the cylinder head material, even piston rings failure[12]. As a result, engine manufacturers strive to design engines that operate knocking free. The knocking occurrence depends on many variables, such as the design of the combustion chamber, equivalence ratio, fuel chemical composition, intake pressure, and intake temperature[8]. Knocking can be avoided by adjusting some parameters, such as compression ratio (CR), spark timing (ST), spark plug location, valve configuration, combustion chamber geometry, intake pressure, and intake temperature[13, 14].

Porpatham *et al.* published work using different compositions of biogas, biogas with hydrogen and the CR influence operating with biogas. In all operating conditions, the engine was knock free and achieved highest levels of thermal efficiency with the highest CR and using a biogas with a composition of 80%CH_4 + 20% CO_2 [3, 7, 15, 16]. In all these papers, the performance of a diesel engine converted to SI engine is studied, using two CRs, 13.1:1 and 15.0:1. Bell *et al*. have evaluated natural gas (NG) compared to three types of simulated biogas (60%NG +40%CO_2, 75%NG +25%CO_2, 55%NG +35%CO_2 +10%N_2) in a SI engine with a CR 11:1. It was found that lean mixtures, delayed the ST and addition of diluents lead to reduction in NOx emissions. The presence of CO_2 in a gaseous fuel reduces the low heating value, and for this reason, reduces the output power and thermal efficiency of the engine [17]. Huang *et al*. presented results from a study in a 7 kW single cylindrical engine, with variable CR (8.0:1 to 15.0:1), operated with simulated biogas using domestic natural gas and CO_2. The fraction of CO_2 was changed from 23% to 40% on a volumetric basis. It was concluded that the primary influence of CO_2 in biogas engine operation was reducing NOx emissions. Also, higher CR led to higher peak pressures and higher brake thermal efficiency [5]. Xing *et al*. experimentally studied cyclical variations in SI engine with biogas and hydrogen mixtures, with a CR of 10.2:1. The results showed that increasing the hydrogen fraction in the mixture decreases the coefficient of variation (COV) of indicated mean effective pressure (IMEP) between 15% and 35% [18]. Chulyoung *et al*. investigated pollutant emissions and thermal efficiency in a gas SI engine with CR 10.2:1 producing 10kW @1200rpm, operating with biogas and hydrogen mixtures with different equivalence ratios. Experimental results showed that the peak values of thermal efficiency, in-cylinder maximum pressure and NOx emissions, were found at an equivalence ratio of 0.83 and the highest percentage of hydrogen [19]. Rakopoulos *et al*. studied the irreversibilities generation in an SI engine with a CR 10.2:1 operating with biogas and hydrogen mixtures. The focal point is on the demonstration of the spatial distribution inside the burned gas of the combustion-generated irreversibilities for the various hydrogen concentration cases examined, which constitute one of the major sources for the defective exploitation of fuel into useful mechanical work that cannot be identified by the traditional first-law analysis [20]. Chandra *et al*. presented the performance analysis of a stationary 5.9 kW diesel engine, converted to SI engine with a CR 12.7:1, operating with natural gas, biogas, and biogas enriched with methane. The ST was changed between 30 and 40 degrees before TDC. Compared with the original diesel fuel operation, there is a decrease in output power generation up to 46.3% using biogas [21]. Carrera *et al*. studied numerically the biogas combustion processes, in a SI engine, with a CR of 13.0:1. This study evaluated the way in which the geometrical parameters, such as CR, and operating parameters like engine speed, equivalence ratio, ST and volumetric concentration of CO_2 in biogas, affected the evolution of the combustion process [22]. Cheolwoong *et al.* conducted a study on the performance and emissions of a 8 liter naturally aspirated SI engine fueled by low calorific biogas blended with hydrogen, and biogas with various methane concentrations. The N_2 dilution test results showed that an increase of inert gas in biogas increased thermal efficiency and reduced NOx emissions, while exacerbating THC emissions and cyclic variations. The engine test results indicated that the addition of hydrogen improved in-cylinder combustion characteristics, extending lean operating limit as well as reducing THC emissions while elevating NOx generation[23]. Kyungtaek *et al*. investigated generating efficiency and NOx emissions of a gas engine generator fueled with biogas–hydrogen blends. Tests were conducted utilizing optimum ST based on the maximum generating efficiencies with varying exhaust gas recirculation rates. Utilizing optimum ST with varying EGR rates, the addition of hydrogen to the biogas increases the generating efficiency of the engine [6]. Gomez *et al.* worked with an 8 kW diesel engine, CR of 15.5:1, converted to SI, finding that the engine achieves high generating efficiencies. For a blend of

50% biogas and 50% methane, a thermal efficiency of 28% was obtained, and the dependence on diesel fuel for use in dual mode was eliminated. After the conversion, the stable operation with this blend was achieved with a ST 12 CAD degrees before TDC. The maximum output power of the SI engine decreases 17.6% after conversion [24].

The purpose of this research was to use biogas blended with natural gas or propane and hydrogen, in a high CR engine. The blends have similar Wobbe index and energy density with respect to a purified biogas. The intention is to improve combustion properties like low heating value, flame speed and flame temperature and avoid power derating compared with diesel engine operation. Knocking threshold fixed the maximal output power for each blend. These blends have a chemical composition with high percentages of CO_2, which yields good knock resistance and potentially high output power and high generating efficiencies. Different strategies were implemented with the objective of finding the best engine operating conditions. These strategies are:

- Transforming a diesel engine with high CR to SI using gaseous fuels.
- Using biogas as main fuel to increase knocking resistance of the blends.
- Blending biogas with natural gas or propane and hydrogen to improve combustion properties.
- Use ST adjusted for optimum generating efficiency, close to the knocking threshold.
- Operating the engine for each blend at the maximum output power, close to the knocking threshold, under stable combustion conditions.
- Using partial throttle opening to maximum output power but limited by the knocking threshold, maximum load is independent of throttle valve % open values.
- Operating the engine with a lean equivalence ratio, to guarantee complete combustion.
- Injecting the blends at a pressure close to 2 bars to increase the output power generation.
- Increasing turbulence intensity at the end of the compression stroke modifying the combustion chamber geometry.

5.3.2 General procedure for testing.

A Lister Petter TR2 compression ignition (CI) engine is used for the research. The engine was converted to SI mode for use with 100% gaseous fuels. The engine has a high CR, with the intention to achieve high generating efficiencies. The engine is connected to an asynchronous electric generator, which is connected to a grid of electrical resistances to simulate an electrical load. In this manner the performance of the engine can be evaluated at different load levels. The most important original specifications of the engine are shown in Table 5.2.1. The tests were carry out in Medellin, Colombia with an altitude of 1500 meters above sea level, with an atmospheric pressure of 85 kPa and 24ºC.

The fuel and blends used in this research are: Biogas and biogas blended with natural gas or propane and hydrogen. The simulated biogas used is a mixture 60% natural gas and 40% CO_2, and the natural gas composition is 94.8 %CH_4, 1.3 %N_2, 2.3 %C_2H_6, 1.1% C_3H_8 and 0.5% CO_2 on a volumetric basis. The blend designations are illustrated with the following two examples: 54B36M10H is composed of 54% **B**iogas, 36% **M**ethane and 10% **H**ydrogen by volume, and 75B15P10H is composed of 75% **B**iogas, 15% **P**ropane and 10% **H**ydrogen by volume. Other blends are specified using the same designation convention. In all the tests the high CR was kept constant with the intention to get high power output and generating efficiencies. The MN of the blends were previously tested [13], the methane number of natural gas was estimated using the software Methane 3.1 from AVL. Table 2 presents blend properties and throttle valve % open values.

Tests were made with an equivalence ratio of 0.9, which was selected because is close to the stoichiometric, but with a slight air excess to ensure complete combustion of the blends. A throttle valve is from a vehicle engine from a Hyundai Atos Prime, with a CR 9.6:1 and 1.1 capacity displacement. Operating at 60% throttle valve opening, the airflow was at the maximum that could be obtained. Larger openings did not increase the volumetric airflow, so this value was considered 100% equivalent throttle valve opening (ETVO). The blends than require more air for combustion, operated close to 90% ETVO at the maximum output power, according to the Table 2. In this research, the engine maximum output power is not limited by the throttle valve opening, but by the knocking threshold and cyclic variations. The

throttle valve controls the airflow and the blends were injected near to the intake port, with a pressure close to 2 bar, so the control of the mixture is independent.

Table 2 Blend properties and throttle valve opening

Fuel Designation	Fuel composition	Fuel properties				Throttle in percentage (ETVO)	Laminar Flame speed (cm/s). Equivalence ratio 0.9 and 1 Atm.
		LHV MJ/m3 fuel	LWI MJ/m3 fuel	Energy density MJ/m3 air	Methane number		
100NG	100% Natural gas	34.55	45.13	3.58	87.2	61.7	34.98
100B	100% Biogas	20.35	20.99	3.44	140.0	75.0	23.57
50B50M	50% Biogas + 50% Methane	27.14	**31.40**	**3.57**	120.0	66.7	30.22
57B38M5H	57% Biogas + 38% Methane +5% Hydrogen	25.00	29.01	3.58	105.3	63.3	30.32
54B36M10H	54% Biogas + 36% Methane +10% Hydrogen	24.22	28.80	3.59	96.5	60.0	31.74
83B17P	83% Biogas + 17% Propane	31.98	31.38	3.64	65.8	58.3	32.83
79B16P5H	79% Biogas + 16% Propane +5% Hydrogen	30.89	31.04	3.65	65.2	56.7	33.91
75B15P10H	75% Biogas + 15% Propane +10% Hydrogen	30.71	30.71	3.77	63.8	55.0	34.95

Because of the random nature of knocking, the knock intensity is different for each cycle. The knock measurement is made over a number of cycles. Cycle to cycle variations in knock intensity are due to a change in composition of the mixture, burning rate variations and differences in pressure, temperature and turbulence. Maximum output power is registered when the average knock peak pressure is in the range between 0.3 and 0.5 bar over 200 cycles. The knock measurement is carried out using the instantaneous pressure curve, measured with a piezoelectric pressure sensor inside the combustion chamber.. Cyclic variation of combustion pressure is an important measure of the operational stability of internal combustion engines. This is quantified by the COV IMEP, which is the standard deviation of IMEP divided by the mean IMEP. For automotive applications, values greater than 5% COV IMEP result in drivability problems for a vehicle [27]. For this research a maximum COV IMEP of 4% is established for the stability limit.

5.3.3. Experimental results.

Table 3 presents the ST for optimum generating efficiencies under maximum output power. The correct phasing of the combustion process results in higher generating efficiencies for each blend. Blend with high MN have low flame speed and combustion is long, the ST must be advanced to adjust combustion phasing. Blends with low MN have high flame speed and combustion is short, the ST is retarded to adjust combustion phasing. The ST for some blends must be retarded to avoid knocking, which occurred most notably with 100GN, 83B17P, 75B15P10H, and 79B16P5H. These blends have relatively low MN (87.2, 65.8, 65.2, and 63.8, respectively). This ST adjustment results in the main phase of combustion occurring late in the expansion stroke with a lower average pressure [28]. Blends such as 100B and 50B50M have high knock resistance, characterized by high MN (140 and 120, respectively). This allow a more advanced ST, which results in combustion events that produce earlier and larger pressure peaks.

Figure 2 shows the instantaneous in-cylinder pressure versus CAD for the blends, in two separate plots for better visualization a) Biogas, natural gas, 50B50M, 57B38M5H and 54B36M10H and b) Biogas, 83B17P, 79B16P5H and 75B15P10H. Each curve is an average of 200 consecutives cycles, which is the same for all figures presented. In each case, the ST is adjusted for optimum efficiency at the maximum output power achieved without knocking. For all tests the average knock peak pressure was in the range between 0.3 and 0.5 bars for 200 consecutive cycles and COV IMEP under 4% to achieve stable combustion. The blend 50B50M has the highest peak pressure because this blend had the highest output

power and early combustion phasing. This blend has favorable combustion properties such as high energy density, high flame speed and high MN (high knock resistance). These characteristics allowed greater output power to be produced, 8.66kW, which is 8.25% higher than 100% diesel operation. The 100B fuel has low energy density but high MN. This mixture allows early combustion phasing but does not have the capacity to increase output power beyond 7.5 kW. The 100B fuel had a derating of 6.25% in output power, compared to the original diesel engine.

Table 3 Spark timing adjusted for optimum efficiency

Blends	ST (CAD BTDC)	Blends	ST (CAD BTDC)
100GN	3	83B17P	4
50B50M	8	79B16P5H	5
57B38M5H	6	75B15P10H	4
54B36M10H	6	100B	12

The blends 83B17P, 79B16P5H, 75B15P10H relative to the blend 50B50M require less air due to lower air/fuel ratio. This results in a reduced mixture flow for these blends, requiring a lower ETVO value and lower cylinder pressure at the intake valve closure. Consequently, the pressure at the end of the compression stroke is lower. The instantaneous pressure curves for the blends 83B17P, 79B16P5H and 75B15P10H are lower than for the blends of 50B50M, 57B38M5H and 54B36M10H because of the output power values are lower. This is because high knock tendency of blends 83B17P, 79B16P5H and 75B15P10H required a delayed ST, which resulted in peak pressures beyond 17 degrees ATDC. The blends 54B36M10H and 57B38M5H are intermediate regarding to peak pressure values. These blends have similar knocking resistance to methane (MN 100) and are similar in peak pressure location and value compared with 100GN.

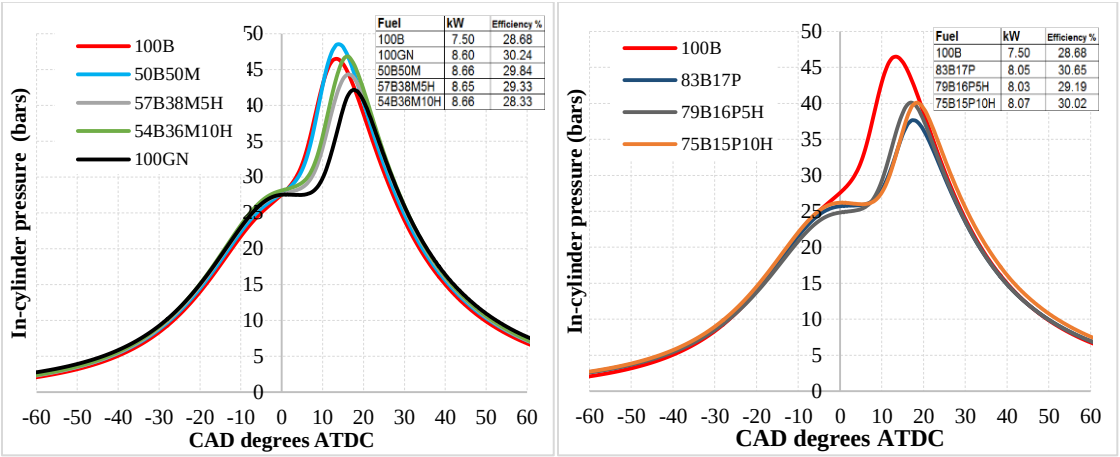

Figure 2 In-cylinder pressure versus CAD to maximum output power, ST for optimum efficiency, knock peak pressure under 0.5 bars and COV IMEP under 4% to 200 cycles.

Figure 3 shows the heat release rate versus crank angle degrees for the blends studied. The blends that show the earliest increase in heat release rate are 100B, 50B50M, 54B36M10H because of the early ST used. The blend 50B50M has a location to the peak heat release rate close to 10 degrees ATDC. The blends 50B50M, 57B38M5H and 54B36M10H achieved the highest output power, close to 8.7 kW, due to the high knock resistance and favorable energy density. The blends 83B17P, 79B16P5H and 75B15P10H, used a late ST, resulting in a later initiation of heat release rate. These blends achieved maximum output power of approximately 8 kW, limited by the knocking threshold. The greatest generating efficiency (30.65%) is achieved with the blend 83B17P, but this blend did not achieved the highest output power because of the high knocking tendency. The fuel 100NG reached 8.60 kW since CO_2 was not present. This fuel achieved a high generating efficiency (30.24%) with a late ST to avoid knocking. The blends that achieved the highest heat release rates are 50B50M, 54B36M10H and 100NG. Blend 50B50M achieved the highest heat release rate with a peak heat release rate location close to 10 degrees ATDC.

The lowest heat release rate resulted from blends 100B, 83B17P and 79B16P5H. For these blends, the maximum output power values were less than 8.1 kW, to 100B the reason was the low energy density, while for the blends 79B16P5H and 83B17P the reason was high knocking tendency, the peak of heat release rate is located close to 15 degrees ATDC.

Figure 4 presents generating efficiency versus ST; red dots indicate the tests whit a knock peak pressure bigger than 0.5 bar, indicating that there is a slight autoignition of the end gas. Blue dots identify tests when the knock peak pressure was lower than 0.5 bar, indicating knock free operation close to the knocking threshold. Blends like 100B and 50B50M used an advanced ST with knocking free operation, allowing more optimal combustion phasing. When ST is advanced, knock tendency is increased the average combustion pressure is higher. Blends like 100NG, 83B17P and 75B15P10H have high laminar flame speed and high flame front speed. These blends despite having a small advance ST burn rapidly and are able to achieve high output power. However, these blends, except natural gas, have high knock tendency evidenced by low MN because of their chemical composition [28]. Small advance ST decreases the knocking possibilitys. However, combustion phasing is not optimal because of the increase of pressure due to combustion, occurs later in the expansion stroke, decreasing the average combustion pressure. Tests were conducted looking for a balance between combustion phasing, low cyclic variations, and being close to the knocking threshold. For all the blends the generating efficiency was the highest at this point. The blends 100GN, 83B17P and 75B15P10H for a ST of 5 CAD degrees BTDC had knock peak pressure values higher of 0.5 bar, indicating that these three blends are more prone to knock, which is consistent with previous MN tests [28].

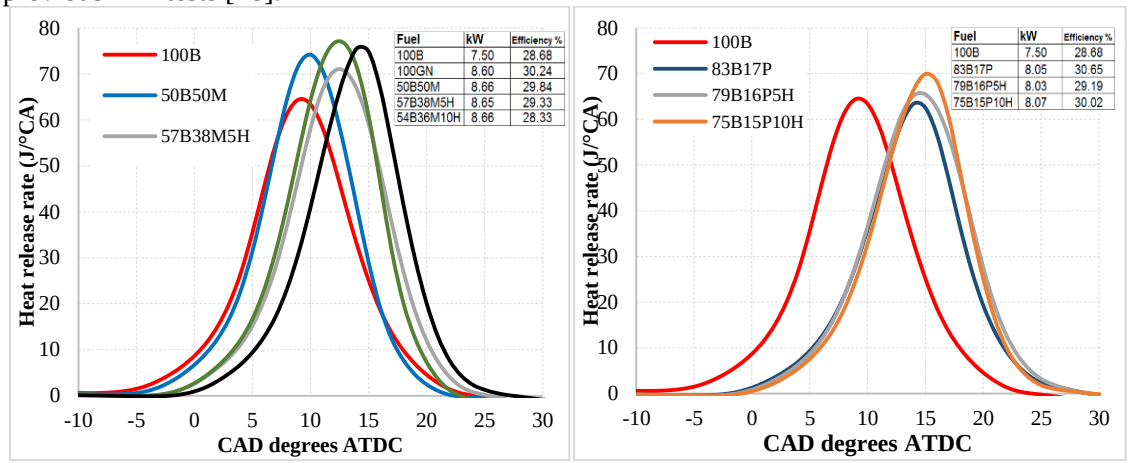

Figure 3 Heat release rate versus CAD to maximum output power achieved for each blend, ST for optimum generating efficiency, knock peak pressure under 0.5 bars and COV IMEP under 4%.

Figure 5 shows a summary of results for generating efficiency and maximum output power. In almost all cases the blends that have achieved greater output power have higher generating efficiency. 50B50M provides a balance between knocking resistance and energy density, allowing this blend to achieve high output power with optimal combustion phasing, achieving high generating efficiency. The blends 57B38M5H and 54B36M10H are blends with similar energy density to 50B50M, but have lower knocking resistance because of the presence of hydrogen. These blends are more prone to knock, requiring a late ST adjustment, decreasing the average combustion pressure and resulting in lower generating efficiency. The blends 83B17P, 75B15P10H and 79B16P5H have low MN, close to 65, biogas with propane additions, between 15-17%, resulting in blends with higher energy density (between 3.64 MJ/m^3 and 3.77 MJ/m^3) than the blend 50B50M. But due to high knock tendency a late ST is required, resulting in a lag in combustion phasing, reducing the average combustion pressure and the generating efficiency. The 100B had acceptable generating efficiency (28.7%) for 7.5 kW of output power, a reduction of 6.25% compared to the original engine operating in diesel mode. This is a good result bearing in mind that it is an alternative fuel with low energy density.

Figure 6 shows the calculated results for specific fuel consumption (SFC). The SFC is calculated from fuel consumption, lower heating value of the blend, and output power. The SFC is a measure of how efficiently an engine uses fuel energy to produce work. Operation with 100NG has the lowest SFC, because there is no diluent (CO_2) in the fuel. The SFC is increased by diluent in the fuel. The blend 50B50M has the lowest SFC to the blends with biogas. The blends 57B38M5H and 54B36M10H have a small increase in SFC. The blends 83B17P, 75B15P10H and 79B16P5H have slightly higher SFC. Biogas has the lowest energy density, resulting in the highest SFC. The blend 50B50M has a critical CR of 16.9:1, as measured on a CFR engine [28]. This is higher than the CR (15.5:1) used in this research, which allows optimal combustion phasing, leading to higher average combustion pressures. Figure 6 also shows the exhaust temperatures measurements, which are taken just downstream of the exhaust valves. The blend 100B has the lowest exhaust temperature, due to the high percentage of CO_2; 100NG has the highest exhaust temperature. The blends 83B17P, 75B15P10H and 79B16P5H, compared to blends 50B50M, 54B36M10H and 57B38M5H, have higher exhaust temperature due to higher adiabatic flame temperature of propane compared with methane.

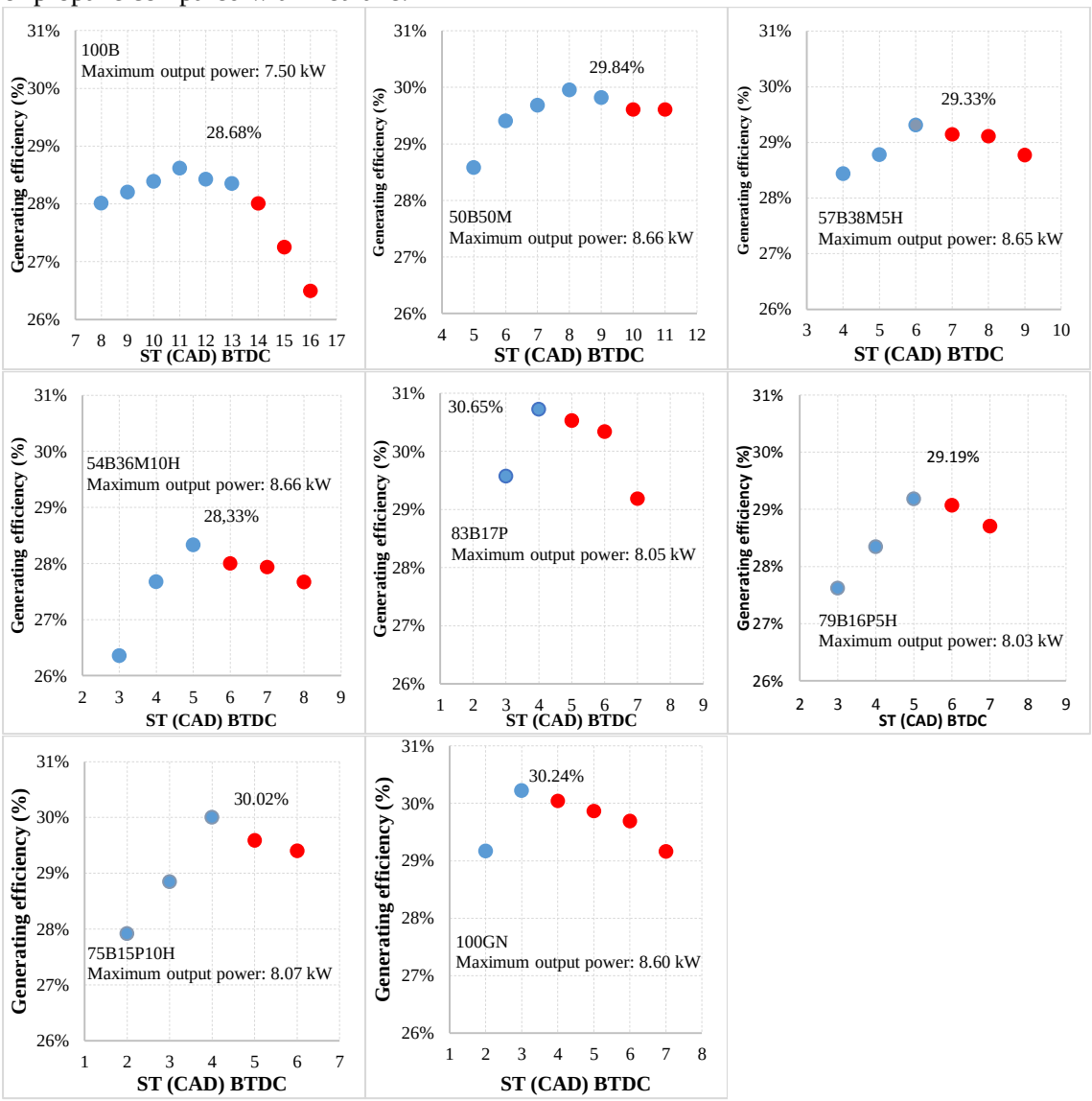

Figure 4 Generating efficiency versus ST, knock peak pressure for 200 consecutive cycles: Red dots bigger than 0.5 bars and blue dots lower than 0.5 bars.

In-cylinder peak pressure during combustion in a SI engine, depends on several factors: Output power, fuel energy, mixture mass, admission pressure, ST, equivalence ratio and throttle valve % open values. Figure 7 shows the average peak pressure in expansion stroke. The blends 50B50M, 54B36M10H and 57B38M5H reached higher output power and therefore higher in-cylinder peak pressures are obtained. The blends 83B17P, 75B15P10H and 79B16P5H require on average 5.6% less air mass than the blend 50B50M, so the cylinder pressure is lower at intake port closure and, consequently, pressures are lower during compression and expansion strokes. Blends than had optimal combustion phasing for generating efficiency were 100B, 50B50M and 57M38M5H, resulting in peak pressure location between 12 and 17 degrees ATDC. For the blends 83B17P, 79B16P5H and 75B15P10H a later ST is required to avoid knocking, resulting in lower peak pressure values and locations greater than 17 degrees ATDC. The blend 50B50M reached the highest peak pressure due to high output power, energy density, optimal combustion phasing, throttle valve % open values, and high knock resistance. Figure 8 also presents the results of the peak pressure location in the expansion stroke. This depends of the ST, in-cylinder pressure at the moment of flame front development, turbulence intensity and flame speed.

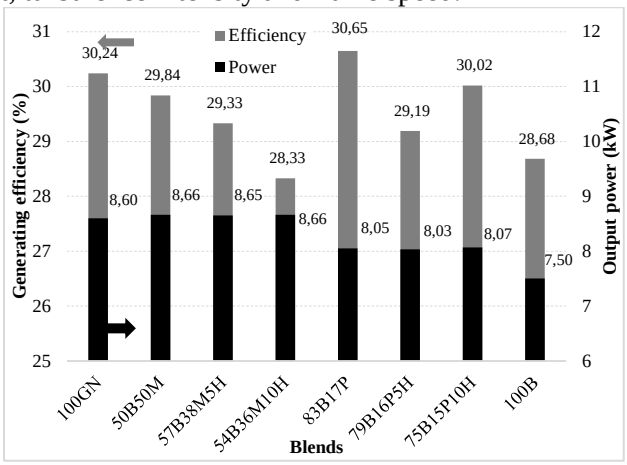

Figure 5 Summary results for generating efficiency and maximum output power.

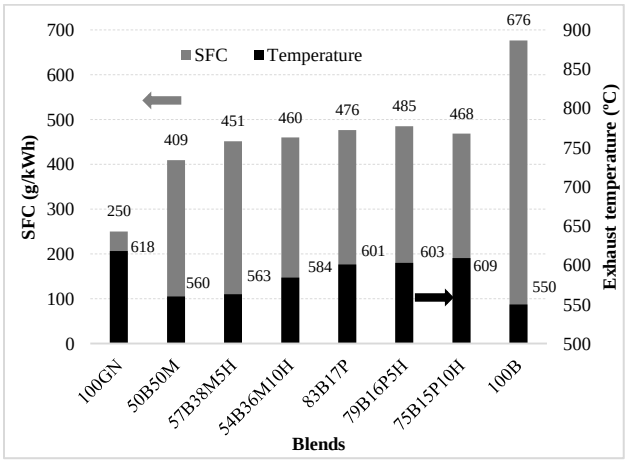

Figure 6 Specific fuel consumption and exhaust temperature

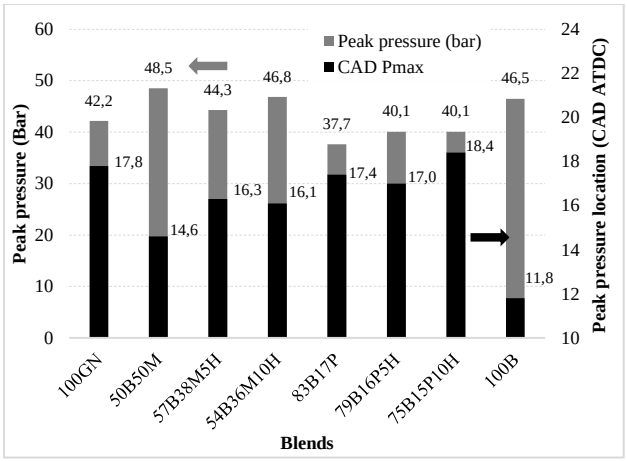

Figure 7 Value and location of peak pressure

Figure 8 shows the 0 to 5% mass fraction burn duration. This period is calculated as the difference between the 5% mass fraction burned location and ST. This parameter can be viewed as the ignition delay time to 0-5% burn duration, values are similar for all blends, between 5.7-6.9 degrees. Figure 8 also shows the 0-50% mass fraction burned duration results. The 100B fuel has the largest 0-50% burn duration. This is due to lower flame speed resulting from high diluent and no higher hydrocarbon species. The 100NG fuel, despite having high flame speed and energy density, has a larger 0-50% burn duration than blend 50B50M, this is because 100NG has a small advance ST. The blends 57B38M5H and 54B36M10H have longer 0-50% burn durations than 50B50M, because these blends require a small advance ST to avoid knocking, resulting in much of the combustion process occurring during the expansion stroke. The blends 83B17P, 79B16P5H and 75B15P10H require a small advance ST to avoid knocking, resulting in a greater displacement of the peak pressure and the longest 0-50% burn durations.

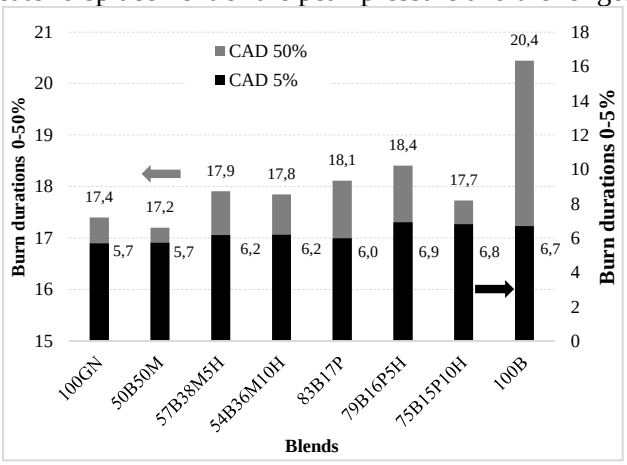

Figure 8 Mass fraction burned durations 0-5% and 0-50%

Figure 9 shows 0-90% and 5-90% mass fraction burn durations. The trends for these two parameters are similar. The 5-90% mass fraction burn duration can be viewed as the combustion duration. Natural gas requires the lowest combustion duration due to the high flame speed and energy density. The blend 50B50M has larger combustion duration than 100GN, because the 50B50M has lower flame speed and energy density. The blends 57B38M5H and 54B36M10H have slightly lower combustion durations than blend 50B50M due to the presence of hydrogen. The blends 83B17P, 79B16P5H and 75B15P10H have lower combustion durations than the blends 50B50M, 57B38M5H and 54B36M10H, because these blends have a higher flame speed and energy density. The fuel 100B had the longest combustion duration because of the lowest energy density and flame speed. In general, the engine used in this research had lower combustion durations than conventional engines because of the high compression ratio.

The global indicated mean effective pressure (IMEPg) is one of the most important parameters to assess the performance of internal combustion engines, because is not dependent on engine size. The IMEPg is proportional to the product of the volumetric efficiency, the air-fuel ratio and combustion efficiency. The IMEPg also depends on the amount of mixture inducted, energy density and equivalence ratio. Figure 10 shows IMEPg for the tests. The IMEPg values are proportional to output power values presented earlier. The blends 83B17P, 79B16P5H and 75B15P10H require lower throttle valve % open values, leading a lower cylinder pressure at intake valve closing. In addition, these blends have lower output power than the blends 50B50M, 54B36M10H and 57B38M5H, leading to lower IMEPg. The blends 50B50M and 54B36M10H have the highest IMEPg. These two blends reached high output powers and have high throttle valve % open values, leading to higher cylinder pressure at intake valve closing.

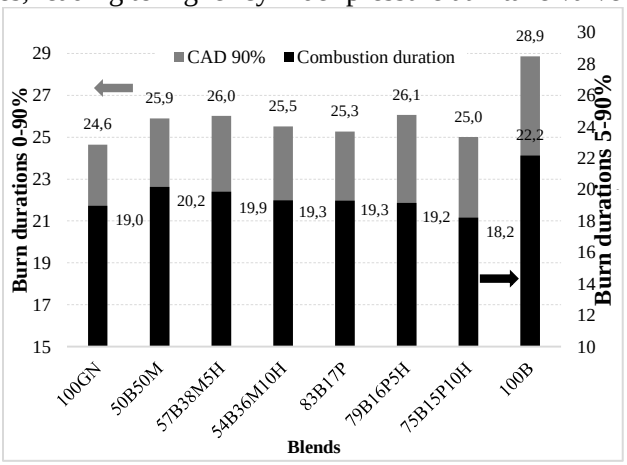

Figure 9 Mass fraction burned durations 0-90% and 5-90% (combustion duration)

Engine operating parameters are directly related to the pollutants emissions. A high CR has been used to produce high generating efficiency, but high levels of NOx are expected due to the high flame temperatures. Similarly, when operating the engine with stoichiometric mixtures the flame temperature reaches its highest values and NOx emissions are high, while lean mixtures result in low NOx emissions accompanied by lower output power. Operating the engine with rich mixtures decreases output power due to poor availability of oxygen and CH_4 and CO emissions increase. An equivalence ratio of 0.9 was used for this research, where the flame temperature is lower than the maximum, there is sufficient availability of oxygen for complete combustion and SFC is low [10,26]. Figure 11 shows the specific emissions of carbon monoxide (CO). The data is presented as specific emissions, which is normalized to account for differences in output power. CO provides a measure of combustion efficiency, where low CO indicates high combustion efficiency and high CO indicates low combustion efficiency. Low CO emissions for fuel 100NG are most likely due to low quenching distance, high flame speed and high flame temperature. For the blend 100B, CO emissions are the highest, likely due to the low flame speed, the low flame temperature and the high percentage of CO_2, which increases the quenching distance. The blend 50B50M has lower CO emissions than the other blends. The blends 50B50M, 54B36M10H and 57B38M5H have lower CO emissions than the blends 83B17P, 75B15P10H and 79B16P5H.

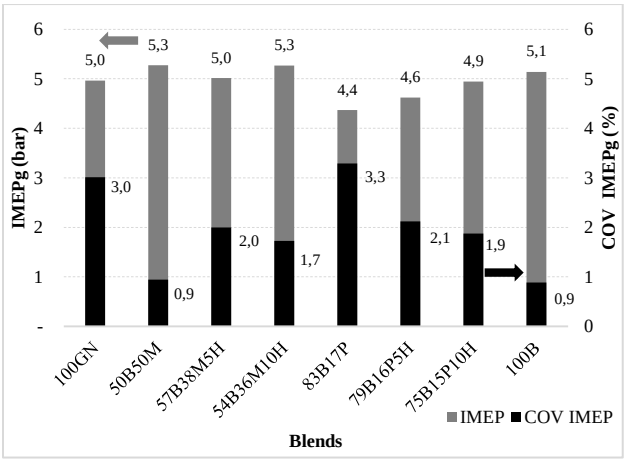

Figure 10 IMEP and COV IMEP.

Figure 11 also presents the specific NOx emissions. NOx emissions are higher when the flame temperature of the fuel is high and when the equivalence ratio is close to 1 due to high combustion temperatures [26]. The fuel 100NG produces the highest level of specific NOx emissions due to the high flame temperature, favoring the formation of NOx. However, the NOx levels for the blends are relatively close, between 6.9-7.8 g/kWh. Among the fuel blends 50B50M had highest NOx value because of the average combustion pressure is greater by the maximum output power, which increases the flame temperature, favoring the NOx formation.

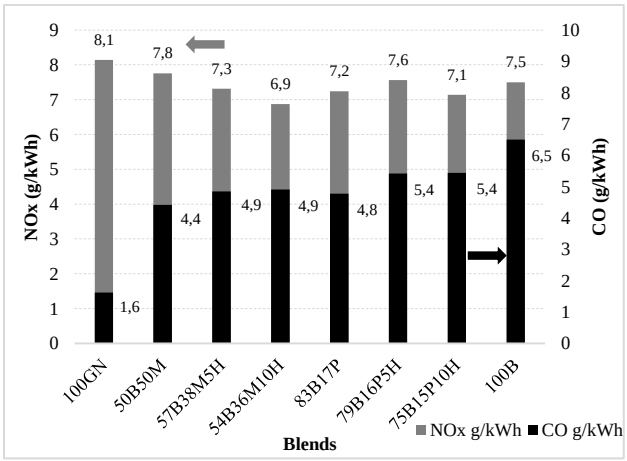

Figure 11 Specific NOx and CO emissions.

5.3.4. Conclusions

Different strategies were implemented to improve generating efficiency of a SI engine compared with the original diesel engine operation. The strategies used were: Transforming a diesel engine with high CR to a SI engine, using biogas as main fuel to increase knocking resistance of the blends, blending biogas with natural gas or propane plus hydrogen addition, using ST for optimum generating efficiency close to the knocking threshold, operating the engine with a lean equivalence ratio and injecting the blends at a pressure of 2 bars to increase the output power. Fuel blends were evaluated while maintaining a 200 cycle average knock peak pressure in the range between 0.3 and 0.5 bar and COV IMEP lower than 4%.

The main observations and conclusions from the test results are the following:

- The best performing blends was 50B50M. This blend is equivalent to a renewable fuel, purified biogas with a chemical composition 80% CH_4 and 20% CO_2. This blend has a good balance between high knocking resistance and energy density.
- The 50B50M blend had the highest output power (8.66 kW), 8.25% higher than 100% diesel fuel operation (8kW @ 1800rpm). The 100B blend reached a power of 7.5 kW, which represents a derating of 6.25% compared with diesel operation.

- After the 50B50M, the blends with the highest output power and generating efficiency were 57B38M5H and 54B36M10H. The fuel 100B had the lowest energy density and resulted in the highest SFC.
- For each output power and blend the engine required a ST adjustment to a correct combustion phasing. The optimum ST is close to the knocking threshold, which lead to the maximum generating efficiency. Correct combustion phasing resulted in a peak pressure location in the range 12-17 CAD degrees ATDC and peak heat release rate close to 10 degrees ATDC.
- The blend 50B50M produced lower CO emissions than the other blends, but had high values of NOx because of the higher average combustion pressure and temperature.

References

1. Patel S., Tonjes D. and Mahajan D., Biogas potential on Long Island, New York: A quantification study. Journal of Renewable Sustainable Energy 3, 043118, 2011.
2. Bond T. and Templeton M.R. History and future of domestic biogas plants in the developing world. Energy for Sustainable Development, 2011. 15(4): p. 347-354.
3. Porpatham E., Ramesh A. and Nagalingam B. Investigation on the effect of concentration of methane in biogas when used as a fuel for a spark ignition engine. Fuel, 2008. 87(8–9): p. 1651-1659.
4. Arroyo J. *et al*. Efficiency and emissions of a spark ignition engine fueled with synthetic gases obtained from catalytic decomposition of biogas. International Journal of Hydrogen Energy, 2013. 38(9): p. 3784-3792.
5. Huang J. and Crookes R.J. Assessment of simulated biogas as a fuel for the spark ignition engine. Fuel, 1998. 77(15): p. 1793.
6. Kyungtaek L. *et al*. Generating efficiency and NOx emissions of a gas engine generator fueled with a biogas–hydrogen blend and using an exhaust gas recirculation system. International Journal of Hydrogen Energy, 2010. 35(11): p. 5723-5730.
7. Porpatham, E., Ramesh A. and Nagalingam B. Effect of hydrogen addition on the performance of a biogas fuelled spark ignition engine. International Journal of Hydrogen Energy, 2007. 32(12): p. 2057-2065.
8. Malenshek M. and Olsen D.B., Methane number testing of alternative gaseous fuels. Fuel, 2009. 88(4): p. 650-656.
9. Zhen X. et al. The engine knock analysis – An overview. Applied Energy, 2012. 92(0): p. 628-636.
10. Heywood J.B., Internal Combustion Engines Fundamentals, ed. M.G. Hill. 1988.
11. Morley D.B. *et al.* Autoignition in Spark-Ignition Engines. Comprehensive Chemical Kinetics. Volume 35, 1997, Pages 661.
12. Heywood J.B. and TAGALIAN J. Flame Initiation in a Spark-Ignition Engine. Combustion and flame 64:243-246, 1986.
13. Karim G.A. The onset of knock in gas fueled spark ignition engines prediction and experiment. Journal of Powertrain and Transport, Vol.14, No. 4, 2007.
14. Schiffgens H.J. *et al*. Concepts for the adaptation of SI gas engines to changing methane number journal of engineering for gas turbines and power. october 1994, Vol. 116.
15. Porpatham E., Ramesh A. and Nagalingam B. Effect of compression ratio on the performance and combustion of a biogas fuelled spark ignition engine. Fuel, 2012. 95(0): p. 247-256.
16. Porpatham E., Ramesh A. and Nagalingam B. Effect of swirl on the performance and combustion of a biogas fuelled spark ignition engine. Energy Conversion and Management, 2013. 76(0): p. 463-471.
17. Bell S.R. and Rathnam S. Fuel composition effects on emissions from a spark-ignited engine operated on simulated biogases, Transactions of the ASME, Vol. 123, January 2001.
18. Xin Z. *et al*. The experimental study on cyclic variation in a spark ignited engine fueled with biogas and hydrogen blends. International. Journal of Hydrogen Energy, 2013. 38(25): p. 11164-11168.
19. Chulyoung J. *et al*. Generating efficiency and emissions of a spark-ignition gas engine generator fuelled with biogas–hydrogen blends. International Journal of Hydrogen Energy, 2009. 34(23): p. 9620-9627.
20. Rakopoulos C.D. and Michos C.N. Generation of combustion irreversibilities in a spark ignition engine under biogas–hydrogen mixtures fueling. International Journal of Hydrogen Energy, 2009. 34(10): p. 4422-4437.
21. Chandra R. *et al*. Performance evaluation of a constant speed IC engine on CNG, methane enriched biogas and biogas. Applied Energy. 2011. 88(11): p. 3969-3977.
22. Carrera J.R. *et al*. Numerical study on the combustion process of a biogas spark-ignition engine. Thermal Science, 2013. 17(1).
23. Cheolwoong P. *et al*. Performance and emission characteristics of a SI engine fueled by low calorific biogas blended with hydrogen. International Journal of Hydrogen Energy, 2011. 36(16): p. 10080-10088.
24. Gómez Montoya J.P. Amell A., Zapata J., Experimental study of spark ignition engine performance and emissions in a high compression ratio engine using biogas and methane mixtures without knock occurrence. Thermal Science: year 2015, vol. 19, no. 6, pp. 1919-1930. DOI 10.2298/TSCI140829119G, 2015.
25. Yu X. *et al*. Optimize combustion of compressed natural gas engine by improving in-cylinder flows. International Journal of Automotive Technology. 2013
26. Korakianitis T., Namasivayam A.M. and Crookes R.J. Natural-gas fueled spark-ignition (SI) and compression-ignition (CI) engine performance and emissions. Progress in Energy and Combustion Science, 2011. 37(1): p. 89-112.
27. Atkins R. An introduction to engine testing and development. Book from SAE International. ISBN 978-0-7680-2099-1. P. 188.
28. Gomez Montoya J.P., Amell A. and Olsen D.B. Prediction and measurement of the critical compression ratio and methane number for blends of biogas with methane, propane and hydrogen. Fuel 186 (2016) 168–175.

5.4 Determination of the optimal operational conditions of a SI engine with high CR.

Abstract

This study attempts to find various ideal operating conditions for a low-power diesel engine, converted to SI with high compression ratio, under stable combustion conditions, high generating efficiency and low pollutant gas emissions without output power derating. The main fuel for the engine is biogas, which is blended with natural gas or propane and hydrogen and two equivalence ratios. The maximum output power measurements are recorded just below the knocking threshold, where the output power and generating efficiency are the highest possible. The lean combustion operation increased the knocking tendency because the throttle valve % opening is higher than when it is close to stoichiometric operation, increasing the air mass flow, decreasing the admission pressure drop, and leading to a higher pressure at the end of the compression stroke, this is different from the conventional tendency studied in SI engines. Therefore, the output power should be decreased to permit operation below the knocking threshold; the combustion quality drops rapidly when the operation is above the knocking threshold. Purified biogas (80% CH_4 and 20% CO_2) with an equivalence ratio of 0.85 achieved the highest output power and generating efficiency, which was even higher than with the original diesel operation; this renewable fuel exhibits an ideal balance between knock resistance, low heating value, flame speed and energy density, resulting in optimal engine performance.

5.4.1 Introduction

The low utilization of biogas for power generation in internal combustion engines is related to the problems that biogas presents for productive use, such as the low heating value or low energy density and low Wobbe index compared with natural gas, gasoline and diesel. In addition, biogas has low flame speed, the presence of sulfur and a high amount of inert gases, which reduces combustion stability and the capacity to produce work. Research and technological developments of internal combustion engines exclusive to use with gaseous renewable fuels are underway to find solutions to problems related to combustion stability during operation, pollutant emissions reduction, and the power derating compared to conventional fuel operation [1-5]. A technological trajectory that can be viable in the range of medium and low power is the use of a diesel engine in spark ignition (SI) mode. A diesel engine is able to operate with a high compression ratio (CR), resulting in high generating efficiency and thereby mitigating some of the negative effects of biogas engine operation [6, 7]. Moreover, to improve the properties of combustion, such as the minimum ignition energy, ignition limits, laminar burning velocity, low heating value or knocking resistance, alternative fuels can be blended with conventional fuels, such as compressed natural gas (CNG) or liquefied petroleum gas (LPG). Additionally, hydrogen can be used to increase the flame speed of biogas blends. These desired blends must be characterized regarding knocking resistance and maximum CR to select an engine and obtain the best possible generating efficiency.

The methane number (MN) and critical compression ratio (CCR) are valuable tools for the diagnosis of alternative fuels and can help in selecting the optimal engine operating conditions. Thermal efficiency in internal combustion engines is fundamentally dependent on the CR. An engine should be operated at the highest possible CR to achieve the highest possible efficiency without the risk of knocking or degradation of mechanical efficiency. The chemical compositions of alternative fuels depend on how they are produced. The chemical composition of a gaseous fuel determines the MN and CCR. However, it is not yet clear what specific engines to these fuels should be used to obtain the best possible thermal efficiencies. For biogas, it is reported that the MN is between 130 and 140, indicating that an engine operating on biogas can work at higher CRs [8]. The mixture of biogas with methane (CH_4) or propane (C_3H_8) and the addition of H_2 results in fuels with higher energy density, higher adiabatic flame temperature, faster flame speed, greater capacity to produce engine power and higher thermal efficiency. These mixtures also reduce the MN of the resultant blend, and thus the knock tendency is greater because the autoignition temperature is decreased [3, 9-13]. The knock limit is defined with regard to the equivalence ratio as the threshold at which knocking starts under specific operating conditions. In SI engine operation, when operating from lean to stoichiometric, the equivalence ratio that initiates knocking

is determined. Using a high CR may result in narrow operating margins, where the engine can exhibit serious problems by the knocking [11, 12].
Significant improvements in generating efficiency are achieved due to output power increases. Gaseous fuels are appropriate for applications with high CR values beyond those typically used for liquid fuels. The improvement in combustion stability associated with the addition of hydrogen allows operation with leaner mixtures or higher EGR rates, which reduce NOx emissions. However, the knock tendency is significantly increased with high hydrogen content. Additionally, the presence of nitrogen (N_2) or carbon dioxide (CO_2), which are diluents, reduces the knock tendency of the resulting blend. SI engine operation with lean mixtures is typically more efficient than operation with stoichiometric mixtures for the same output power level. However, extremely lean mixtures lead to power derating and reduced efficiency due to increases in cyclic variation and CO and HC emissions [15]. The most compelling reason to operate an SI engine with a lean fuel-air mixture is that low pollutant emissions can be achieved with no aftertreatment. When the mixture is rich, there is not enough oxygen to complete combustion, and the emission of CO is high. Lean combustion operation results in low CO and THC emissions up to the lean limit, beyond which CO and THC increase. This phenomenon depends on the fuel. For light hydrocarbons near the equivalence ratio of 0.7, there is a significant increase in the THC concentrations due to misfire, which also leads to a decrease in thermal efficiency [16]. NOx emissions are present in the combustion products due to reactions between nitrogen and oxygen. Although NOx contains NO and NO_2, in SI engines, NO concentration is greater than NO_2. NOx is higher when the equivalence ratio is close to 1, where the greatest flame temperatures are realized. Rich and lean mixtures tend to decrease NOx emissions significantly. The availability of O_2 also limits the formation of NOx, which is one reason NOx emissions are low for rich mixtures [16].
The lean mixture limit depends on the fuel chemical composition and engine specifications; for lean operation, the cycle variability leads to, in some cycles, the mixture being too lean to be ignited. The flame propagation limit is occurs when the flame front cannot consume the air-fuel mixture before it is extinguished. During the expansion stroke, the mixture ahead of the flame front is cooled, leading to a low flame speed. If the pressure and temperature drop quickly, it is possible for the flame to be extinguished, which is referred to as the partial combustion [17]. Several techniques can be used to extend the lean limit, such as improving fuel-air mixing, increasing the CR, increasing the spark ignition energy, adding fuels with higher flame speeds and increasing the turbulence intensity during combustion [17].
The purpose of this research is to determine the optimal operating conditions of a diesel engine converted to SI under stable combustion, high generating efficiency and low emissions, without power derating, using biogas blended with natural gas or propane and hydrogen. These blends have Wobbe indexes and energy densities similar to those of purified biogas of 80% CH_4 and 20% CO_2. The combustion stability is defined with COV IMEP lower than 4% on average for 200 consecutive cycles, and the knock peak pressure cannot be higher than 0.5 bar on average for 200 cycles. Knocking threshold is maintained in the range between 0.3-0.5 bar to maximize output power and generating efficiency. Engine operation close to the knocking threshold result in high generation efficiency. The optimal blend and equivalence ratio are determined in this research.

5.4.2. Experimental setup and general procedure for testing

The crank angle was measured using an angular encoder, Kistler 2614B4, with a resolution of 0.1 crank angle degrees (CAD). A Kistler measurement system designated as “KiBox To Go” type 2893A was designed specifically to measure and analyze the combustion in real-time for internal combustion engines. KiBox uses a zero-dimensional thermodynamic model based on energy conservation; it was used because of its simplicity, its lower time consumption for the program execution, and its relatively accurate results. The zero-dimensional model provided a satisfactory combustion heat analysis, which determined the main thermodynamic parameters, and the engine characteristics could be set easily. Using piezoelectric pressure sensors while the engine was running, calculations for the thermodynamic zero point correction and thermodynamic loss angle were performed. The calculation of the heat release was performed without taking into account the wall heat losses and with a constant polytropic exponent, which could change according to the fuel used. The combustion analysis system used the Siemens-VDO algorithm for the

calculation of knocking values. The measurements of combustion chamber pressure, intake pressure and crank angle allowed a detailed analysis of the combustion process in the Lister Petter TR2 engine. The measurements of knock peak pressure, IMEP, cyclic variations (COV IMEP), peak pressure, engine speed, combustion duration, and heat release rate were performed simultaneously from during each cycle. Figure 5.2.2 shows the experimental setup of the test cell.

The fuel and blends used in this research include natural gas, biogas, and six blends of biogas with methane or propane and hydrogen additions. The biogas used was a 60% natural gas and 40% CO_2 blend, and the natural gas composition was 94.8% CH_4, 1.3% N_2, 2.3% C_2H_6, 1.1% C_3H_8 and 0.5% CO_2 by volume. In each case, the output power was the maximum possible, as the ST of each blend was adjusted for optimum generating efficiency without knocking. The MNs of the blends were tested previously [13], and the MN of the natural gas was estimated using the software Methane 3.1 from AVL. Table 2 presents various blend properties. The following analysis of estimated properties may support some of the analysis results. 1. The addition of 5% to 10% hydrogen to blends of biogas with methane and biogas with propane, although the hydrogen has a high specific heat ratio, does not significantly change the specific heat ratio of the blends; thus, the effect over the end gas temperature is expected not to have significant effects. 2. The addition of hydrogen reduces the stoichiometric air fuel ratio of the blends. 3. The energy density is similar for all blends except biogas and natural gas.

Table 2 Blend properties and throttle valve % opening

Fuel Designation	Fuel composition	Fuel properties				Throttle (ETVO)		Stoichiometric Air fuel ratio (kg air/kg blend)	Specific heat ratio to the mixture at 1 bar and 25 °C.
		LHV MJ/m3 fuel	LWI MJ/m3 fuel	Energy density MJ/m3 air	Methane number	Equiv. ratio 0.9	Equiv. ratio 0.6		
100NG	100% Natural gas	34.55	45.13	3.58	87.2	61.7	76.7	16.,5	1.3851
100B	100% Biogas	20.35	20.99	3.44	140.0	75.0	91.7	6.08	1.3844
50B50M	50% Biogas + 50% Methane	27.14	**31.40**	**3.57**	120.0	66.7	85.0	10.19	1.3877
57B38M5H	57% Biogas + 38% Methane +5% Hydrogen	25.00	29.01	3.58	105.3	63.3	80.0	9.32	1.3872
54B36M10H	54% Biogas + 36% Methane +10% Hydrogen	24.22	28.80	3.59	96.5	60.0	78.3	9.45	1.3874
83B17P	83% Biogas + 17% Propane	31.98	31.38	3.64	65.8	58.3	75.0	8.45	1.3834
79B16P5H	79% Biogas + 16% Propane +5% Hydrogen	30.89	31.04	3.65	65.2	56.7	73.3	8.56	1.3834
75B15P10H	75% Biogas + 15% Propane +10% Hydrogen	30.71	30.71	3.77	63.8	55.0	71.7	8.64	1.3835

In the first part of the tests for each blend, the tests were performed with two equivalence ratios: the first was 0.9, selected because it is close to the stoichiometry but has enough oxygen to be close to complete combustion; and the second was 0.7, selected to reduce emissions of NOx and CO. In the second part of the tests, for blend 50B50M, five tests were conducted with different equivalence ratios with the intention of finding the best equivalence ratio for this blend and determining the effect of the throttle valve % open value on knocking. Table 2 shows the blend properties and throttle valve % opening. In this case, the maximum output power was limited not by the throttle valve % open but by the knock threshold and the cyclic variation. Knocking measurement was conducted using the instantaneous pressure curve taken with

a piezoelectric pressure sensor and was then filtered with a smoothed average pressure curve; peak pressures were measured in each cycle, and the maximum peak pressure was the knock value of that cycle, which was then averaged over 200 consecutive cycles [18]. Cyclic variability is an important measure of the internal combustion engine's operation stability, measured with COV IMEP. Maximum output power was then measured with stable combustion and knock-free operation.

Table 3 Additional blend properties

Fuel Designation	Laminar flame speed (cm/s) at 35 bar and 850K.		Ignition delay time (s) at 35 bar and 850K.		Quenching distance (mm) at 35 bar and 850K.		Minimum Ignition Energy (mJ) at 35 bar and 850K.	
	Equivalence ratio: 0.7	Equivalence ratio: 0.9	Equivalence ratio: 0.7	Equivalence ratio: 0.9	Equivalence ratio: 0.7	Equivalence ratio: 0.9	Equivalence ratio: 0.7	Equivalence ratio: 0.9
100NG	3.44	7.33	0.682	0.533	0.53	0.25	2.78	0.35
100B	2.16	4.36	0.952	0.743	0.91	0.46	11.63	1.79
50B50M	2.67	5.67	0.923	0.721	0.73	0.35	6.14	0.81
57B38M5H	2.66	5.65	0.916	0.715	0.75	0.36	6.53	0.88
54B36M10H	2.76	5.88	0.894	0.698	0.73	0.35	6.21	0.83
83B17P	3.28	6.97	0.586	0.457	0.57	0.27	3.06	0.40
79B16P5H	3.34	7.14	0.642	0.501	0.57	0.27	3.02	0.39
75B15P10H	3.41	7.26	0.687	0.537	0.57	0.27	2.99	0.40

Table 3 presents some additional blend properties, with the intention of supporting comparative analysis from tests and results. Laminar flame speed was calculated numerically using Chemkin with Grimech 3.0 reaction mechanism. Ignition delay time was also calculated using Chemkin with San Diego reaction mechanism. Quenching distance and minimum ignition energy were calculated using Lefevre model [21].

5.4.3. Experimental results

5.4.3.1 Engine operation comparison using two equivalence ratios.

Table 4 presents ST values adjusted for optimal generating efficiency. Figure 2 presents the test results for each blend with two equivalence ratios. Figure 2a shows the comparison of power derating by changing the equivalence ratio from 0.9 to 0.7. The blends 100B, 83B17P, 79B16P5H, and 75B15P10H have high-power derating as shown by the change in the equivalence ratio, with 100B having the highest power derating of approximately 38%. The blends 50B50M, 57B38M5H and 54B36M10H had output power on average, 7% lower, so even these blends exhibit higher output power than the original diesel engine operation (8 kW @ 1800 rpm). In general, the blends 50B50M, 57B38M5H and 54B36M10H obtained better results related with output power and generating efficiency than the blends 83B17P, 79B16P5H, and 75B15P10H because the former blends have higher MNs and better balance between knock resistance and density energy. The equivalence ratio changed from 0.9 to 0.7 for each test, force to reduce the output power and the generation efficiency because of knocking tendency is increased. This result, in turn, reduced the output power and adjusted the ST, thus avoiding being above the knocking threshold. Figure 2b presents the results for generating efficiency from the engine tests at maximum output power for each blend related to the change in the equivalence ratio; in general, the generating efficiency decreases with the increase of air in the mixture, and heat losses are increased due to the higher amounts of exhaust gasses. The generation efficiency also drops because the maximum output power should be decreased, and the ST should be adjusted to avoid knocking. For the equivalence ratio of 0.7, the blends 83B17P, 79B16P5H and 75B15P10H obtained higher generating efficiencies than the blends 50B50M, 57B38M5H, and 54B36M10H because the former have higher energy density and flame speed. However, due to these mixtures having lower MNs, the output power must be reduced to avoid knocking. According to the tests, the knocking resistance is a factor with greater impact than the energy density for achieving high output power, but a balance is required. Biogas has the highest MN but a low energy density.

Table 4 Spark timing adjusted for optimum generating efficiency

Blend	ST (°BTDC) Equiv. ratio: 0.9	ST (°BTDC) Equiv. ratio: 0.7
100GN	3	3
50B50M	8	7
57B38M5H	6	5
54B36M10H	6	5
83B17P	4	4
79B16P5H	5	4
75B15P10H	4	3
100B	12	10

Figure 3a shows the calculation results of specific fuel consumption (SFC) for this research; this figure has particularly vital importance because the output power is a response variable, measured in each case near the knock threshold. SFC is a measure of how efficiently an engine uses a fuel to produce work, regardless of the engine size. 100NG had the lowest values for SFC, because natural gas is a conventional fuel without the presence of inert gasses. The blend 50B50M has a good balance between reactivity and knocking resistance, yielding an ideal value of SFC, particularly for an alternative fuel. The blends 57B38M5H and 54B36M10H have an intermediate position for SFC. The blends 83B17P, 79B16P5H and 75B15P10H have an SFC that is slightly higher because these blends cannot achieve an output power higher than 8.1 kW with an equivalence ratio of 0.9 due to being limited by knocking. Biogas has the lowest energy density due to its high percentage of CO_2, resulting in the highest SFC. The increase of nitrogen in the air when the equivalence ratio changes from 0.9 to 0.7 increases the heat loss in exhaust gasses due to the higher gas quantity, and therefore, all of the blends have a higher SFC. Low equivalence ratios reduce turbulent flame speed; the burn rate is diminished because the quenching distance is increased. Furthermore, the CH_4 emissions are higher, and power losses are increased because of the unburned CH_4.

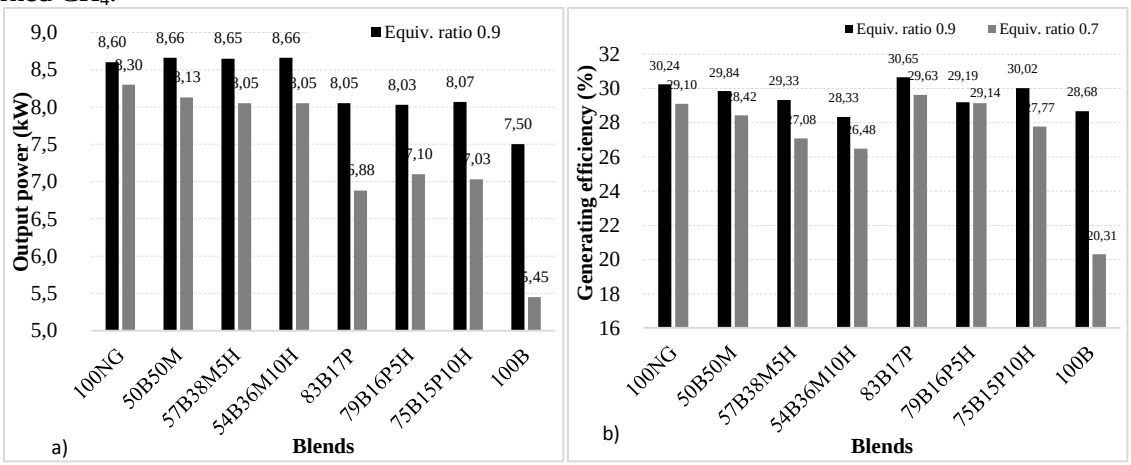

Figure 2 a) Maximum output power b) generating efficiency. Two equivalence ratios, ST adjusted for optimum efficiency, knock peak pressure lower than 0.5 bar, and a COV IMEP lower than 4%.

Figure 3b shows the combustion duration, measured in CAD degrees, between 5% and 90% of the mass burned. 100NG is the fuel with the lowest combustion duration; due to the high flame speed and high energy density, it required a lower mixture mass than the other blends to achieve maximum output power, and the combustion occurred at a higher mean pressure. The blend 50B50M has a slightly longer combustion duration than 100NG. Because 50B50M has lower flame speed and lower energy density, it requires greater fuel mass to reach the maximum output power than 100NG. 50B50M also has better combustion phasing than 100NG due to its high knocking resistance, allowing the heat release to occur at a higher pressure. The blends 57B38M5H and 54B36M10H require less time for combustion than 50B50M due to the presence of hydrogen, which increases flame speed and results in faster combustion;

this time may be smaller, but due to these two blends requiring an ST adjustment to avoid knocking to maximum output power, the combustion phasing is not ideal. The blends 83B17P, 79B16P5H, and 75B15P10H have shorter combustion durations than the blends 50B50M, 57B38M5H and 54B36M10H because these blends have higher flame speeds and higher energy density. 100B takes the longest time to burn fuel, despite having better combustion phasing, due to its low energy density and its low flame speed; additionally, the fuel mass must be greater due to its low heating value. Reducing the equivalence ratio increases the combustion duration because the flame speed is decreased by the increase in the amount of nitrogen in the mixture. According to the test results the blends 100B, 50B50M, and 57B38M5H have a CCR higher than the CR used in the Lister Petter engine (CR of 15.5:1). The other blends have a lower CCR than that used in the research. However CFR engine operation results in higher knocking tendency compared to the Lister Petter engine which speed is 1800 rpm. Thus, it is possible to operate the Lister Petter engine with the blends proposed, but a reduced ST is required in some cases to avoid knocking, which could result in non-ideal combustion phasing and the reduction of generating efficiency.

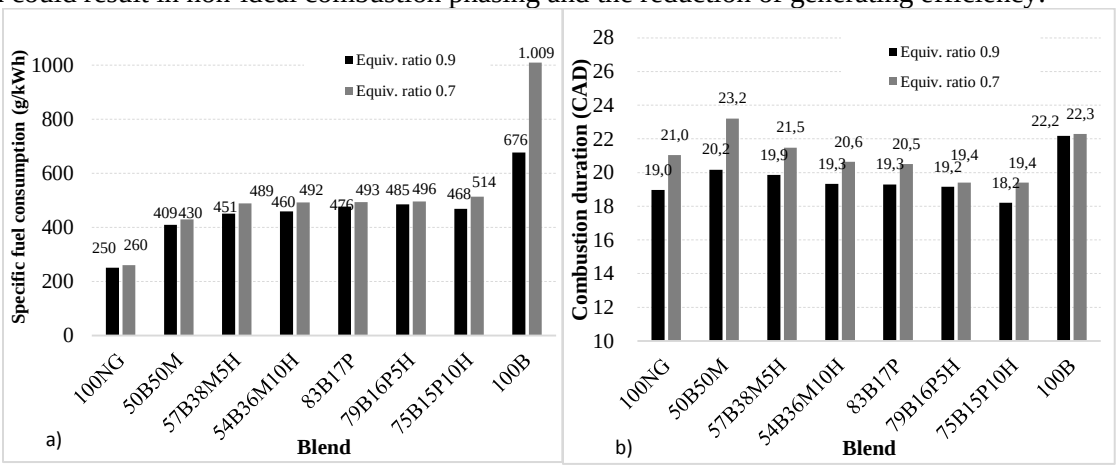

Figure 3 a) Specific fuel consumption b) combustion duration. ST adjusted for optimum efficiency, a knock peak pressure lower than 0.5 bar and a COV IMEP lower than 4% for 200 cycles.

IMEP is one of the most important parameters for evaluating the performance in internal combustion engines because IMEP does not depend on engine size; IMEP is work per cycle divided by the displaced volume. IMEP reflects the product of the volumetric efficiency (ability to inject air into the engine), the fuel-air ratio (effective use of air for combustion) and the conversion efficiency of fuel into energy. IMEP also depends on the fuel amount injected, intake pressure, low heating value and equivalence ratio. Figure 4a shows the results of IMEP calculation for the tests. The IMEP increases as the mixture becomes more lean because, when the mixture is leaner, a higher throttle valve % open is required; the upper air quantity is then admitted, yielding a higher mixture density in the inlet stroke and increased pressure at the end of the compression stroke. The blends 83B17P, 79B16P5H and 75B15P10H have higher energy density than the other blends and require a lower mixture mass, requiring a lower throttle valve % open and resulting in lower pressure at the intake, compression and expansion strokes. Moreover, these blends have lower output power, limited by knocking, than the blends 50B50M, 57B38M5H, and 54B36M10H with lower IMEP. 100NG has an intermediate position with respect to IMEP compared with the other blends because 100NG achieves higher output power and has the highest low heating value, which requires a lower mixture mass. A low throttle valve % open is required, leading to lower intake and compression pressures. The blends 54B36M10H and 50B50M have the highest values for IMEP, and these two blends obtain high output powers. They also require a high throttle valve % open, admitting a higher mixture mass, pressure and density at the intake stroke are higher.

Figure 4b shows the calculation results of COV IMEP; these values are not intended to indicate which blends have better cyclic variation, but COV IMEP serves as control data when recording the maximum output power. The maximum output power was recorded when the COV IMEP was lower than 4%. For each blend and equivalence ratio of this research the COV IMEP was lower than 4%, indicating good

combustion stability for the tests engine. In general, lean mixtures have higher IMEP COV values. The COV IMEP depends on the cycle-to-cycle differences in the masses of the air and fuel, amount of trapped burned gasses in the cylinder, engine speed, intake pressure, ST, knock intensity, turbulence intensity and equivalence ratio. The blends 50B50M and 100B have the lowest COV IMEP due to the correct combustion phasing, while the blends 100NG and 83B17P have the highest values for the COV IMEP because of the small ST used.

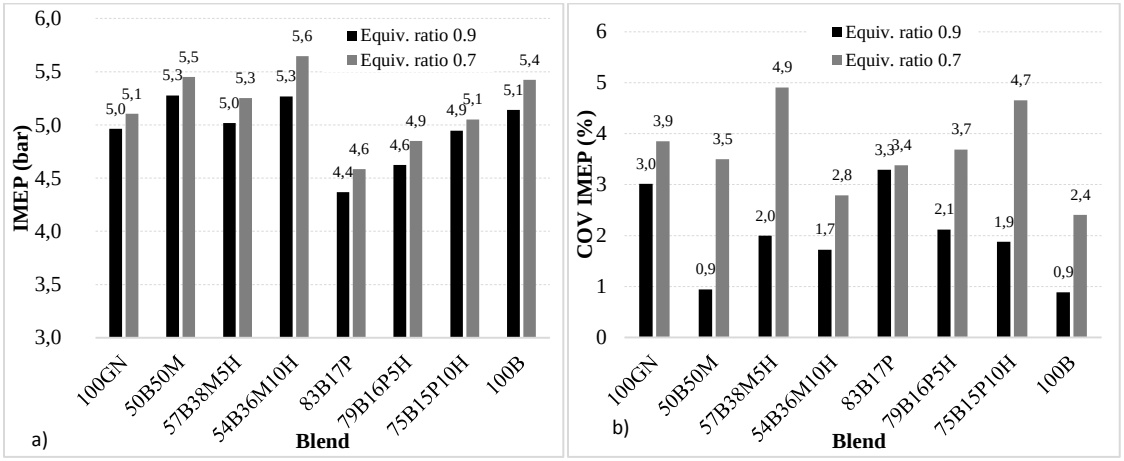

Figure 4 a) IMEP b) COV IMEP, with ST adjusted for optimum efficiency, knock peak pressure lower than 0.5 bar and COV IMEP lower than 4% for 200 cycles.

Figure 5a shows the CO specific emissions for the research blends; CO emissions measure the quality of combustion when a blend is burned under different engine operating conditions, including pressure, temperature and flame speed. The blend 100NG showed the lowest CO emissions. Because of a low quenching distance, the volume of gas near the walls that is quenched is small, reducing the mixture volume impacted by incomplete combustion. The high flame speed allows the fuel to burn faster, avoiding areas of incomplete combustion. High flame temperature increases the chemical kinetics of CO oxidation, reducing the amount of CO emission. For 100B, CO emissions are the highest due to the low flame speed, the low flame temperature and high percentage of CO_2, which increases the quenching distance. Near the lean combustion limit, CO emissions are increased due to the low combustion properties; the blends with high percentages of inert gas operating with an equivalence ratio of 0.7, have higher levels of CO emissions because of the larger quenching distance. In general, greater oxygen availability in lean mixtures reduces the value of CO emissions because there is more oxygen to complete fuel oxidation, as could be observed for each blend operating with a lean mixture. The 50B50M has lower CO emissions than other blends, except for natural gas, because 50B50M has a high flame speed, which results in a high peak pressure. The blends 50B50M, 57B38M5H and 54B36M10H have lower CO emissions than the blends 83B17P, 75B15P10H, and 79B16P5H due to the former blends having higher pressure during the combustion process.

NOx emissions are present in the combustion products from hydrocarbon fuels due to high temperature reactions between nitrogen and oxygen originating from combustion air. Although NOx consists of NO and NO_2 in SI engines, NO appears in greater quantity. NOx increases as the equivalence ratio is close to 1. Figure 5b shows the NOx-specific emissions; high flame temperatures favor NOx formation, and 100NG presents the highest levels of NOx emissions for this reason. All NOx emissions are in a similar range, but this range is less for 100NG, between 6,9-7.8 g/kWh for the equivalence ratio of 0.9 and between 6.0-6.7 g/kWh for the equivalence ratio of 0.7. The blends 50B50M, 54B36M10H, and 57B38M5H have a higher output power than the blends 83B17P, 79B16P5H, and 75B15P10H.

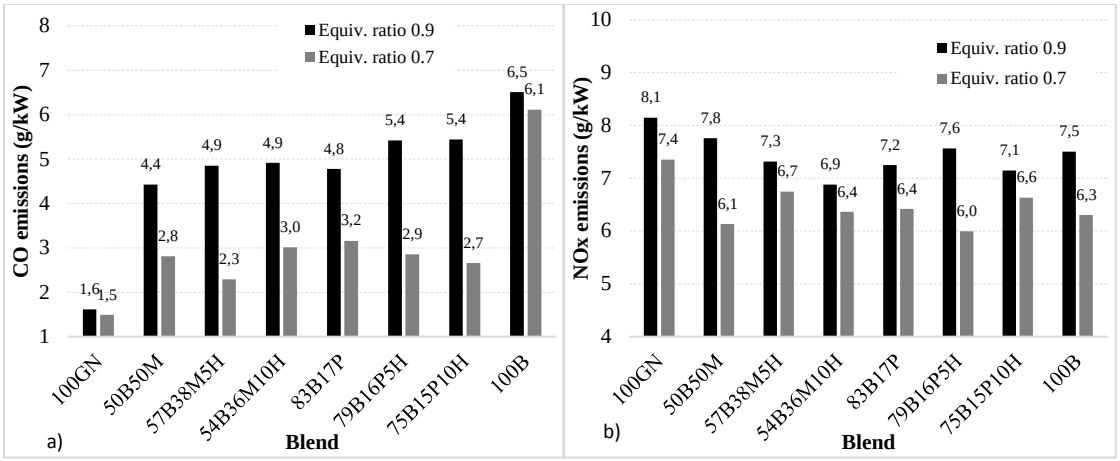

Figure 5 a) CO-specific emissions and b) NOx-specific emissions.

5.4.3.2 Ideal equivalence ratio for the blend 50B50M

To find the ideal engine operation conditions, from the results obtained with the blends studied in section 3.1, the blend 50B50M was selected. This blend obtains the highest output power and generating efficiency, compared with the other blends, and this blend has a good balance between knock resistance, flame speed and energy density. Maximum output power tests were recorded just below the knocking threshold to find the variation with the equivalence ratio. Figure 6a presents the test results for generating efficiency and output power. The ideal operating conditions for the blend resulted in an equivalence ratio of 0.85. The maximum output power is close to 8.7 kW with a generating efficiency close to 30%, suggesting that these conditions are ideal for engine operation. At these conditions using 50B50M a higher output power and higher generating efficiency than the original diesel engine is obtained. Figure 6b presents the SFC. The equivalence ratio of 0.85 has the lowest SFC value. Exhaust temperature for this equivalence ratio is 28ºC lower than for the equivalence ratio of 0.9 due to the lower flame temperature.

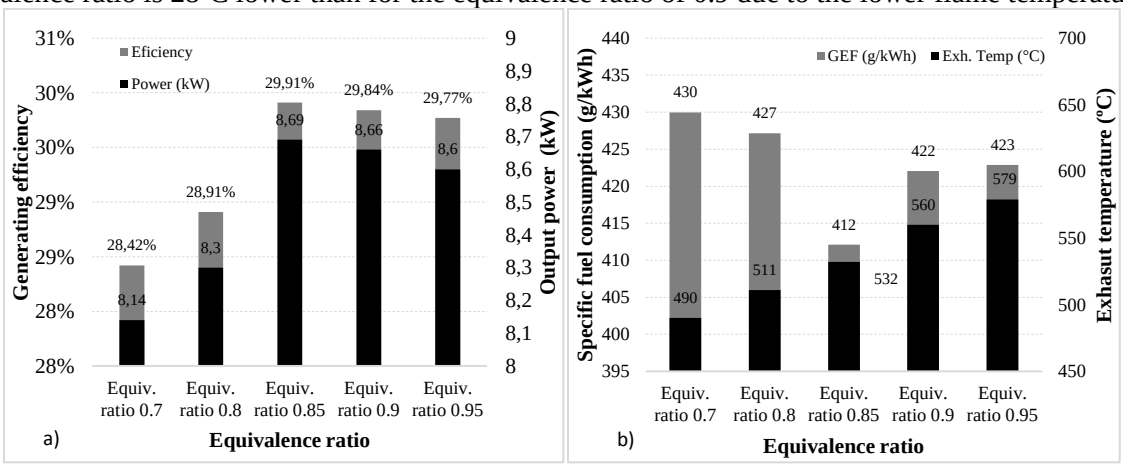

Figure 6 a) Generating efficiency and output power; b) SFC and exhaust gases temperature

Figure 7a shows that, for the ideal equivalence ratio of 0.85 for the blend 50B50M, the peak pressure is 4.2 bar higher compared to the equivalence ratio of 0.9, and the highest value for the peak pressure is close to 60 bar, slightly increasing the output power and the generating efficiency. Figure 7a also shows the ideal location for the peak pressure, which is just less than 12 degrees ATDC, the lowest value compared with the other equivalence ratios, indicating that the flame speed is higher for this equivalence ratio because the ST used for each equivalence ratio was the same. Using the equivalence ratio of 0.85, there is a decrease in pollutant emissions, as shown in Figure 7b, reducing CO emissions by 37.3% and NOx emissions by 6.79% compared to tests with an equivalence ratio of 0.9. The change in the

equivalence ratio from 0.9 to 0.85 slightly increases the oxygen availability, allowing more CO to react, release energy and produce more CO_2. Moreover, the addition of air slightly decreases the flame temperature because of the excess air, which decreases the NOx emissions.

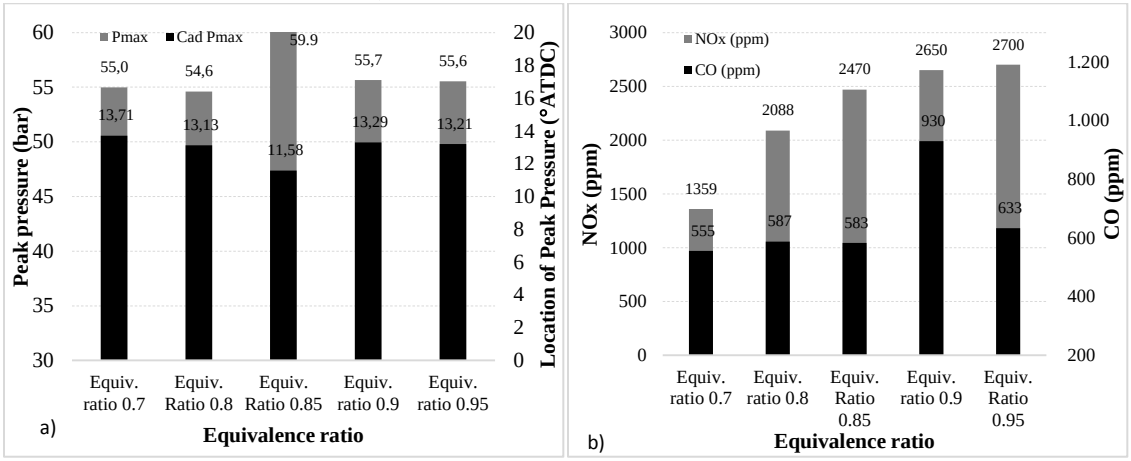

Figure 7 a) Maximum pressure and its location; b) Emissions of NOx and CO in ppm.

Figure 8a shows the pressure curves measured during the intake stroke versus the crank angle for the test with the blend 50B50M and different equivalence ratios. At the end of the intake stroke, at -180 degrees ATDC, it is observed that the blend with the equivalence ratio of 0.7 has the lowest pressure drop because the highest throttle valve % open is used to allow more air flow. In the figure, this space is indicated by a rectangle overlaid on the plot. Figure 8b presents the curves of instantaneous in-cylinder pressure versus crank angle near TDC. At the end of the compression stroke, the pressure with equivalence ratio of 0.7 has a higher value than those for the other equivalence ratios used. The pressure difference with the change in equivalence ratio between 0.7 and 0.9 is 4.95 bar at the end of the compression stroke, as highlighted by the rectangle overlaid on the plot. Each test is conducted at maximum output power, close to the knocking threshold. This pressure difference at the end of the compression stroke, as will be discussed in more detail in the next section, results in all blends with an equivalence ratio of 0.7 having a knock tendency higher than the blends with an equivalence ratio of 0.9. This result occurs because, in all the tests presented in section 3.1, the output powers for blends with an equivalence ratio of 0.7 were lower than for the blends with an equivalence ratio of 0.9. For the blend 50B50M with an equivalence ratio of 0.85, the highest peak pressure occurs because the output power and generation efficiency are maximized with this equivalence ratio. Operating the blends with a leaner mixture results in increasing the knocking tendency, but if the operation uses mixtures near stoichiometric mixtures, high NOx and CO emissions result. The equivalence ratio 0.85 for the blend 50B50M has a favorable balance, yielding maximum output power and generation efficiency, low CO and NOx emissions, and stable combustion conditions.

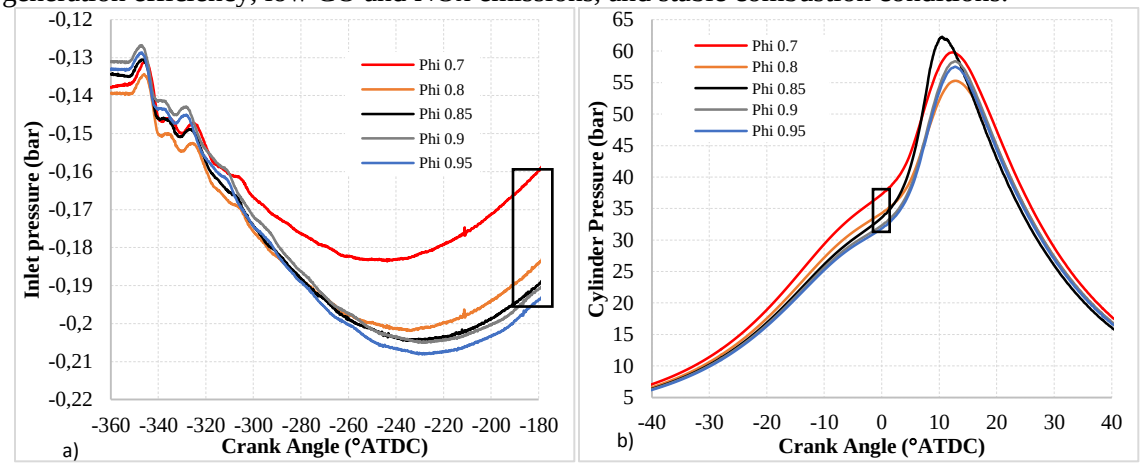

Figure 8 a) Inlet pressure; b) Instantaneous pressure in the cylinder

5.4.3.3 Effect of throttle opening to obtain lean mixtures.

To change the equivalence ratio from 0.9 to 0.7 to make the mixture leaner, the throttle valve % open value is increased, decreasing the pressure drop during the intake stroke. A higher knocking tendency was observed for an equivalence ratio of 0.7 compared to 0.9. Lean the mixture decreases the flame temperature and the ignition delay time is increased. However, reducing the pressure drop in the intake stroke results in increased cylinder pressure at intake valve closing, which is related with higher pressure at the end of compression stroke. Increased pressure accelerate autoignition reactions at the end gas, leading to an increased knocking tendency. In similar testing conducted in a CFR engine it was concluded that leaner mixtures permit increases CCR due to the decrease in knocking tendency [13]. Thus, the CFR results appear to show the opposite trend of the results presented in this paper. There are several important differences between the diesel engine converted to SI results presented herein and the CFR results. The CFR engine does not use a throttle valve, and the pressure in the intake manifold was constant at 100 kPa. Additionally, the CFR engine operates at 950 rpm, about half the speed of the Lister Petter engine. A analysis was performed on the effect of the throttle valve on knocking tendency to the Lister Petter engine. The results are shown in Table 5. The analysis shows that there are competing effects on the knock tendency. Consequently, engines operating under different operating conditions could respond differently to changes in equivalence ratio and admission pressure depending on the magnitude of each effect.

Table 5 Effects related to the throttle opening to obtain leaner mixtures.

Mixture properties and parameters	Change equivalence ratio from 0.9 to 0.7	Increase in inlet pressure	Final effect on knocking
Specific heat ratio (Cp/Cv)	↑	↑	Increases the knock tendency
Inlet pressure	↑	↑	Increases the knock tendency
Mixture density	↑	↑	Increases the knock tendency
Pressure in compression stroke	↑	↑	Increases the knock tendency
Peak pressure	↑	↑	Increases the knock tendency
Temperature in compression stroke	↑	↑	Increases the knock tendency
Flame temperature	↓	↑	Reduces the knock tendency
Laminar flame speed	↓	↓	Increases the knock tendency
Turbulent flame speed	↓	↑	Increases the knock tendency
Inert gases in mixture	↑	↑	Reduce the knock tendency
Ignition delay time	↑	↓	Increases the knock tendency
Residual burned gases	↓	↓	Reduce the knock tendency

The difference in pressure at the end of the compression stroke between the 0.7 and 0.9 equivalence ratio cases is 4.95 bar for the blend 50B50M. It is assumed that this difference can be generalized as 3 bar on average to analyze all the blends. By increasing the air quantity, the specific heat ratio is increased. The addition of natural gas and hydrogen to the biogas also increases the specific heat ratio of the mixture. The temperature at the end of the compression stroke can be estimated using the intake temperature (300K on average), a CR of 15.5:1 and the respective specific heat ratio value. Using the temperature and pressure at the end of the compression stroke, it is possible to estimate the adiabatic flame temperature (Tad) under these conditions using Chemkin with the reaction mechanism Grimech 3.0. Table 6 presents the estimated temperature at the end of the compression stroke for the mixtures with an equivalence ratio of 0.7 and pressure of 26 bar. Temperatures at the end of the compression stroke are higher for all the blends

compared to the mixtures with an equivalence ratio of 0.9 and a pressure of 26 bar. The table also presents the results to the adiabatic flame temperature. When making the mixture leaner, there are two facts that effect flame temperature. The first is an increase in the amount of air, which tends to decrease the flame temperature. The second is increasing the specific heat ratio, which tends to increase the flame temperature. Chemkin simulation results show that, by changing the equivalence ratio from 0.9 to 0.7, with an increased pressure in 3 bar at the end of the compression stroke, the final effect is to reduce the adiabatic flame temperature. Thus, the dominant effect is the increase in the amount of air. On average there is a reduction of 228K in the adiabatic flame temperature, which reduces the knocking tendency.

Table 6 Temperature at the end of the compression stroke and adiabatic flame temperature, conditions at the end of the compression stroke.

Blends	Equivalence ratio of 0.9 and pressure of 26 bar			Equivalence ratio of 0.7 and pressure of 29 bar		
	Specific heat ratio	Compression Temp. (K)	Tad (K)	Specific heat ratio	Compression Temp. (K)	Tad (K)
100B	1.384	947	2,485	1.387	954	2,264
50B50M	1.388	955	2,557	1.390	961	2,325
57B38M5H	1.387	954	2,549	1.389	960	2,321
54B36M10H	1.387	954	2,553	1.390	960	2,324
83B17P	1.383	944	2,551	1.386	952	2,324
79B16P5H	1.383	944	2,554	1.386	952	2,326
75B15P10H	1.383	944	2,557	1.386	952	2,329

Turbulent flame speed (S_T) decreases because the increase in the amount of air reduces laminar flame speed. However, the increase in pressure at the end of the compression stroke tends to increase S_T. To estimate the combined effect, two simulations in CFD Fluent were performed to simulate the fluid dynamics and turbulence. Using the blend 50B50M, the only parameters varied were the equivalence ratio and the inlet pressure. The combustion model is partially premixed combustion, the turbulence model is K-epsilon RNG, the ignition model is the "Spark Ignition model," and the turbulent combustion model is the Zimont model [22]. From these simulations, at the end of the compression stroke, the turbulence intensity, mixture density and Reynolds number were calculated. This information was used to model S_T using the Gülder model [23] as follows:

$$\frac{S_T}{S_L} = 1 + 0.62\left(\frac{u'}{S_L}\right)^{0.5} \mathrm{Re}_T^{\,0.25} \qquad \text{Equation 5.4.1}$$

The results are presented in Table 7.It is observed that decreasing the equivalence ratio to 0.7 reduced the turbulent flame speed, leading to reduced turbulent flame speed (9.26 m/s on average) for all the blends with equivalence ratios of 0.7. In turn, this result caused an increase in the knock tendency because the time required to burn the mixture increased, allowing more time to the end gas autoignition. Ignition delay time is the most important property in assessing the knocking tendency of fuels and air mixtures under different conditions of pressure and temperature. The ignition delay time was estimated using Chemkin with the model Homogeneous 0-D reactor and using the San Diego mechanism, which had one of the best estimation results of MN and CCR [13]. The pressure and temperature conditions used correspond to the estimated pressure at the end of the compression stroke. Reducing the equivalence ratio tends to increase the ignition delay time due to the air excess. Increasing the pressure at the end of the compression stroke tends to decrease ignition delay time. Table 8 shows the combined effect. According to the Chemkin simulations, ignition delay time decreases, on average for all the blends, by 0.0025 seconds due to the change in the equivalence ratio from 0.9 to 0.7. This result is equivalent to the engine, at 1800 rpm to have autoignition advanced by 27 CAD degrees. In this case, the effect of pressure and temperature is more significant than the effect of increasing excess air. This behavior was observed in tests for all the blends.

Table 7 Estimated turbulent flame speed using the Gülder model.

	Equivalence ratio of 0.9 and pressure of 26 bar				Equivalence ratio of 0.7 and pressure of 29 bar			
Blends	**SL (m/s)**	**u` (m/s)**	**Re_T**	**S_T (m/s)**	**SL (m/s)**	**u` (m/s)**	**Re_T**	**S_T (m/s)**
100B	0.24	58.7	68,062	37.5	0.14	58.8	68,816	29.5
50B50M	0.30	58.7	68,062	42.5	0.18	58.8	68,816	32.9
57B38M5H	0.30	58.7	68,062	42.5	0.18	58.8	68,816	33.0
54B36M10H	0.32	58.7	68,062	43.5	0.19	58.8	68,816	33.9
83B17P	0.33	58.7	68,062	44.3	0.20	58.8	68,816	35.0
79B16P5H	0.34	58.7	68,062	45.0	0.21	58.8	68,816	35.6
75B15P10H	0.35	58.7	68,062	45.7	0.22	58.8	68,816	36.2

Table 8 Estimation of the ignition delay time due to the change in equivalence ratio.

Blends	**Equivalence ratio of 0.9 and pressure of 26 bar**			**Equivalence ratio of 0.7 and pressure of 29 bar**		
	Specific heat ratio	**Compression Temp. (K)**	**Ignition delay time (s)**	**Specific heat ratio**	**Compression Temp. (K)**	**Ignition delay time (s)**
100B	1.384	947	0.031	1.387	954	0.026
50B50M	1.388	955	0.025	1.390	961	0.022
57B38M5H	1.387	954	0.026	1.389	960	0.024
54B36M10H	1.387	954	0.026	1.390	960	0.024
83B17P	1.383	944	0.016	1.386	952	0.014
79B16P5H	1.383	944	0.015	1.386	952	0.014
75B15P10H	1.383	944	0.015	1.386	952	0.014

5.4.4 Conclusions

This research presents test results for a Lister Petter biogas engine with a high compression ratio. Using blends with methane or propane and hydrogen additions, operating conditions are optimized to achieve high output power and generating efficiency and low pollutant emission. A analysis is performed to better understanding of the effect related with the increased knocking tendency with the change in the equivalence ratio from 0.9 to 0.7. The main conclusions from this work are as follows:

- The blend 50B50M, equivalent to a purified biogas, shows the highest output power and high generating efficiency due to a good balance between knocking resistance and energy density. The best equivalence ratio for this blend is 0.85.
- The purified biogas is able to operate in a diesel engine converted to SI with high CR, for low-output power generation, without power derating and with high generating efficiency. The output power and generating efficiency are higher than those obtained using the original diesel engine. The operation is stable and with low CO and NOx emissions.
- Opening the throttle valve to make the mixture leaner increases the knocking tendency.
- The maximum output power is not limited by the throttle valve % open value but by the knocking threshold and cyclic dispersion.
- The results when opening the throttle valve to change the equivalence ratio from 0.9 to 0.7 for all the blends are two. First, a leaner mixture is obtained and second the cylinder pressure at intake valve closure increases. These two responses have competing effects on knocking tendency. In general, the knocking tendency increases mainly the ignition delay time and turbulent flame speed decrease, due to the pressure increasing at the end of the compression stroke.
-Biogas with an equivalence ratio of 0.7 achieves relatively low values of output power of 5.45 kW and generating efficiency close to 20% because of the high knock tendency during lean combustion. Biogas operation is improved with an equivalence ratio close to a stoichiometric.
- All the blends, except biogas, had output powers over 8 kW, maximum output power of diesel engine.

References

1. Davis, S.G., et al., An optimized kinetic model of H2/CO combustion. Proceedings of the Combustion Institute, 2005. 30(1): p. 1283-1292.
2. A. Roubaud, r.r., d. Favrat,, Lean-Burn Cogeneration Biogas Engine with Unscavenged Combustion Prechamber: Comparison with Natural Gas. Applied Thermodynamics, 2002. 5(4): p. 169-175.
3. Porpatham, E., A. Ramesh, and B. Nagalingam, Investigation on the effect of concentration of methane in biogas when used as a fuel for a spark ignition engine. Fuel, 2008. 87(8–9): p. 1651-1659.
4. Vu, T.M., et al., Effects of diluents on cellular instabilities in outwardly propagating spherical syngas–air premixed flames. International Journal of Hydrogen Energy, 2010. 35(8): p. 3868-3880.
5. Mehrzad Kaiadi, P.T., Ashish Shah, Extending the performance, fuel efficiency and stability of stoichiometricspark ignition natural gas engines – Gas engine research at KCFP 2007-2012, S.G.C. AB, Editor. 2013.
6. T.Korakianitis, A.M.N., R.J.Crookes, , Natural-gas fueled spark-ignition (SI) and compression-ignition (CI) engine performance and emissions. . Progressin Energy and Combustion Science,. , 2010. 1: p. 1-24.
7. Porpatham, E., A. Ramesh, and B. Nagalingam, Effect of compression ratio on the performance and combustion of a biogas fuelled spark ignition engine. Fuel, 2012. 95(0): p. 247-256.
8. Malenshek, M. and D.B. Olsen, Methane number testing of alternative gaseous fuels. Fuel, 2009. 88(4): p. 650-656.
9. Porpatham, E., A. Ramesh, and B. Nagalingam, Effect of hydrogen addition on the performance of a biogas fuelled spark ignition engine. International Journal of Hydrogen Energy, 2007. 32(12): p. 2057-2065.
10. Lee, S., et al., Effect of n-Butane and propane on performance and emission characteristics of an SI engine operated with DME-blended LPG fuel. Fuel, 2011. 90(4): p. 1674-1680.
11. Karim, G.A., The onset of knock in gas fueled spark ignition engines prediction and experiment Journal of KONES Powertrain and Transport, Vol.14, No. 4, 2007.
12. Karim, G.A., Autoignition and Knock in Engines Fueled with Hydrogen and Hydrogen Supplemented Gaseous Fuel Mixtures, U.o.C. Mechanical Engineering, Editor. 1997.
13. Gómez Montoya, J.P., A.A. Amell, and D.B. Olsen, Prediction and measurement of the critical compression ratio and methane number for blends of biogas with methane, propane and hydrogen. Fuel, 2016. 186: p. 168-175.
14. Korakianitis, T., A.M. Namasivayam, and R.J. Crookes, Natural-gas fueled spark-ignition (SI) and compression-ignition (CI) engine performance and emissions. Progress in Energy and Combustion Science, 2011. 37(1): p. 89-112.
15. Karim, G.A., Autoignition and Knock in Engines Fueled with Hydrogen and Hydrogen Supplemented Gaseous Fuel Mixtures, U.o.C. Mechanical Engineering, Editor.
16. Heywood, Jhon B. Internal Combustion Engine Fundamentals. 1988. McGraw hill.
17. Quader, A., "What Limits Lean Operation in Spark Ignited Engines - Flame Initiation or Propagation?," SAE paper 760760.
18. Gomez Montoya J.P. and Amell A. Doctoral thesis "Determination of the optimal operating conditions of an SI engine with high CR, using gaseous fuels from renewable sources". Universidad de Antioquia. 2016.
19. Gómez Montoya J.P. Amell A., Zapata J., Experimental study of spark ignition engine performance and emissions in a high compression ratio engine using biogas and methane mixtures without knock occurrence. Thermal Science: year 2015, vol. 19, no. 6, pp. 1919-1930. DOI 10.2298/TSCI140829119G, 2015.
20. Atkins R. An introduction to engine testing and development. Book from SAE International. ISBN 978-0-7680-2099-1. P. 188
21. Lefebvre, A.H., Ignition Theory, in Gas Turbine Combustion, T. Francis, Editor. 1999: USA. p. 50-52.
22. V. Zimont. Gas Premixed Combustion at High Turbulence. Turbulent Flame Closure Model Combustion Model. Experimental Thermal and Fluid Science, 21:179-186, 2000
23. O.L., G., Turbulent premixed flame propagation models for different combustion regimes. Twenty-Third Symposium (International) on Combustion, 1990, pp. 743–750.

5.5 Effect of increasing turbulence intensity on knocking tendency of a SI engine with high CR.

Abstract

This research presents the results of experimental tests carried out on a diesel engine converted to spark ignition (SI), keeping the engine's high compression ratio, while applying a Piston Combustion Chamber Geometry Change (PCCGC) to increase the turbulence intensity at the end of the compression stroke and during the combustion process. The increase in turbulence intensity was intended to increase the turbulent flame speed of the biogas, during the flame front expansion in the cylinder, in order to compensate for the low laminar flame speed of biogas. The results presented study the effect of increasing turbulence intensity on knocking tendency, using biogas mixed with natural gas or propane and hydrogen additions. All the tests, before and after the PCCGC, for each blend and equivalence ratio, were taken below the knocking threshold with low cyclic variation, and the spark timing was adjusted for optimum generating efficiency. The increase in turbulence intensity due to the PCCGC was simulated using CFD Fluent 13.0, in which 13 combustion chamber geometries were considered. The geometry selected had greatest turbulence intensity and turbulent kinetic energy. The turbulence intensity increase was measured indirectly through the duration of combustion, using the periods to 5%, 50%, and 90% of mass burned. It was found that the increase in turbulence intensity increased the engine's knocking tendency, reducing the maximum output power for all the blends in order to remain under the knocking threshold. Biogas was not affected by the conditions of high pressure, high temperature, and high turbulence. Purified biogas derating 14% of its maximum output power. For all the blends, the measures of peak pressure, maximum heat release rate, indicated mean effective pressure, and exhaust temperature were lower after the PCCGC. The knocking tendency is increased with greater turbulent flame speed; also blends with higher laminar flame speeds are more prone to knock.

5.5.1 Introduction

Most natural gas (NG) commercial vehicles are using converted diesel engines. The combustion chamber in these engines is most commonly located in the piston crown and a flat cylinder head is used. The inlet port of these engines often generates a highly swirling gas motion to enhance the diesel combustion process. In the conversion to SI engine, the original inlet port is most often used. The original combustion chamber is, however, not directly suitable for SI operation as the compression ratio (CR) is often too high, and the flow structure is optimized for spray combustion rather than the flame front propagation of a SI engine. But the question is how the piston crown should be modified in order to minimize emissions and at the same time achieve a high generating efficiency. There are two opinions on this matter [1]. The first opinion holds that a fast combustion process is desired, enabling operation at lean equivalence ratios, without large cycle-to-cycle variations. Lean mixtures should be favorable from a thermodynamic point of view as the specific heat ratios during the expansion stroke are higher. A higher CR would also be possible as the knocking tendency is reduced with lean mixtures, which would compensate for the higher heat losses to the walls due to the greater bulk flow and turbulence used to increase the combustion rate. The resulting nitrogen oxides (NOx) emission should be low with this strategy, However, unburned hydrocarbons (HC) could be a problem with lean mixtures as flame quenching and partial burn would be expected [2]. The second opinion holds that a minimal amount of in-cylinder flow velocity and turbulence is desired in order to reduce the heat losses to the walls and hence improve the generating efficiency. The slower combustion expected with this strategy should reduce the maximum pressure and temperature during the expansion stroke, leading to low NOx emissions. This strategy could be effective for engines operating with an equivalence ratio equal to one and using a three-way catalyst, but expected to be less suitable for lean mixtures, as the cycle-to-cycle combustion variations would be severe [1-3].

The piston combustion chamber geometry has no effect on the turbulence levels during the intake stroke, but is important at the end of the compression stroke and during the expansion stroke, moment when the high turbulent intensity is required to guarantee high turbulent flame speed during combustion. Combustion fluid-dynamic (CFD) numerical simulations are used as a tool to estimate the changes involved in the combustion process by the PCCGC. Simulation results suggest which geometries will have a higher turbulent kinetic energy (TKE), higher turbulence intensity, higher peak pressure, higher

temperature, and shorter combustion duration [1, 2, 4, 5]. The first part of the combustion process (between 0-0.5% mass burned) is mostly affected by the fuel chemical composition, turbulence intensity and equivalence ratio. The intermediate part of the combustion (0.5-5% mass burned) is mostly influenced by the bulk speed and the turbulence intensity. The combustion rate in SI engines is proportional to the speed at which the turbulent flame front propagates through the unburned mixture, this velocity depending predominantly on the degree of turbulence in the combustion chamber at the end of the compression stroke [1]. Although the bulk speed influences the first part of the combustion, its impact on the overall combustion rate is less important than turbulence intensity. Turbulence intensity and average bulk speed change during the compression and expansion strokes. One method for increasing the turbulence intensity at the end of the compression stroke is to increase the percentage of combustion chamber area [1, 2, 6].

Several dimensionless parameters are used to characterize turbulent premixed flames. The dimensionless parameter used to define the turbulence here is the turbulent Reynolds number. The characteristic chemical reaction time is the residence time in a laminar flame, which is defined as the relation between the flame thickness and the laminar flame speed. The characteristic physical reaction time is the relation between the integral scale length and the turbulence intensity. The ratio of the characteristic eddy turnover time to the laminar burning time is called the Damkohler number, which is an inverse measure of the influence of the turbulent flow on the chemical processes occurring in the flame [5]. The relation of the laminar flame front thickness over the Kolmogorov scale length is a measure of the stretch or local distortion to which a laminar flame is subjected by the turbulent flow. The relation between turbulent intensity and laminar flame speed is a measure of the relative strength of turbulence. Different regimes of turbulent flames are apparent in the plot of Damhkoler number versus turbulent Reynolds number. In the Borghi diagram the reaction sheet regime, propagating reaction fronts are wrinkled and convoluted by the turbulence. SI engines operate at high speeds and high turbulence, located in this regime [5][7]. Although the mean in-cylinder speed may have an effect on the initial combustion rate, distorting the development of the first flame front and increasing the burn surface, the main mechanism for improving combustion is turbulence. The circular flow motion has been observed to improve combustion through turbulence produced close to the end of the compression stroke, as the flow is compressed into a reduced volume. The rotating vortices that make the circular movement tend to break into smaller structures and their kinetic energy is gradually converted into TKE [7, 8]. In SI engines, the flame fronts are highly wrinkled with interconnected reaction zones [5].

Increasing the in-cylinder turbulence intensity with the PCCGC increases the turbulent flame speed and combustion rate and decreases the combustion duration, which reduces the time required for the flame front to reach the walls, reducing heat losses and leading to higher generating efficiency [9]. The time required by the flame front to reach the farthest points from the spark plug must be less than the ignition delay time of the end gas – which is being compressed by the flame front and by the movement of the piston – in order to prevent knocking. As the geometry of the piston is modified in order to increase the turbulence intensity and turbulent flame speed, the geometry of the fastest combustion will also result in the highest NOx values due to the increases in pressure and temperature. However, in the case of lean mixtures, NOx levels can be maintained for all geometries [2]. High turbulence in the combustion chambers reduces total hydrocarbon (THC) and carbon monoxide (CO) emissions due to good mixing. Essentially, there are three kinds of turbulence in SI engines: Swirl, tumble, and squish. Swirl occurs when there is a rotational movement of the mixture around an axis perpendicular to the combustion chamber. Tumble is when the rotational movement occurs on an axis transverse to the combustion chamber. And lastly, squish refers to the small eddies formed by the combustion chamber geometry [10, 11].

The combustion chamber geometry in an SI engine is a dominating factor, which controls the in-cylinder bulk flow, where the highest movement scales like swirl, tumble, and squish produce high levels of turbulence at the time of combustion and during the expansion stroke. The intake stroke results in high mixture speeds and high turbulence, which almost disappear at the end of the compression stroke. Both mean speed and turbulence intensity decrease rapidly close to TDC, since there is no production of turbulence in this range. In non-turbulent mixtures the flame propagation is laminar, but when there is turbulence the flame front wrinkles and the reaction zone is thinner than with laminar combustion.

Additionally, the turbulent flame speed is several times higher than the laminar flame speed, depending on the turbulence intensity. The initial phase of the combustion process depends primarily on the degree of turbulence around the spark plug at the time of ignition, this first phase persisting until many eddies have been completely burned. Notably, it is the variations that occur in this phase of combustion that are responsible for the cyclical variations observed in the engine's operation. The combustion chamber geometry affects the critical combustion process in this initial phase. In turbulent mixtures, large eddies are divided into smaller swirls and transfer the TKE. Eventually, the smallest eddies dissipate energy into heat. There are two mechanisms that explain the increased flame front speed because of the turbulence: The first considers that the turbulent eddies are thinner than the laminar flame front, which leads to increases the local heat transfer and mass rates in the flame front. The second considers that the turbulent eddies are wider than the thickness of the flame front [10, 12].

There are different combustion chamber geometries for the pistons in SI engines, depending on the kind of engine, fuel, engine power, and engine brand. Flat piston geometry is the simplest kind of combustion chamber. With this flat geometry, the swirling flow resulting from the intake stroke does not change significantly during the compression and expansion strokes, resulting in a low degree of turbulence during combustion. A cylindrical chamber geometry results in an increased angular velocity of swirl flow, as the the mixture is forced into the chamber, the resulting flow is *believed* to be a complex toroidal rotation. The presence of squish, and the dramatic increase in swirl turbulence, lead to an increase in turbulence intensity, causing the surface area of the flame front in the first part of the combustion to be increased compared to the case of flat piston geometry. In a square combustion chamber the combustion rate is increased due to the small turbulence scales resulting from the breaking of the swirls in the corners of the combustion chamber. Another combustion chamber geometry used is cross-shaped at the top and cylinder-shaped at the bottom. The flow in this kind of combustion chamber is very complex, the swirling motion of the overall inflow breaking into small swirls in all the corners of the cross, close to TDC [1, 2]. During the intake stroke, many annular vortices are broken, increasing TKE, as the inlet flow hits the intake valve and the flow through the intake stroke produces shear layers. Although TKE is high, it cannot be directly used to increase the combustion rate, since dissipation makes it difficult to maintain the high level of TKE until the end of the compression stroke. The annular vortices are influenced by the geometry of the intake port and the lift of the valves, the TKE remaining the same during the intake stroke for two different combustion chambers [12].

This research did a CFD study of 13 different piston combustion chamber geometries. Most of the geometries used in these simulations were based on the results of previous research. Among these shapes are: square, clover, cone, cross, and cylindrical, among others. The volume of the combustion chamber was kept similar in order to preserve the CR. With the progress in computation technology, there are increasing simulation studies of fluid mechanics, including the numerical solution of the Navier-Stokes equations, which may include the solution of a detailed chemical kinetic mechanism. However, there are few simulation studies using CFD for SI engines with alternative fuels, the most important:

Mardi et al. [13] used CFD to investigate the effects of exhaust gas recirculation (EGR) and the initial pressure of the charge on the performance and emissions of an SI engine. The engine was powered separately with gasoline and some alternative fuels. The simulation results were compared with experiments with good closeness. The results show that the non-production of CO_2, CO, and THC, and the high flame speed and low heating value of hydrogen (H_2), makes H_2 an ideal alternative compared to other fuels. Furthermore, increasing EGR from 0% to 20% reduces NOx emissions. The results show that an increase in EGR causes a decrease in the IMEP due to the low flame speed and the low combustion rate, while specific fuel consumption (SFC) increases with increasing EGR. An EGR of 10% is a reasonable running condition, leading to a significant reduction of NOx while the effects on CO and on the IMEP are still favorable.

Keveh et al. [14] used open-cycle CFD to study an SI engine running on blends of methane and hydrogen with a detailed kinetic mechanism (Grimech 3.0). This study investigated the effect of the addition of hydrogen to methane. CFD simulations were done using Fluent 6.3 software. The key results are: with optimal ST, all fuel is burned before 10 degrees ATDC; hydrogen reduces the combustion duration,

expands the lean limit, and reduces CO and CO_2 emissions; intake valves and piston movement are two factors for the generation of velocity vortices in the combustion chamber. This work demonstrates the high capacity of CFD to solve the three-dimensional combustion process in an SI engine.

Harshavardhan et al. [15] did a CFD analysis of the air flow inside the cylinder and the interaction of air and fuel for different piston head shapes. The flows are transient, compressible, and of a turbulent nature. They found that geometry with a centered combustion chamber resulted in 51% higher turbulence intensity and the TKE increased 21% with better stratification of the charge, better evaporation of the fuel, and higher TKE at injection time.

Kosmadakis et al. [16] investigated the combustion of H_2 in an SI engine with EGR using CFD. A simplified geometry was used to investigate combustion and NOx emissions. The results of the simulations, which were run using custom CFD code, were compared with experimental results in order to validate the combustion model, which incorporates an expression for the residual gases in the laminar flame speed calculations. Kosmadakis et al. [17] also did an investigation, again running custom CFD code, of the formation mechanisms for NOx emissions in an SI engine using blends of methane and hydrogen. The work focused on the mechanism for NOx formation at various equivalence ratios.

Duan et al. [18] carried out numerical and experimental research to control the flashback in a H_2 engine. The work focused on optimizing the timing and pressure of H_2 injection with the purpose of reducing the distribution in the concentration of the mixture upon admission, and controlling the mixture temperature through the intake valve to avoid flashback.

Changwei et al. [19] numerically investigated the combustion in an SI engine running on H_2 and gasoline, using CFD calculations. There was agreement between the calculations and in-cylinder pressure measurements. The calculations showed that the addition of H_2 increases the turbulent flame speed. Changwei et al. [20] also developed a correlation for laminar flame speed and validated the use of CFD simulations in SI engines with H_2 and gasoline. The values estimated with the correlation were satisfactorily in agreement with the experimental results. The correlation is similar to that presented by Metghalchi [21]. Calculations were performed using CFD AVL FIRE. The two correlations are implemented using the ECFM combustion model to calculate the combustion process with different H_2 levels.

There is contradictory literature about whether faster combustion may increase or decrease the knocking tendency in SI engines. Faster combustion allows less time for end-gas autoignition to occur, but also increases the end-gas pressure and temperature, which may reduce the ignition delay time for autoignition. There are two studies that show that a greater combustion speed increases the knocking tendency, which is the focus of this research: Chen and Raine did a study to propose using the time duration from ignition to 70% mass fraction burnt as an explanatory variable, the hypothesis being that knocking cycles have shorter mass fraction burnt duration than normal cycles. The simulation results suggest that increasing burning rate will promote knock, which is in agreement with the experimental results presented [22]. Breaux et al. presented a paper, which seeks to quantify engine performance consequences and identify fundamental similarities across a range of high-speed, medium-bore, lean-burn SI engines. They show that changes in flow structure and turbulence intensity result in changes to the rate of heat release, cylinder wall heat rejection, and cycle-to-cycle combustion variability. In-cylinder turbulence was manipulated by changing the extent of intake-port induced swirl, as well as varying the degree of piston-generated turbulence. Increasing in-cylinder turbulence leads to reduced cycle-to-cycle variability and increased knocking tendency [23].

A literature search reveals no studies on how to increase the turbulent flame speed, and consequently reduce the combustion duration, during the flame front expansion in a SI engine with high CR. There is no information on the best combustion chamber geometry for biogas or for blends of biogas with methane or propane and hydrogen additions. The effect of turbulence intensity on knocking tendency is not clear. The relation between the methane number and the ideal turbulence intensity to achieve high maximum output power is also unclear. The purpose of the PCCGC was to increase the maximum output power, which was 8.6 kW with purified biogas presented in a previous paper. However, the increase in turbulence intensity increases the knock tendency, forcing a reduction in output power in order to remain under the knocking

threshold. A diesel engine converted to SI with high CR and high turbulence intensity is used. The current study's purpose is to study the effect of increasing turbulence intensity on the knocking tendency in a high CR SI biogas engine running on blends of biogas with natural gas or propane and hydrogen additions. The new knocking conditions are of lower pressure and temperature, higher turbulence intensity. Knocking is a predominant limiting phenomenon for maximum output power in SI engine.

5.5.2 General procedure for testing

The fuel and blends used in this research are: Natural gas, biogas, and six blends of biogas with either methane or propane, with additions of hydrogen. The simulated biogas used is a mixture of 60% natural gas and 40% CO_2. Before the PCCGC, the natural gas used had the following composition: 94.8% CH_4, 1.3% N_2, 2.3% C_2H_6, 1.1% C_3H_8, and 0.5% CO_2, on a volumetric basis. After the PCCGC the natural gas had the following composition: 95% CH_4, 2.5% C_3H_8, and 2.5% CO_2, again by volume. Both natural gases have similar LWI (close to 45 MJ/m^3 fuel), energy density (close to 3.6 MJ/m^3 air), and methane number (approximately 87.2). In each case the output power was the maximal possible, the ST adjusted independently for each blend to achieve optimum generating efficiencies close to knocking threshold. The MNs of the blends were tested previously [13], and the MN of the natural gas was estimated using Methane 3.1 software from AVL. Table 1 presents the properties of the blends. The laminar flame speed was determined numerically using Chemkin, with the Grimech 3.0 kinetic mechanism.

Because of their high CR, diesel engines have a good capacity to admit air, overcoming the resistance of a partially open butterfly throttle valve without significant declines in generating efficiency. This allows for the operation at maximum output power limited by knocking and cyclic dispersion. In this research, the engine maximum output power operation was not limited by the butterfly throttle valve opening. The butterfly throttle valve controlled the airflow while the blends were injected near to the inlet port at an average pressure of 2.5 bar, giving independent control of the mixture.

Table 1 Blend properties

Blend designation	Blend composition	Blend properties				Laminar flame speed (cm/s), equivalence ratio of 0.9, 1 atm, and 25 °C
		LHV MJ/m^3 fuel	LWI MJ/m^3 fuel	Energy density MJ/m^3 air	Methane number	
100GN	100% Natural gas	34.55	45.13	3.58	87.2	34.98
100B	100% Biogas	20.35	20.99	3.44	140.0	23.57
50B50M	50% Biogas + 50% Methane	27.14	**31.40**	**3.57**	120.0	30.22
57B38M5H	57% Biogas + 38% Methane +5% Hydrogen	25.00	29.01	3.58	105.3	30.32
54B36M10H	54% Biogas + 36% Methane +10% Hydrogen	24.22	28.80	3.59	96.5	31.74
83B17P	83% Biogas + 17% Propane	31.98	31.38	3.64	65.8	32.83
79B16P5H	79% Biogas + 16% Propane +5% Hydrogen	30.89	31.04	3.65	65.2	33.91
75B15P10H	75% Biogas + 15% Propane +10% Hydrogen	30.71	30.71	3.77	63.8	34.95

5.5.2.1 PCCGC to increase the turbulence intensity

Twelve geometries in addition to the original geometry were simulated with CFD, with the purpose of determining the geometry with the highest turbulence intensity at the end of the compression stroke and during the combustion process. The CFD simulations were done in Fluent 13.1 with 3D dynamic meshes that simulate the engine piston movement, with a similar CR and an engine speed of 1800 rpm. The actual cylinder and piston measurements were used, while the cylinder head and the combustion chamber were simplified in order to facilitate the meshing. The combustion model used was partially premixed combustion, the turbulence model was k-epsilon RNG (2 equations), and the ignition model was the SI model. The partially premixed combustion model defines a laminar flame speed value by default, which is a parameter dependent on the fuel composition and equivalence ratio. A UDF was used to modify these

values according to the Chemkin simulations for each blend. The correlation defined by Metghalchi y Keck was used to simulate combustion at high pressure and high temperature, [21]. The partially premixed combustion model was based on the "C equation model" [25]. The turbulent combustion model was based on the work of Zimont et al. [26], involving the solution of the transport equation for the reaction progress variable, the closure of this equation being based on the definition of turbulent flame speed. The solution of the energy equation was based on the solution of a simplified detailed mechanism. San Diego and DM19 mechanisms [27-29] were used for their good estimates of the MN. The geometry that gave the best results for high TKE and high turbulence intensity at the end of the compression stroke was the simple cylindrical geometry, while the CR was preserved.

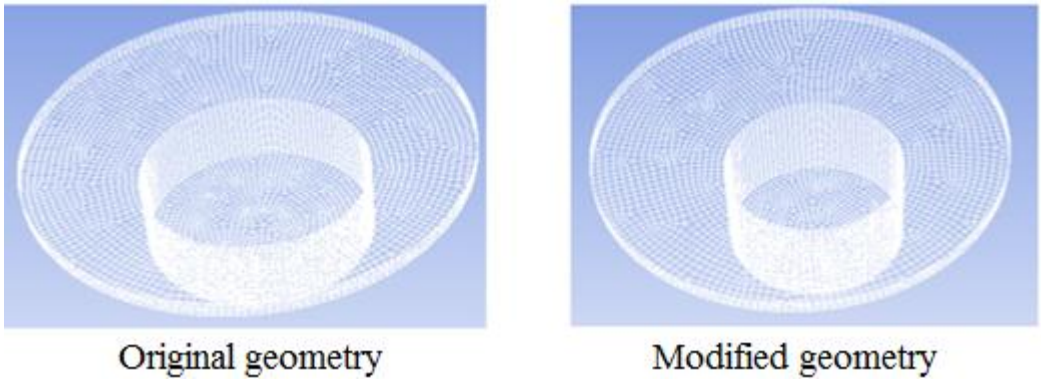

Figure 2 Original geometry and modified geometry

5.5.3 CFD and experimental results of the tests before and after the PCCGC.

5.5.3.1 CFD simulations results

Figure 2 presents the original geometry mesh and modified geometry mesh at TDC, which is a simple cylindrical geometry, with a ratio of 0.37 between the bowl diameter and piston diameter. According to the results of [10], combustion chamber geometry affects exhaust emissions in SI engines. In that study, the dimensionless parameters of every bowl type were deduced and compared with others, based on engine operating conditions. The best bowl was found to be the hemispherical (d/D = 0.37). Results indicate that bowls increase both heat transfer and flame speed. Figure 3 presents the images of the flame front development taken from Fluent simulations. It is observed that a spherical flame front is generated from the spark, the flame front traveling through the unburned mixture to the walls. The blue color represents the unburned mixture and the red color the burned mixture, while yellow and green indicate flame formation.

Figure 4 presents the results of the CFD simulations, for the 13 geometries evaluated, in terms of a) turbulent kinetic energy (TKE) and b) mass burn fraction. The goal was for the TKE and turbulence intensity to be greater than for the original engine geometry near top dead center. In addition, the increase in turbulence intensity should reduce the duration of combustion by increasing the burn rate. The results indicate that geometries d/D 0.37, cone trunk, square B, and square A deliver higher levels of TKE at the end of the compression stroke and during the combustion period, as compared to the original geometry. With geometry d/D 0.37, the mass burn fraction is increased from 0.5 to 0.72 at 730 CAD degrees. However, other geometries such as clover, Quartette, Quartette B, and cross decrease TKE and turbulence intensity with respect to the original geometry. Geometry d/D 0.37 proved to be the best, as it achieved the greatest increases in TKE and turbulence intensity.

Figure 5 compares the values of various variables for geometry d/D 0.37 and the original geometry. The results show that there was an increase in turbulent kinetic energy and turbulence intensity, leading to a higher turbulent flame speed and higher burn rate. This results in a quicker combustion with the modified geometry trying to increasing knocking resistance. On the other hand, the modified geometry increased the pressure and the temperature, decreasing knocking resistance. The increases in the magnitudes of the

mass burn fraction, TKE, and the turbulence intensity were greater than the increases in pressure and temperature.

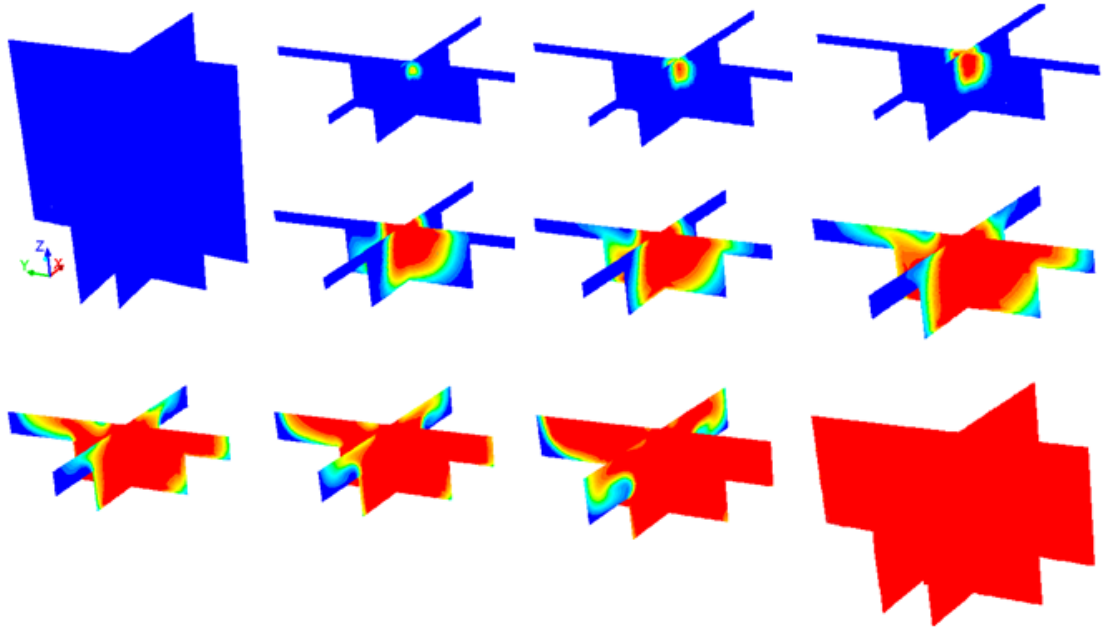

Figure 3. Flame front development in Fluent

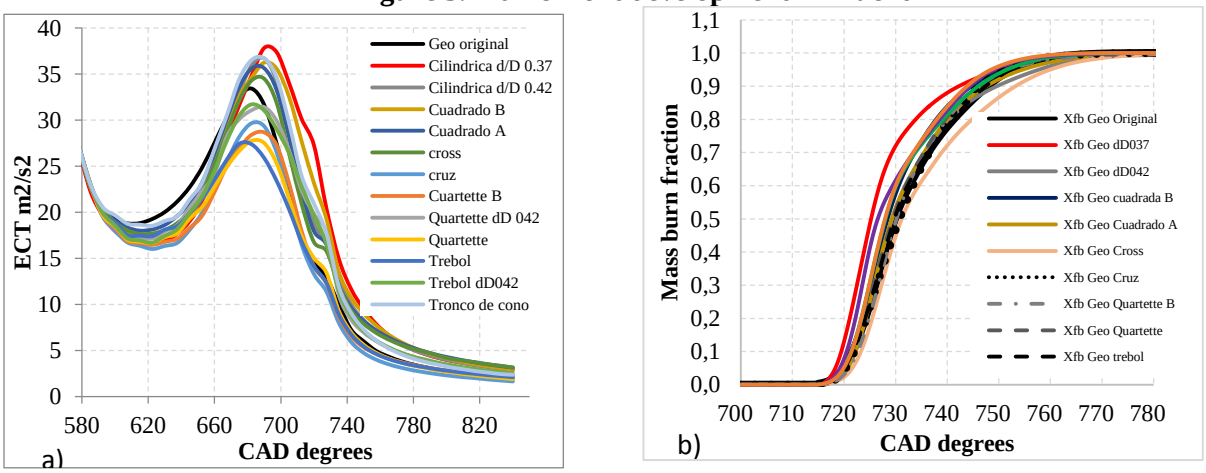

Figure 4 a) Turbulent kinetic energy and b) mass burn fraction of for all simulated geometries

Figure 6a presents the Damköhler (Da) number, which indicates that the relationship between the characteristic physical flow time and the characteristic chemical time. The Da was smaller for geometry d/D 0.37 at all points. The characteristic physical flow time depends on the integral scale and the turbulence intensity; since the turbulence intensity increased, the flow time decreased. This leads to improved chemistry inside the combustion chamber, which can burn a fuel faster. Figure 6b also presents the Reynolds number on the integral scale, comparing CFD simulations for geometry d/D 0.37 and the original geometry. At the end of the compression stroke and during combustion, the Reynolds number was greater for geometry d/D 0.37. At TDC the modified geometry increased the turbulence levels by 66% with respect to the Reynolds number on the integral scale. The Damköhler number and the Reynolds number validated the geometry change from the original to d/D 0.37.

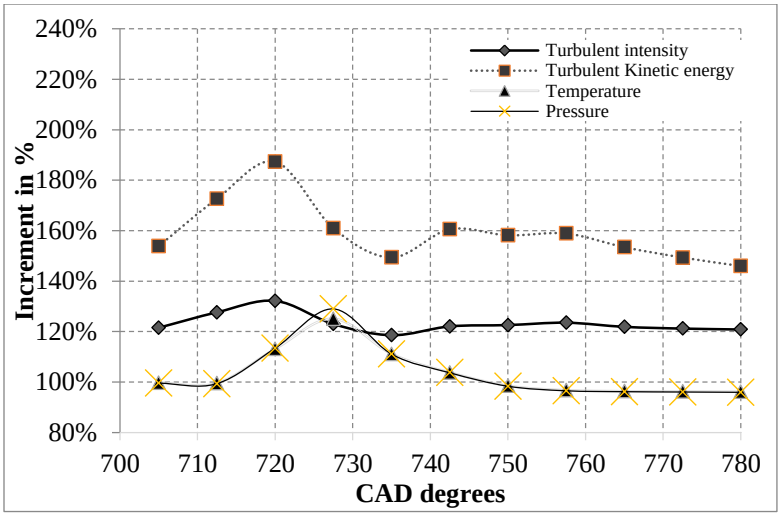

Figure 5 Magnitude of various variables, CFD simulations, original geometry vs d/D 0.37

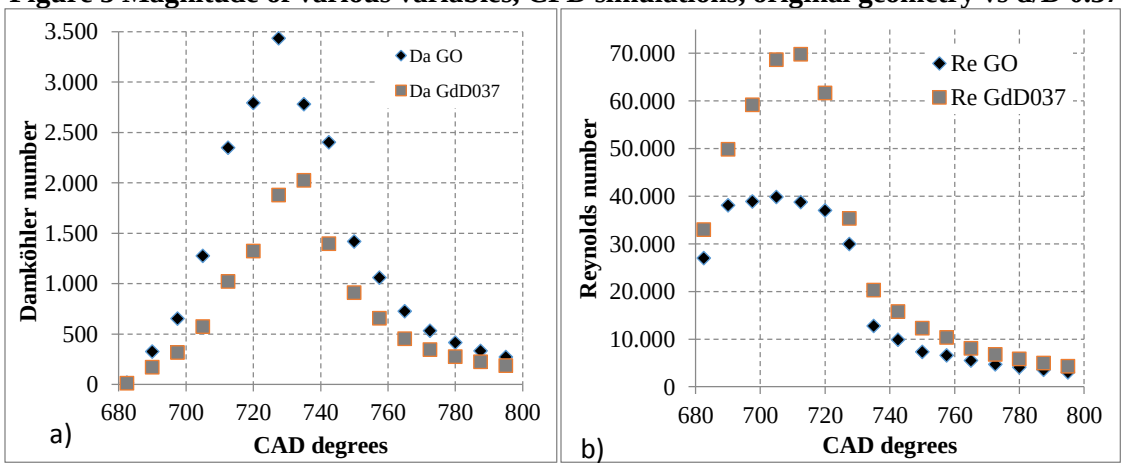

Figure 6 a) Damköhler number and b) Reynolds on the integral scale. CFD simulations for the ideal geometry, original vs. d/D 0.37

5.5.3.2 Experimental results

Figure 7a shows the results of the measurements and calculations of output power and generating efficiency for the tests before and after the PCCGC. The purpose of the PCCGC was to increase the turbulence intensity in-cylinder at the moment when combustion begins, in order to induce a greater turbulent flame front speed. After the PCCGC, the first observable effects were a change in the sound of engine operation and that the engine had a greater knocking tendency than before for all the blends studied in this research. This made it necessary to operate the engine at lower output powers, so that the knock peak pressure would average between 0.3 and 0.5 bar over 200 consecutive cycles. Operation with 100NG had a power derating of 27.2% after the PCCGC, due to the increase in knocking tendency. The increase in turbulence intensity clearly increased the engine knocking tendency, apparently for two reasons: 1. The increase in turbulence intensity increases the heat transfer from the flame front to the end gas, which results in higher end gas temperatures. 2. Higher pressure at the end of the compression stroke, which increases the end gas pressure, reduces the end gas ignition delay time. Blends 83B17P, 79B16P5H, and 75B15P10H had a 40% power derating, on average, while blends 57B38M5H and 54B36M10H had a 30% of power derating, on average, all blends being limited by the increased knocking tendency. According to the results, blends with a higher MN have lower power derating, while blends with low MN have greater power derating. Blend 50B50M, with a MN of 120, had a power derating of 14.5%, while 100B achieved a comparable output power to operation before the PCCGC, but now the maximum output

power to 100B was limited by the knocking threshold. Figure 7b presents the generating efficiencies, which were reduced for all the blends after the PCCGC due to the reduced output power related with the increase in knocking tendency to operate the engine below the knocking threshold. Generating efficiency was reduced by 6.34%, on average, for all the blends. The smallest reduction in generating efficiency was 1% for blend 50B50M. Blends 83B17P, 79B16P5H, and 75B15P10H had a generating efficiency reduction of 12%, on average, due to the drastic output power reduction. Pure biogas had a generating efficiency reduction of 3.3%. The new engine characteristic result in a SI engine with high knocking tendency because of the conditions of high pressure, temperature and turbulence, is clear than the engine is not a conventional SI engine. Figure 8a presents the ST for optimum generating efficiency before and after the PCCGC. Due to the increased engine knocking tendency after the PCCGC, a lower ST advance was required to prevent knocking. In general, all of the ST advances were low; the blends with high MNs had STs greater than 4 CAD degrees before top dead center (BTDC), while low MN blends had STs of 2 or 3 CAD degrees BTDC. The low ST advance values are due to the objective to obtain the maximum possible output power under the knocking threshold. The exhaust temperatures are shown in Figure 8b. All tests after the PCCGC resulted in lower exhaust gas temperatures due to the engine's reduced output power. Notably, lower exhaust temperatures indicate lower flame temperatures, and as all the tests were carried out near the knocking threshold, it can be concluded that knocking occurred at a lower temperature after the PCCGC. The average exhaust temperature difference was 35.7°C.

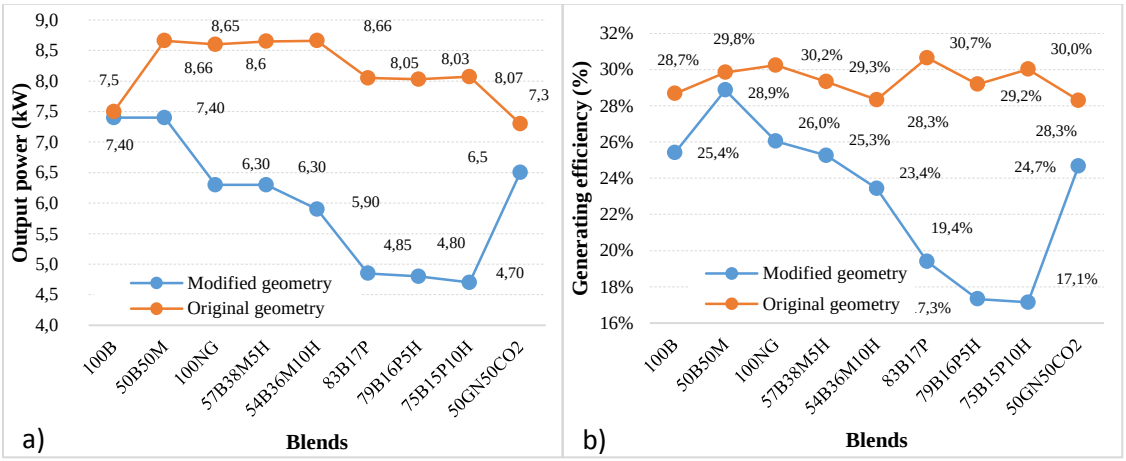

Figure 7 a) Output power and b) Generating efficiency, before and after the PCCGC

Diesel engines have high volumetric efficiencies, overcoming the resistance of the throttle valve at partially open positions without significant declines in generating efficiency. This is shown in Figure 7b by the results before the PCCGC, where values above 30% in generating efficiency were obtained. Figure 9 indicates that after the PCCGC, although achieving a lower output power, the throttle valve open percentage was reduced by 25%, on average. In the case of biogas, the throttle valve position was reduced from 75% to 53% open while achieving a similar power output. Due to these low throttle valve open percentages, large pressure drops are expected on the intake stroke. Comparing biogas performance before and after the PCCGC provides a crucial reference because the output power is similar, besides engine speed, and equivalence ratio were all similar, and thus the amount of air and fuel required to reach the maximum output power.

Figure 10 shows in-cylinder pressures. Figure 10a presents a comparison before and after the PCCGC for fuels 100B and 50B50M. The pressure during the compression stroke was higher after the PCCGC, the new pressure curves having a different shape and resulting in higher pressures at the end of the compression stroke despite the fact that the CR was similar to the original geometry. For biogas, compared at similar output power, the pressure at the end of the compression stroke was higher by about 9 bar after the PCCGC. For 50B50M, while producing 1.2 kW less after the PCCGC, the pressure at the end of the compression stroke was higher by about 8 bar. Even with the reduced output power, the final pressure at the end of the compression stroke was considerably higher for the blend, which increased the

engine's knock tendency. According to the results obtained in the runs before the PCCGC, the ideal peak pressure location should be in the range of 12-17 degrees ATDC. Due to the reduced ST advance used with the new geometry, the peak pressure locations move forward slightly in the expansion stroke, leading to the generating efficiency decreases. Biogas and 50B50M had the best combustion phasing, the high knock resistance permitting a more advanced ST. Their peak pressure locations were around 17 CAD degrees ATDC, with lower peak pressures, signifying that knocking occurred at lower pressure and temperature but with greater turbulence. Figure 10b shows the in-cylinder pressure after the PCCGC for all the blends. In general, the shapes of the new curves were different, with higher pressures at the end of the compression stroke for all the blends, and the location of the peak pressures shifted close to 20 CAD degrees ATDC, due to the small ST used to avoid detonation.

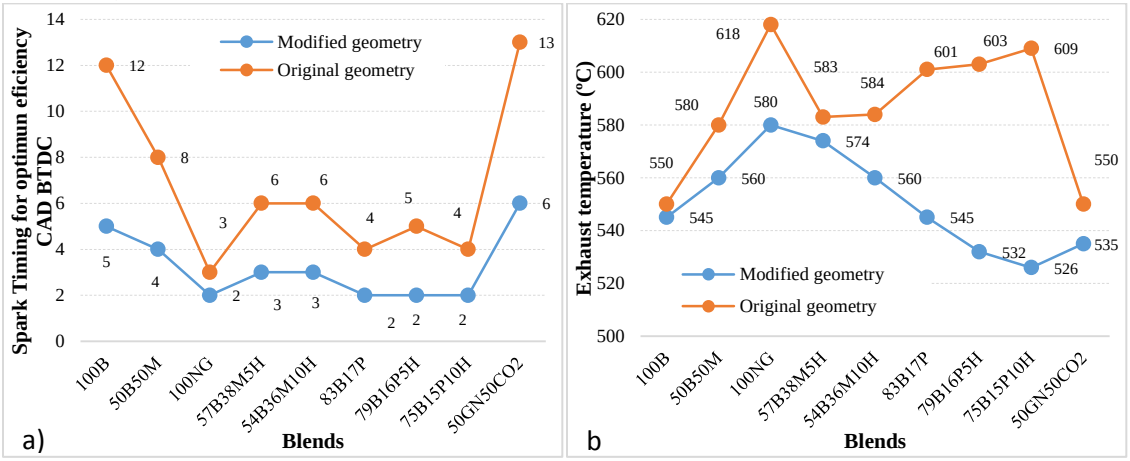

Figure 8 a) ST adjusted for optimum generating efficiency, b) Exhaust temperature, before and after the PCCGC

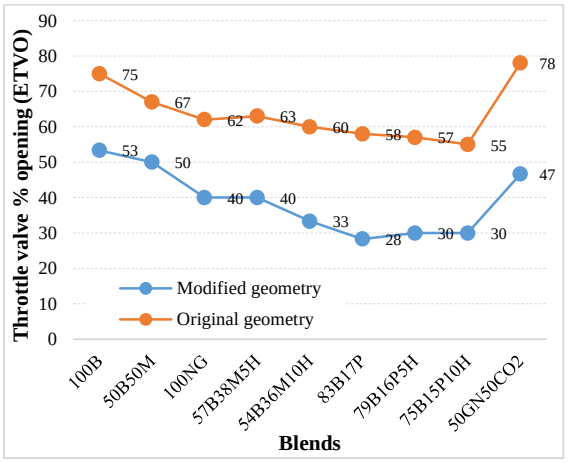

Figure 9 Throttle valve % opening, before and after PCCGC

Figure 11 shows the calculated heat release rates. Figure 11a compares before and after the PCCGC for blends 100B and 50B50M. Due to the smaller ST after the PCCGC, the heat release starts after TDC. Before the PCCGC, biogas had a ST of 12 CAD degrees BTDC and heat release started at 8 CAD degrees BTDC. After the PCCGC, biogas had a ST of 5 CAD degrees BTDC and heat release started at 2 CAD degrees ATDC. Thus in the case of biogas, there was an increase in the ignition delay time after the PCCGC, adding approximately 3 CAD degrees to the delay before the initiation of heat release. This suggests that the increased turbulence delays the kernel onset to the flame front formation, as described in literature [5, 6, 30]. The greater ST before the PCCGC resulted in better combustion phasing, where the maximum heat release rates occurred at close to 10 CAD degrees ATDC, while the maximum heat release rates after the PCCGC were closer to 15 CAD degrees ATDC, as is shown in Figure 11b. This caused the

generating efficiency to decrease due to non-ideal combustion phasing. Furthermore, the increased turbulence caused the heat release to complete earlier. In the case after PCCGC, biogas heat release occurred between 2 and 29 CAD degrees ATDC, taking 27 CAD degrees to complete the heat release. Before the PCCGC, biogas heat release occurred between -8 and 24 CAD degrees ATDC, taking 32 CAD degrees to complete the heat release, requiring 5 CAD degrees more before PCCGC. This suggests that the reduced combustion duration after the PCCGC is due to the higher turbulence intensity, indirectly measuring the turbulence intensity increase achieved by the PCCGC.

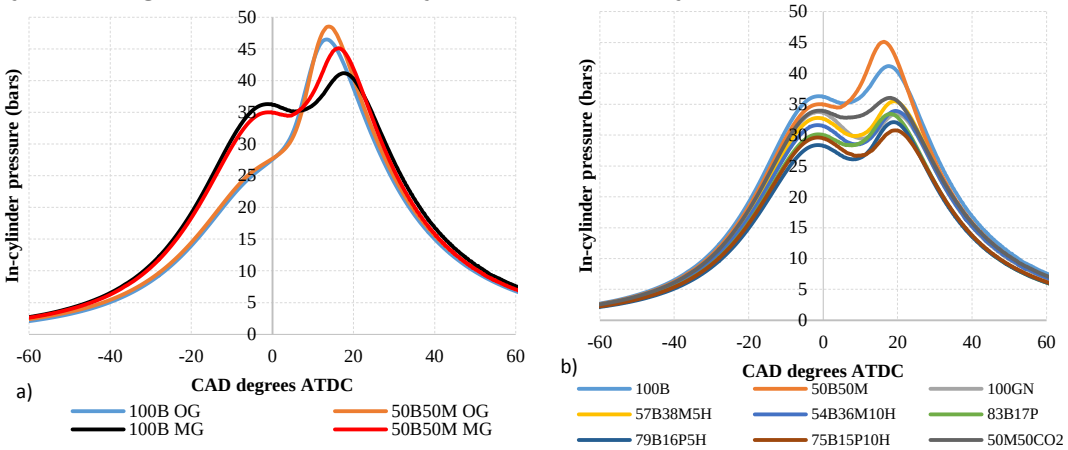

Figure10 In-cylinder pressure a) comparison before and after PCCGC b) all blends after PCCGC

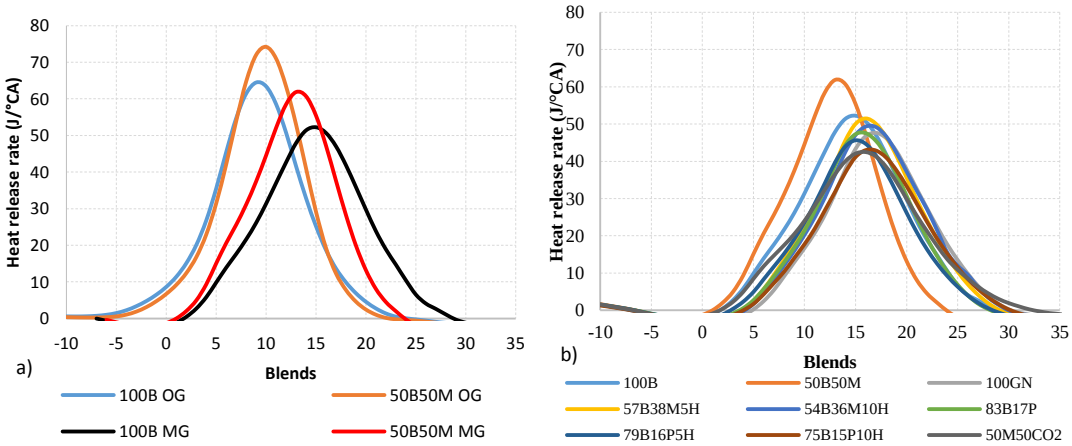

Figure 11 Heat release rate a) Comparison before and after PCCGC b) All blends after PCCGC

Figure 12 presents the mass fraction burn duration to 5% and 50% for before and after the PCCGC. Before the PCCGC the 0-5% burn duration range was between 5.7 and 6.9 CAD degrees for all blends, while after the PCCGC the range was between 6.5 and 8.5 CAD degrees, even with lower output power for all the blends. The increased interval indicates a greater delay for the flame front formation, caused by the increased turbulence intensity, which increases the resistance to flame front formation as could read with biogas which increase 1.5 CAD degrees to 0-5% burn duration, but to 0-50% burn duration was reduced from 20.4 CAD to 18.4 CAD degrees, indicating that after flame front formation the 0-50% burn duration is decreased by 2 CAD degrees by the increase in turbulence intensity with similar operational conditions. For blend 50B50M the decrease was 1.2 CAD degrees. For other blends, the 0-50% burn duration was 17.7 to 18.4 CAD degrees before the PCCGC, and after the PCCGC was 16.7 to 18.3 CAD degrees. In general it is clear that the 50% mass fraction burn duration was reduced by the increase in the turbulence intensity by the PCCGC, which increased turbulent flame speed.

Figure 13 presents the mass fraction burn duration to 90%, as well as the combustion duration between 5%-90% burn, before and after the PCCGC. For biogas, the 0-90% burn duration decreased by 4 CAD degrees and for blend 50B50M it decreased by 4.7 CAD degrees, on average. For the other blends, the 0-

90% burn duration was in the range of 24.6-26.1 CAD degrees before the PCCGC, while after the PCCGC the range was 23.1-24.5 CAD degrees. For both biogas and 50B50M, the combustion duration (5%-90% burn) decreased by 5.5 CAD degrees. For the other blends, the combustion duration was 18.2-19.9 CAD degrees before the PCCGC, while after the PCCGC, the combustion duration was 14.8-16.6 CAD degrees. In general the PCCGC resulted in an increase in the turbulence intensity, which increased the turbulent flame speed for all blends, decreasing combustion duration under conditions of lower output power and near to knocking threshold, knocking occurred at lower pressure and temperature but higher turbulence.

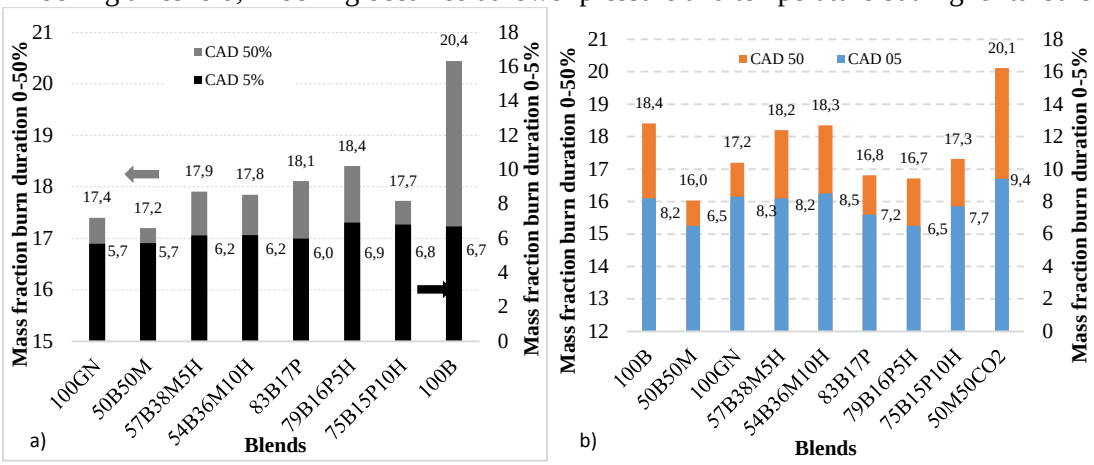

Figure 12 Mass fraction burn duration to 5% and 50% a) before and b) after the PCCGC

Figure 14 shows the average peak pressure and location over 200 cycles. The average peak pressure decreased for all the blends; for biogas it decreased by 5.2 bar, for blend 50B50M it decreased 5.1 bar, and for natural gas it decreased by 7.5 bar. To biogas the maximum output power after the PCCGC was not limited by the energy density, but by the occurrence of knocking. Biogas and 50B50M have high MNs, achieving output powers above 7.4 kW. The highest peak pressures were not above 43.4 bars, a pressure that before the PCCGC was common in the engine operation. Knocking occurred at lower pressure and temperature, and higher turbulence intensity, after the PCCGC. This increase in knocking tendency had a stronger effect on fuels with a high laminar flame speed, which is proportional to the turbulent flame speed. Thus after the PCCGC, due to more turbulent conditions, blends that contain propane were the most affected, followed by blends 54B36M10H, 57B38M5H, and natural gas. 50B50M and 100B, having MN above 120, were the least affected, reaching the highest output powers and maximum peak pressures.

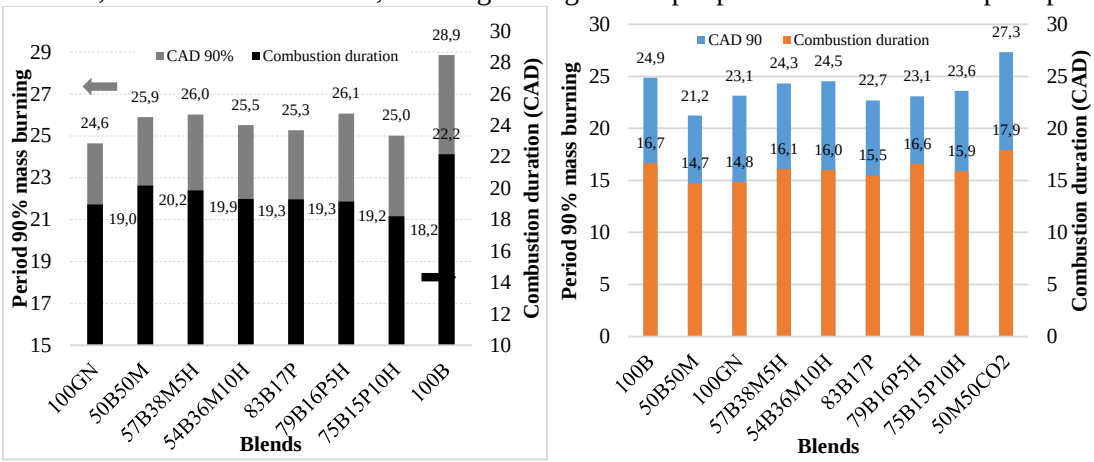

Figure 13 Mass fraction burn duration to 90% and combustion duration measured between 5%-90% a) before b) after the PCCGC

Figure 15 presents the global indicated mean effective pressure (IMEPg) and coefficient of variation in indicated mean effective pressure (COV IMEPg) before and after the PCCGC. Biogas' IMEPg had a reduction of 0.2 bar, while blend 50B50M had a reduction of 0.5 bar. Before the PCCGC, other blends

IMEPg's varied between 4.4 and 5.3 bar, while after the PCCGC their IMEPg's varied between 4.1 and 4.5 bar, indicating that knocking occurred at a lower IMEPg after the PCCGC. For all blends the maximum values for peak pressure, heat release rate, IMEPg, and exhaust temperature were lower after the PCCGC, indicating that the increase in engine knocking tendency was only due to the increased turbulence intensity, since there were no other modifications made to the engine. Knocking tendency appears to increase with increasing turbulent flame speed, blends with higher laminar flame speeds were more affected by knocking. The COV IMEP served as control data while measuring the maximum output power, required to be less than 4% on average over 200 cycles, as can be seen in figure 15.

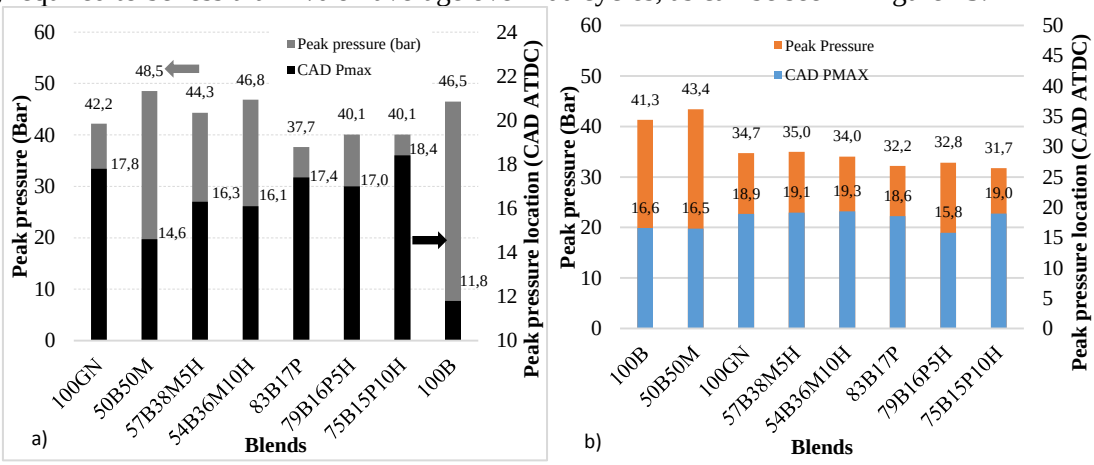

Figure 14 Peak pressure and location a) before b) after the PCCGC

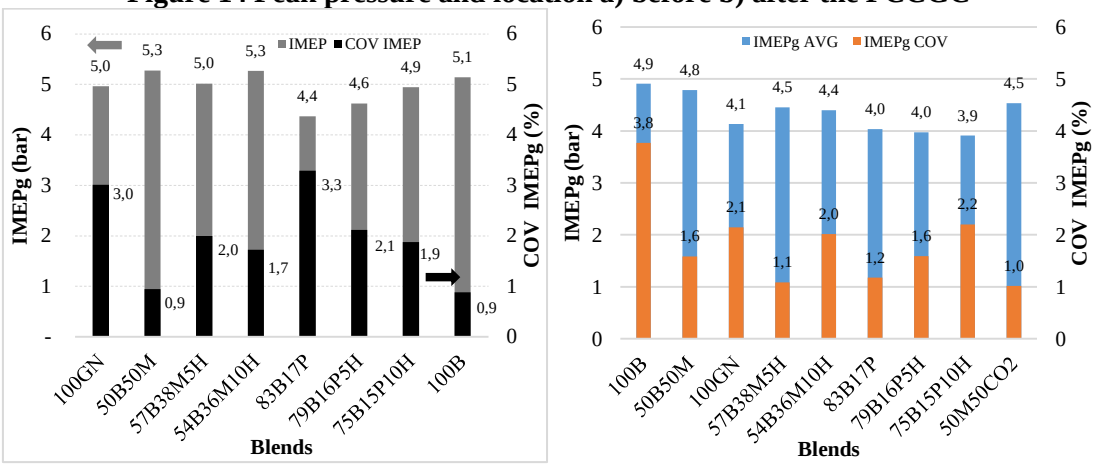

Figura 15 IMEP and COV IMEP a) before and b) after the PCCGC

5.5.4 Conclusions

This research presents the results of experimental tests performed on an SI engine with a high CR and with the PCCGC, with a bowl diameter to piston diameter ratio of 0.37, in order to increase the turbulence intensity at the end of the compression stroke and during the combustion process. The general purpose was to find the best operating conditions for biogas, which is one of the main alternative fuels. The main comments and conclusions of this research are presented:

- The combined effect of a high CR and high turbulence intensity in the SI engine resulted in a higher knocking tendency. After the PCCGC, knocking occurred at lower end-gas pressure and temperature, but with greater turbulence intensity. Therefore, all blends reached lower output power and reduced generating efficiency after the PCCGC.
- The blends most affected by the increased knocking tendency were those with high laminar flame speeds and low methane numbers, forcing a greater reduction in output power in order to be under the knocking threshold. Blend 75B15P10H was the most affected by the PCCGC.

- Biogas and purified biogas produced the highest output powers, even greater than natural gas, due to the high knock resistance under extreme conditions of pressure, temperature, and turbulence.
- The pressure during the compression stroke was higher after the PCCGC for all blends, while peak pressure and combustion temperature were lower.
- For all the blends lower ST was required after the PCCGC in order to achieve the maximum output power while remaining under the knocking threshold.
- After the PCCGC the throttle valve open percentage was 25% smaller on average.

References

1.Johansson, B. and K. Olsson, Combustion Chambers for Natural Gas SI Engines Part I: Fluid Flow and Combustion in International Congress and Exposition, S.T.P. SERIES, Editor. 1995: Detroit, Michigan.

2.Olsson, K. and B. Johansson, Combustion Chambers for Natural Gas SI Engines Part 2: Combustion and Emissions in International Congress and Exposition, S.T.P.S. 950517, Editor. 1995.

3.Wise, D.M., D.B. Olsen, and M. Kim, Development of a Lean Burn Methane Number Measurement Technique for Alternative Gaseous Fuel Evaluation. Proceedings of the ASME 2013 Internal Combustion Engine Division Fall Technical Conference.

4.Heywood, J.B., Combustion and its modeling in spark ignition engine, in International Sympsium Comodia 94.

5.Heywood, J.B., Internal Combustion Engines Fundamentals, ed. M.G. Hill. 1988.

6.Heywood, J.B. and J. TAGALIAN., Flame Initiation in a Spark-Ignition Engine. COMBUSTION AND FLAME 64:243-246,

7.Bates, S.C., Flame Imaging Studies of Flame Development in a SI Four-Stroke Engine, in Engine Research Department, W. General Motors Research Laboratories, Michigan, Editor.

8.Bonatesta, F., Premixed Combustion in Spark Ignition Engines and the Influence of Operating Variables ed. http://dx.doi.org/10.5772/55495. 2013.

9.Mehrzad Kaiadi, P.T., Ashish Shah, Extending the performance, fuel efficiency and stability of stoichiometricspark ignition natural gas engines – Gas engine research at KCFP 2007-2012, S.G.C. AB, Editor. 2013.

10.Zefaan, H. 2012, "Combustion chamber geometry effects in spark ignitionengine exhaust emissions", Australian Journal of Mechanical Engineering, Vol. 10, No. 1, pp.29-40, http://dx.doi.org/10.7158/M11-799.2012.10.1.

11.Karim, G.A., Autoignition and Knock in Engines Fueled with Hydrogen and Hydrogen Supplemented Gaseous Fuel Mixtures, U.o.C. Mechanical Engineering, Editor.

12.YU, X., et al., Optimize Combustion Of Compressed Natural Gas Engine By Improving In-Cylinder Flows International Journal of Automotive Technology, 2013. Vol. 14, No. 4, pp. 539−549.

13.Mardi K, M., S. Khalilarya, and A. Nemati, A numerical investigation on the influence of EGR in a supercharged SI engine fueled with gasoline and alternative fuels. Energy Conversion and Management, 2014. 83: p. 260-269.

14.Zaker, K., et al., Open cycle CFD investigation of SI engine fueled with hydrogen/methane blends using detailed kinetic mechanism. International Journal of Hydrogen Energy, 2015. 40(40): p. 14006-14019.

15.Harshavardhan, B. and J.M. Mallikarjuna, Effect of piston shape on in-cylinder flows and air–fuel interaction in a direct injection spark ignition engine – A CFD analysis. Energy, 2015. 81: p. 361-372.

16.Kosmadakis, G.M., et al., CFD modeling and experimental study of combustion and nitric oxide emissions in hydrogen-fueled spark-ignition engine operating in a very wide range of EGR rates. International Journal of Hydrogen Energy, 2012. 37(14): p. 10917-10934.

17.Kosmadakis, G.M., D.C. Rakopoulos, and C.D. Rakopoulos, Investigation of nitric oxide emission mechanisms in a SI engine fueled with methane/hydrogen blends using a research CFD code. International Journal of Hydrogen Energy, 2015. 40(43): p. 15088-15104.

18.Duan, J., F. Liu, and B. Sun, Backfire control and power enhancement of a hydrogen internal combustion engine. International Journal of Hydrogen Energy, 2014. 39(9): p. 4581-4589.

19.Ji, C., et al., Numerical investigation on the combustion process in a spark-ignited engine fueled with hydrogen–gasoline blends. International Journal of Hydrogen Energy, 2013. 38(25): p. 11149-11155.

20.Ji, C., et al., Development and validation of a laminar flame speed correlation for the CFD simulation of hydrogen-enriched gasoline engines. International Journal of Hydrogen Energy, 2013. 38(4): p. 1997-2006.

21.M. Metghalchi, J.K., Burning velocities of mixtures of air with methanol, isooctane, and indolene at high pressure and temperature. COMBUSTION AND FLAME 48:191-210 (1982).

22.Chen Y. and Raine R. A study on the influence of burning rate on engine knock from empirical data and simulation. Combustion and Flame 162 (2015) 2108–2118.

23.Breaux B., Hoops C. and Glewen W. The Effect of In-Cylinder Turbulence on Lean, Premixed, Spark-Ignited Engine Performance Journal of Engineering for Gas Turbines and Power. AUGUST 2016, Vol. 138 / 081504-1

24.Juan Pablo GÓMEZ MONTOYA, Andres AMELL, Jaime ZAPATA, Experimental study of spark ignition engine performance and emissions in a high compression ratio engine using biogas and methane mixtures without knock occurrence. Thermal Science: Year 2015, Vol. 19, No. 6, pp. 1919-1930. DOI 10.2298/TSCI140829119G, 2015.

25.2006, F.U.s.G.S., F. Inc, Editor.

26.V. Zimont. Gas Premixed Combustion at High Turbulence. Turbulent Flame Closure Model Combustion Model. Experimental Thermal and Fluid Science, 21:179-186, 2000.

27.Combustion Research Group. <http://web.eng.ucsd.edu/mae/groups/combustion/mechanism.html>. UC San Diego. Web page was accessed inMarch, 2015.

28. Martinez *et al* reduced chemical kinetic mechanism for CFD simulations of high BMEP lean-burn natural gas engines. Proceedingsof the ASME internal combustion engine division spring technical conference;2012.

29. J.P. Gómez Montoya et al. Prediction and measurement of the critical compression ratio and methane number for blends of biogas with methane, propane and hydrogen/ Fuel 186 (2016) 168–175

30. Gatowski J.and Heywood J.B. Flame Photographs in a Spark-Ignition Engine. Combustion and Flame 56: 71-81.

5.6 Biogas SI engine operating under conditions of high CR and high turbulence intensity.

Abstract

A change of paradigm is presented; biogas is more powerful than diesel, natural gas, and some blends studied. A diesel engine was converted to SI, to be used with gaseous fuels. The engine had a high compression ratio with the intention to achieve high generating efficiencies; combustion chamber geometry was modified to increase the turbulent flame speed and thus reduce the knocking tendency. The fuels used were: Natural gas, biogas, and seven blends of biogas with methane or propane and hydrogen additions. The blends were used to improve biogas' combustion properties and determine the best blend for the research. Biogas (60% fuel and 40% CO_2) was simulated using 3 different fuels: Two different natural gases, with methane numbers (MN) 87 and 75, and pure methane with MN 100; these test are used to estimate the sensitivity of knocking to the biogas base fuel's chemical composition. Maximum output power is just below the knocking threshold. Biogas in a SI engine with high compression ratio and high turbulence intensity resulted in the fuel with the highest output power generation, because of the high knocking resistance and improved turbulent flame speed by the increase in the turbulent intensity at the end of the compression stroke. Due to the high turbulence intensity after the change in the combustion chamber geometry, the knocking tendency of the engine was increased, requiring a reduction in the output power, compared to the original geometry. There is a direct relation between MN and maximum output power energy density. There is an inverse relation between maximum output power with energy density, laminar flame speed and adiabatic flame temperature. The ideal turbulent flame front is a flame front that burns at high pressure and high turbulence intensity using a fuel with high knocking resistance, low laminar flame speed and low flame temperature. Blends with a low MN must be burned with low turbulence intensity and blends with a high MN must be burned with high turbulence intensity.

5.6.1 Introduction

Biogas is the product of anaerobic digestion of organic matter, which can be formed spontaneously in landfills or in a controlled manner in digesters. It is now viewed as an important energy source because of the current efforts to reduce the use of and dependence on fossil fuels. Biogas production technology provides a unique set of benefits, such as improving the environment for users merely by reusing the organic material in trash, and being a sustainable energy resource. Despite increased research on digesters, the use of biogas in internal combustion engines for power generation is not increasing significantly due to the problems associated with biogas, such as low heating value, low flame speed and high content of inert gases, which have led to biogas being considered an energetically poor fuel [1-8].

Knocking is an abnormal combustion phenomenon, which adversely affects the performance, emissions, and service life of spark ignition (SI) engines. The normal combustion event of a SI engine can be described as a turbulent flame front that originates at the spark plug and moves through the air and fuel mixture in a controlled way, mainly governed by the chemical kinetics of the oxidation process. The portion of the unburned mixture ahead of the flame front is called "end gas". During normal engine operation, the flame front propagates through the end gas, consuming the mixture in a controlled way. By contrast, knocking describes a phenomenon of abnormal combustion that produces an audible sound due to the autoignition of the end gas before it is consumed by the flame front, leading to a rapid increase of the in-cylinder pressure and extremely localized temperatures. When knocking occurs, the mixture burns quickly and releases energy between 5 to 25 times faster than during normal combustion, causing large pressure waves with an amplitude of several bar and speeds of up to 2000 m/s. These pressure waves cause high-frequency oscillations of the in-cylinder pressure, producing a sharp sound [9, 17].

The knocking threshold is a measure to determine the onset of knocking. Habitually, the knocking value is quantified as the maximum change in in-cylinder peak pressure as measured with a piezoelectric sensor. The knocking threshold can be defined as the point at which the knocking becomes audible. However, in this research the knocking threshold was defined as half the peak pressure measured at the onset of audible knocking; knocking threshold is not audible during engine operation, but measured with an in-cylinder pressure sensor. This knocking threshold establishes the maximum output power that can be produced by

an SI engine under stable combustion conditions. For this research, the knocking threshold was defined as a knock peak pressure between 0.3 and 0.5 bars, on average over 200 consecutives cycles [18]. Biogas was the only blend than could take advantage of the engine's characteristics: 1. High compression ratio for high output power and high generating efficiency, fitting due to biogas' high knock resistance 2. High turbulence intensity and, consequently, increased turbulent flame speed, which is usually low for biogas due to its low laminar flame speed. Other blends could not take advantage of the high turbulence intensity after the change in the combustion chamber geometry due to their high knocking tendency [22].

The final ideas from this research are presented below in the section of conclusions and comments, according to the test results of the global research and the following own considerations:

First, knocking has some special characteristics: 1. Knocking is a random vibrational phenomenon, which is completely evident when the engine is operating in this condition. The engine's entire structure vibrates in proportion to knocking intensity. Knocking intensity changes cycle-to-cycle even at constant engine operation, air flow, fuel flow, and spark timing (ST). 2. Knocking generates high-frequency pressure waves. The oscillations of the in-cylinder pressure are caused by the random locations in the end gas autoignition. Each end gas autoignition point generates a pressure wave, which travels inside the combustion chamber in different directions and interacts with other pressure waves generated by others autoignition points. Thus a variable pressure field is created in the combustion chamber, the expansion waves and the reflection of these waves by the chamber walls creating the oscillatory pressure-versus-time record, as can be measured at a given point with a piezoelectric pressure sensor. Some autoignition points cause autoignition at other points, due to the increase in pressure and temperature at a local autoignition point. 3. Knocking releases energy faster and causes faster temperature rises. The fuel's energy is released by autoignition, and with increased knocking intensity, the heat release rate is increased as well, resulting in higher temperature rises [22].

Second, knocking depends on several factors, mainly: 1. Fuel chemical composition. Blends that include gases like hydrogen (H_2), carbon monoxide (CO), and propane (C_3H_8) are more prone to knocking. On the other hand, methane has the highest knock resistance, and inert gasses like carbon dioxide (CO_2) and nitrogen (N_2) increase the knock resistance of the blend. Fuel chemical composition is vital for determining the knocking tendency, which has been quantified with MN. 2. Laminar flame speed. Fuels with a high laminar flame speed have a high turbulent flame speed, and a high turbulent flame speed reduces combustion duration and thus probability of knocking. However, according to test results, extreme turbulence intensity can increase the knocking tendency and blends with high laminar flame speed can have a high knocking tendency. 3. Spark timing. ST is the most common way of controlling knocking, reducing the end gas temperature by delaying the ST. However, this may reduce engine performance. 4. Turbulence intensity. A reduction in combustion duration results in a lower knocking tendency, which can be obtained by increasing the turbulent flame speed by increasing the turbulence intensity at the end of the compression stroke. However, in this research it was found that high turbulence intensity resulted in a higher knocking tendency. Thus each blend must be matched with its ideal combustion chamber geometry. Blends with low MN must be burned with low turbulence intensity and blends with high MN, such as biogas, must be burned with a high turbulence intensity to take advantage of the high turbulent flame speed [23]. 5. Compression ratio. A higher CR results in higher pressure and temperature at the end of the compression stroke, which increase the knocking tendency. MN methodology also measures the critical compression ratio for each fuel under specific operating conditions. 6. Pressure at the end of the compression stroke. Depending on the throttle valve opening percentage, the equivalence ratio, and fuel chemical composition, a higher pressure at the end of the compression stroke increases the knocking tendency. 7. Temperature at the end of the compression stroke. Depending on the change in specific heat ratio, lean mixtures increase the temperature at the end of the compression stroke, increasing the knocking tendency. 8. Equivalence ratio. Lean combustion reduces the knocking tendency because the excess nitrogen increases the ignition delay time of the end gas. However, this research found that lean combustion increased the knocking tendency due to the dominant effect of the higher pressure at the end of the compression stroke reducing the ignition delay time. 9. Inlet pressure and temperature. Increasing the inlet pressure leads to higher pressure at the end of the compression stroke, reducing the ignition delay

time of the end gas. The inlet temperature has a similar effect, and thus a higher inlet pressure or temperature increases the knocking tendency. 10. Number of spark plugs. If the flame front is generated in different places at the same time, the probability of knocking is reduced due to the lower combustion duration. 11. Combustion chamber design. If the distance between the spark plug and the walls is reduced, changing the combustion chamber geometry, the time to burn the mixture is reduced and thus the knocking tendency is also reduced. 12. Flame temperature. Fuels with high flame temperatures will have a higher knocking tendency, as the heat transfer from the flame front to the end gas is higher, reducing the ignition delay time. 13. Amount of residual gases and exhaust gas recirculation. In both cases, the presence of inert gases at the initiation of combustion reduces the flame temperature and thus the knocking tendency [9,12,22].

This paper presents the final research results with the main goal of finding the best operating conditions for biogas in a named biogas SI engine, which is a diesel engine transformed to SI using a high CR to achieve high output power and generating efficiencies, and modifying the combustion chamber geometry to increase the turbulence intensity at the end of the compression stroke and during combustion with respect to the original diesel piston geometry. The intention was to increase the turbulent flame speed and reduce the probability of knocking, as knocking reflects the outcome of a competition between the flame front and the pre-combustion reactions of the end gas. Knocking will not occur if the flame front consumes the whole mixture before pre-combustion reactions cause end gas autoignition. Blends of biogas with methane or propane and hydrogen additions, were used to improve biogas' combustion properties, such as minimum ignition energy, ignition limits, laminar flame speed, energy density, and low heating value. The combustion chamber geometry modification resulted in a higher knocking tendency, which is the result of the more extreme pressure, temperature, and turbulence conditions after the modification. In general, as the knocking tendency of the engine was increased, natural gas and all of the blends required a reduction of the output power in order to be below the knocking threshold. Before the combustion chamber modification, all blends obtained output powers greater than 8 kW @ 1800 rpm, the maximum output power of the original diesel engine as presented previously, whereas biogas obtained 7.5 kW, limited by its low energy density and low heating value [22]. This paper also presents the main concepts required to design biogas SI engines, namely high CR and high turbulence intensity. There is a relation between methane number (MN) and maximum output power, enabling that a biogas SI engine be used similarly to a CFR engine to test the knocking tendency of gaseous fuels. Laminar flame speed, energy density, and adiabatic flame temperature are compared with MN to determine relation between properties.

5.6.2 Experimental setup and general procedure for testing

Scheme 1 Main details of the engine conversion

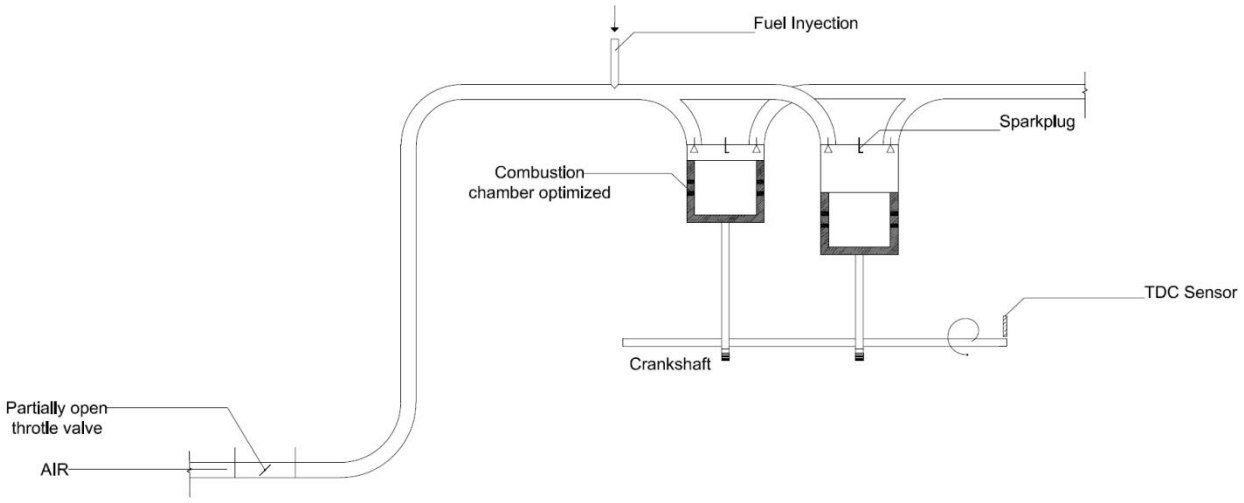

The following actions were performed to transform the engine from diesel to biogas SI engine: 1. Diesel injectors were removed and replaced with high-capacity spark plugs. The spark plugs were added to the

power supply system, and a sensor located on the crankshaft to program the ST. 2. The smallest commercial throttle valve available was used for controlling the equivalence ratio. 3. Blends were injected close to the inlet port at a pressure between 2 and 3 bars. Blends were mixed using a mixer, while the fuel and air were controlled independently to ensure the correct equivalence ratio. 4. Combustion chamber geometry was optimized using CFD simulations to increase turbulence intensity during combustion. Scheme 1 presents the main details of the engine conversion.

5.6.2.1 General procedure for testing

All tests presented used a modified combustion chamber geometry, which produced high turbulence intensity at the end of the compression stroke. The tests showed that greater turbulence intensity led to a greater knocking tendency for all blends except for biogas [22]. The fuels used in this research were: biogas and various biogas blends with natural gas or propane and hydrogen additions. To simulate biogas, 3 different gases were used as base fuel: methane with a MN of 100, natural gas with a MN of 87, and natural gas with a MN of 75. These base fuels were used to estimate interchangeability problems due to variations in their chemical composition. Table 1 presents the base fuels designations and chemical compositions, and Table 2 presents their properties. The simulated biogas used was a mixture of 60% base fuel and 40% CO_2.

Table 1 Base fuels designation and chemical composition

Fuels	Designation	CH_4	C_3H_8	C_2H_6	CO_2	N_2
Methane	M NM 100	100,0%	0,0%	0,0%	0,0%	0,0%
Natural gas A	GN NM 87	95,0%	2,5%	0,0%	2,5%	0,0%
Natural gas B	GN NM 75	87,3%	3,4%	7,1%	1,4%	0,8%

In each case the engine was operated at maximum output power, close to the knocking threshold, and for each blend the ST was adjusted for optimum generating efficiencies. MN of the natural gas was estimated using software Methane 3.1 from AVL. Table 3 presents some blend properties using methane as base fuel in biogas. The tests for all the blends were done with an equivalence ratio of 0.9, which was selected as it generally obtained the highest output power with a slight air excess to ensure complete combustion of the blends. A sweep of the equivalence ratio to biogas was performed.

Table 2 Base fuels properties at standard conditions

Fuels	LHV MJ/m^3 fuel	LWI MJ/m^3 fuel	Va m^3 air/m^3 fuel	Energy density MJ/m^3aire	MN	Laminar flame speed (cm/s)
M NM 100	33,93	45,59	9,52	3,56	100	39,11
GN NM 87	34,54	45,83	9,67	3,57	87,2	39,82
GN NM 75	36,98	46,32	10,31	3,59	75,3	40,95

5.6.3 Experimental results

5.6.3.1 Experimental results for all blends with three base fuels to simulate biogas, at an equivalence ratio of 0.9

All the results presented are after the combustion chamber modification. Figure 2 presents the spark timing (ST) for optimum efficiency.. Biogas base fuels used were methane with an MN of 100, natural gas with an MN of 87, and natural gas with an MN of 75. Due to the combustion chamber modification and the resulting high knocking tendency, the ST had to be delayed by some CAD degrees. Blends 100B and 50GN50CO2 showed the highest knock resistance, allowing for an ST that could obtain good combustion phasing. Blends with an MN below 90 required 2 CAD degrees to the ST. In general, blends with high MN could use advanced ST. Blends that used methane as a base fuel could use more advanced ST than blends that used natural gases with MN of 87 and 75. The small chemical difference between GN NM 87 and GN NM 75, which is mainly related to a reduction in methane concentration and an increase in propane and ethane concentrations, resulted in all blends with GN NM 75 as a base fuel having higher

knocking tendency compared to the blends that used GN NM 95 as a base fuel. The knocking tendency was very sensitive to changes in chemical composition.

Figure 3 presents the maximum output power. All runs were performed close to and below the knocking threshold. The original diesel engine produced a maximum of 8.0 kW @ 1800 rpm, represented in Figure 3 by a red line. The blends that used methane as a base fuel obtained higher output power because of its higher knocking resistance, while the blends that used GN NM 75 as a base fuel obtained the lowest output powers because of the highest knocking tendency. Blends 100B, 50B50M, and 50GN50CO2, all having MN greater than 120, obtained the highest output powers compared to the other six blends. These blends are made up of biogas with different proportions of methane and carbon dioxide, which achieved better results than natural gas and the blends of biogas enriched with methane or propane and hydrogen additions. Biogas is the only blend than obtained better output power than the original diesel. Before the change in combustion chamber geometry, the output power of biogas was 7.5 kW, limited by its low energy density. After the change in combustion chamber geometry high turbulence intensity increased the turbulent flame speed [23], combined with biogas' knocking resistance, obtained the highest output power 8.6 kW, limited by the knocking threshold. Biogas operated well under extreme conditions of pressure, temperature, and turbulence. All of the blends that had propane in their chemical composition experienced a power derating of approximately 38% due to the high knocking tendency of the engine after the combustion chamber geometry change. All blends, except 100B achieved a power output greater than 8 kW before the change in combustion chamber geometry, with a maximum output power of about 8.7 kW, which appeared to be the generation limit of the engine. For both 75B15P10H and pure propane the power derating was close to 55%, which is the result of the increase in knocking tendency due to the increase in turbulence intensity. This suggests that every blend must use a specific combustion chamber geometry. Blends with high MN could use combustion chamber with high turbulence intensity and blends with low MN must use combustion chamber with low turbulence intensity. Low heating value and flame speed are the properties that commonly limit the maximum output power due to the fuel's capacity to produce work. However, as presented in this research, knocking resistance is another important property that must be kept in mind. Engine power depends on the fuel's mass flow and low heating value. Since biogas has a lower low heating value, it must use a greater amount of fuel mass than conventional fuels, requires a greater throttle valve opening percentage.

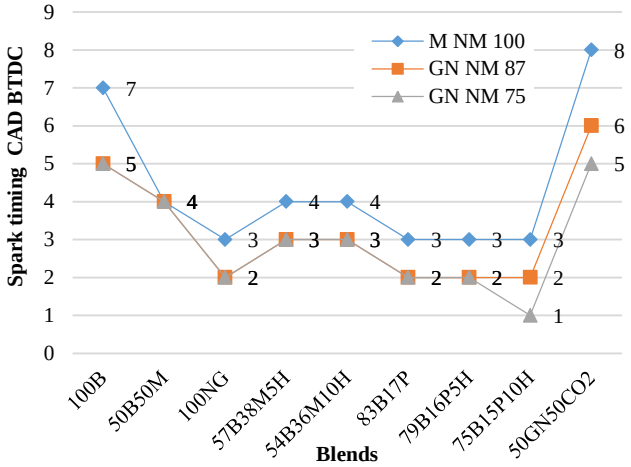

Figure 2 Spark timing for optimum efficiency, close to and below the knocking threshold. Biogas base fuels: Methane, natural gas with an MN of 87, and natural gas with an MN of 75

Figure 4 shows generating efficiencies. The original diesel engine produced 8.0 kW@1800 rpm with a generating efficiency of 27.6%, represented in Figure 4 by the red line. Before the combustion chamber geometry change, all blends had a greater generating efficiency than the original diesel engine at the maximum output power. After the combustion chamber geometry change, because of the increase in knocking tendency, only blends 100B and 50B50M obtained higher generating efficiencies than 28%, with the advantage of producing 8.6 kW output power with biogas. The engine operation parameters were

optimized for biogas operation due to the high CR and high turbulence intensity at the end of compression stroke. The blends with propane in their chemical composition had an average generating efficiency reduction of 39% because of the low output power limited by knocking. Before the combustion chamber modification, natural gas obtain an output power of 8.6 kW with a generating efficiency of 30.24%, whereas after the combustion chamber modification the output power was reduced to 7.4 kW and generating efficiency to 26.7%. These values are similar to the simulated poor biogas (50GN50CO2), which produced a comparable output power and generating efficiency to natural gas after the combustion chamber geometry change. 57B38M5H and 54B36M10H also experienced a reduction in output power (18%) and generating efficiency (11%).

Figure 5 presents the in-cylinder pressures. All tests were performed close to the knocking threshold. Figure 5a presents the curves for 100B and 50B50M using biogas base fuels methane, natural gas with an MN of 87, and natural gas with an MN of 75. Biogas achieved the highest pressure at the end of the compression stroke and the highest peak pressure during combustion, its high MN and knocking resistance allowing it to obtain the highest output power. Blends that used methane as a biogas base fuel reached higher pressures at the end of the compression stroke due to their higher knocking resistance, which could increase the output power close to knocking threshold, while blends that used natural gas with MN of 75 as a biogas base fuel reached lower pressures at the end of the compression stroke, and consequently lower output powers close to knocking threshold. Figure 5b presents the pressure curves for all blends that had methane as a biogas base fuel. As can be seen, biogas and biogas blends with natural gas achieved higher pressures than other blends. As proportion of propane and hydrogen were increased, a lower pressure value was achievable due to the lower knocking resistance of these blends. Blends that obtained higher output powers had higher pressures at the end of the compression stroke, biogas achieving the highest pressures. Because of the ST used with biogas operation, the best combustion phasing was obtain for this fuel, the peak pressure occurring at less than 14 CAD degrees. According to test results, the ideal peak pressure location was between 12-17 degrees ATDC, before the change in the combustion chamber geometry. A late ST will result in the peak pressure occurring after 17 CAD degrees, with lower average combustion pressure, resulting in reduced output power and generating efficiency.

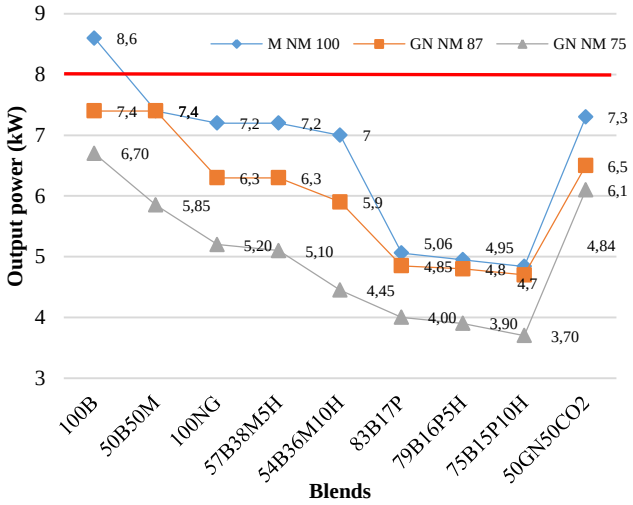

Figure 3 Maximum output power, close to the knocking threshold. Biogas base fuels: Methane, natural gas with an MN of 87, and natural gas with an MN of 75.

Figure 6 presents the net heat release rate. Figure 6a compares 100B and 50B50M, using as biogas base fuels: Methane, natural gas with MN of 87, and natural gas with MN of 75. According to the test results before the change in the combustion chamber geometry, the ideal location for the peak heat release rate was between 10-12 degrees ATDC. After the geometry change, biogas with pure methane was the only blend that could achieve a peak heat release rate at less than 12 CAD degrees ATDC. Although biogas had the lowest laminar flame speed of all the blends, the high turbulence intensity increased the turbulent flame speed of the biogas significantly, while the good combustion phasing and the high output power

permitted the biogas to achieve a good location for the peak heat release rate. Figure 6b presents the heat release rate curves for all blends made with methane as a biogas base fuel, the greatest peak heat release rate being with pure methane due to it having the shortest combustion duration. 50B50M peak heat release rate occurred close to 15 CAD degrees ATDC, a non-ideal combustion phasing because of the low output power of this blend, which resulted in a low average combustion pressure. All blends that had propane in their chemical composition had their peak heat release rate occurring after 15 CAD degrees ATDC, due to the low average combustion pressure, which resulted in reduction of generating efficiencies.

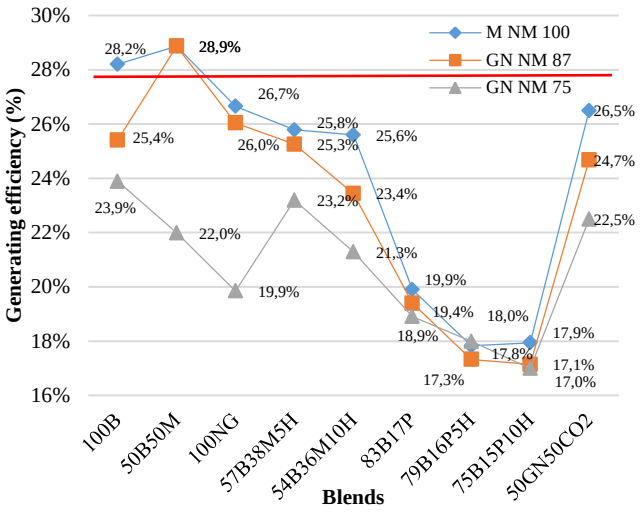

Figure 4 Generating efficiency, tests close to the knocking threshold. Biogas base fuels: Methane, natural gas with MN of 87 and, natural gas with MN of 75.

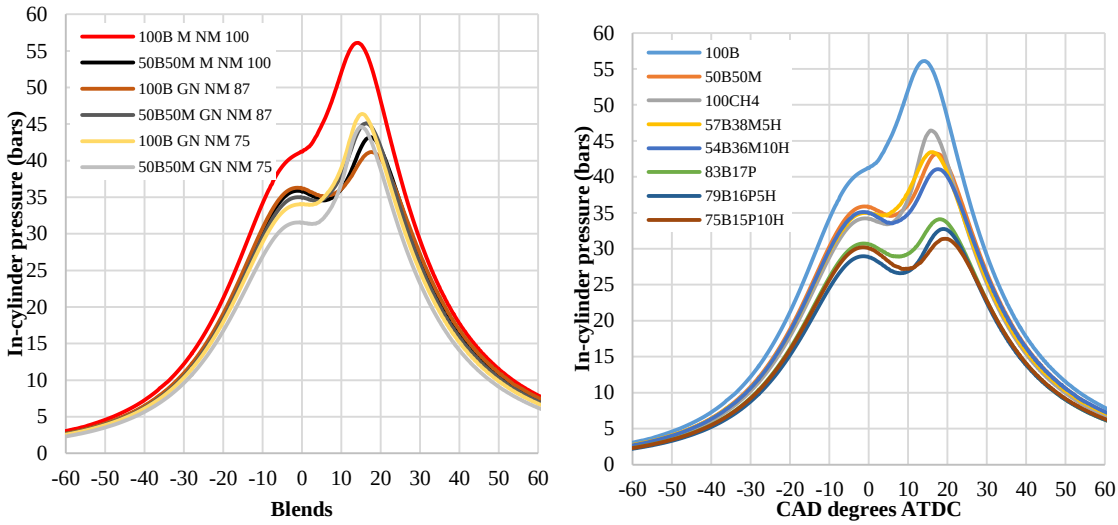

Figure 5 In-cylinder pressure, close to the knocking threshold. a) 100B and 50B50M, biogas base fuels: Methane, natural gas with MN 87, natural gas MN 75 b) Blends with methane as base fuel.

Figure 7 presents the summary of peak pressure values and location, using methane as a base fuel. Biogas blends with propane had lowest peak pressures of around 32.2 bar and occurring at more than 15.8 CAD degrees ATDC. Biogas had the greatest peak pressures and locations. For natural gas, poor biogas, and biogas blended with methane and hydrogen additions, the peak pressure values were between 40.3 and 44.7 bars, the peak pressure occurring between 15.4 and 17.6 CAD degrees ATDC. Biogas' chemical composition resulted in special fuel properties, such as low heating value, low laminar flame speed, and high knocking resistance, leading to specific operating conditions. A good balance of fuel properties and operating conditions leads to good peak pressure and location. Knocking serves as a quantitative measure of the mismatch between fuel properties and engine operating conditions. In order to achieve the

maximum output power in SI engines, with respect to ideal mixture properties and engine operating conditions, better matched settings result in higher output power. Biogas achieved the best results of the different possibilities under extreme conditions of pressure, temperature, and turbulence.
Figure 8 presents throttle valve % openings for all the blends with the different biogas base fuels. In general the throttle valve % openings were low for all the blends, this value depending on the output power, the equivalence ratio, and fuel composition. The biogas of pure methane required the largest opening because of its highest output power and the high fuel mass required. Lower throttle valve % openings resulted in higher inlet pressure drops, but according to the test result of the global research, this did not lead to a considerable loss in generating efficiency.

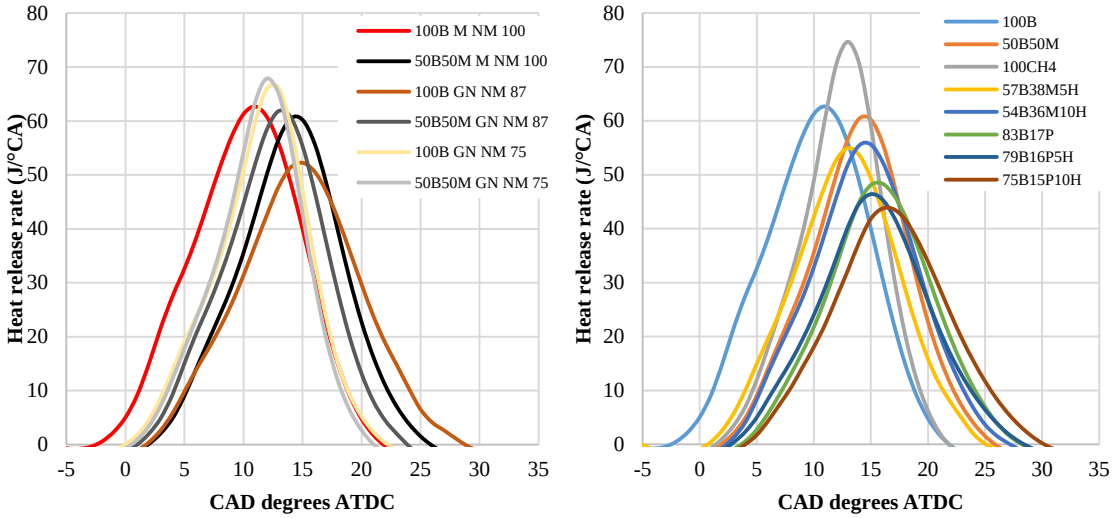

Figure 6 Net heat release rate, close to and below the knocking threshold. a) 100B and 50B50M, biogas base fuels: Methane, NG MN 87, NG MN 75. b) All blends with methane as a biogas base fuel

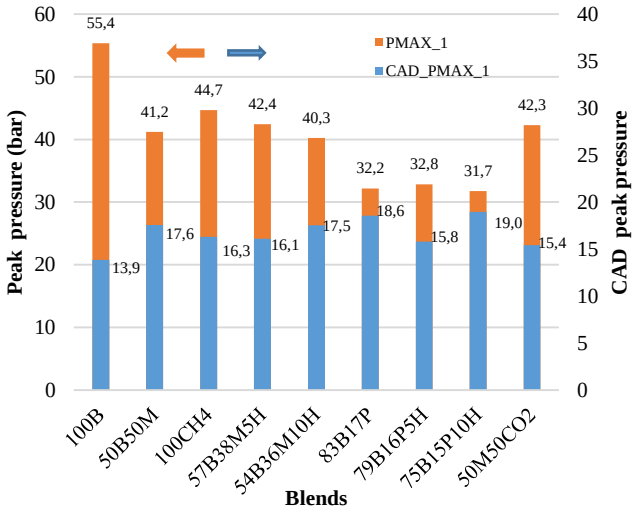

Figure 7 Peak pressures and locations. Base Fuel: Methane

Figure 9 presents the periods to 5% and 50% mass burned, using methane as a base fuel. These periods were calculated between the ST and the CAD to 5% and 50% mass burned. The only fuel faster than biogas was pure methane, but the output power of methane was 14% lower than that of biogas. Biogas has 40% CO_2 in its chemical composition, and thus the mixture mass of biogas is much greater than the mixture mass of methane. Although biogas's laminar flame speed is the lowest compared with all the blends in this research, the high turbulence intensity resulted in biogas' high turbulent flame speed, leading to its quick periods to 5% and 50% mass burned. Figure 10 presents the periods to 90% mass

burned and the combustion durations between 5-90% mass burned, using methane as a base fuel. In general and according to the results, the combustion duration of the engine is lower than in conventional SI engines, due to the high CR and the high turbulence intensity at the end of the compression stroke. For biogas, the combustion duration was only 15.3 CAD degrees, as measured between 5-90% mass burned. The period from ST until 90% mass burned, including ignition delay time to create the flame front kernel, was 21.8 CAD degrees for biogas. The combustion process occurs at higher speeds, than conventional SI engines, as a result of extreme conditions of pressure, temperature, and turbulence, which work in a good balance for biogas combustion. Conventional SI engines can have combustion durations greater than 30 CAD degrees, suggesting that this engine varies significantly from conventional SI engines.

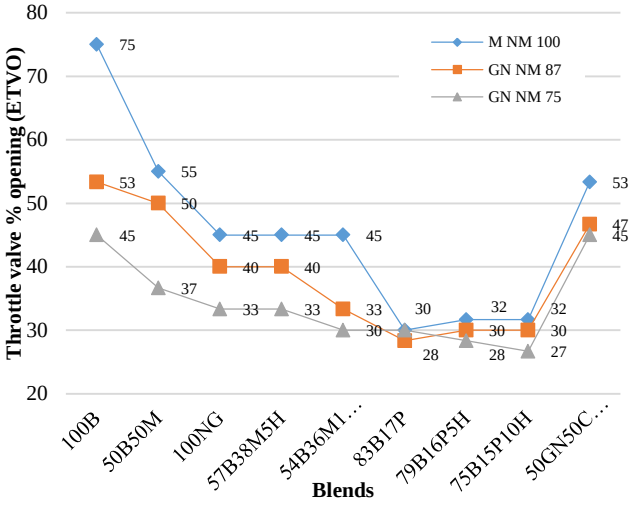

Figure 8 Throttle valve % opening. Biogas base fuels: Methane, NG MN of 87, and NG MN of 75

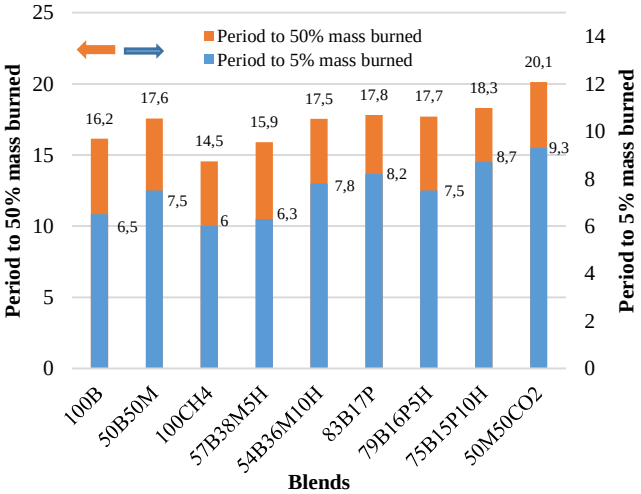

Figure 9 Periods for 0-5% and 0-50% mass fraction burned, base fuel: Methane

Figure 11 presents the IMEP and COV IMEP, using methane as a base fuel. All the blends get the knocking threshold at different IMEP. Knocking threshold depends on pressure, temperature, chemical composition, and turbulence intensity. Biogas had the highest output power at knocking threshold in this study. This relates to biogas having the highest IMEP, its combustion occurring at high average pressure because of its high knocking resistance. Blends 50B50M, 100CH4, 57B38M5H, and 54B36M10H had similar IMEP, all lower than biogas IMEP, because of their lower output powers limited by knocking. Blends 83B17P, 79B16P5H, and 75B15P10H had similar IMEP, the lowest of all the blends due to the propane content, which has a high knocking tendency, leading to the knocking threshold being at low

output powers. COV IMEP was lower than 2.7% for all the blends, which indicates high engine operation stability. Three different biogas presented the lowest COV IMEP. While it is common that high levels of CO_2 lead to higher COV IMEP values [7], the high pressure and turbulence intensity in this research reduced the COV IMEP for the biogas.

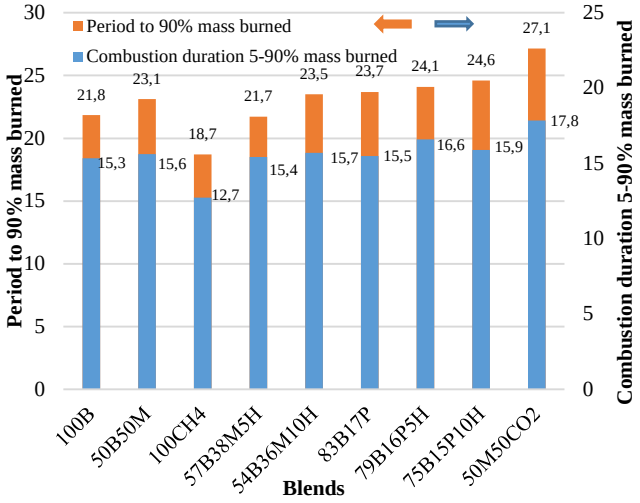

Figure 10 Period 0-90% mass fraction burned, 5-90% combustion duration, base methane.

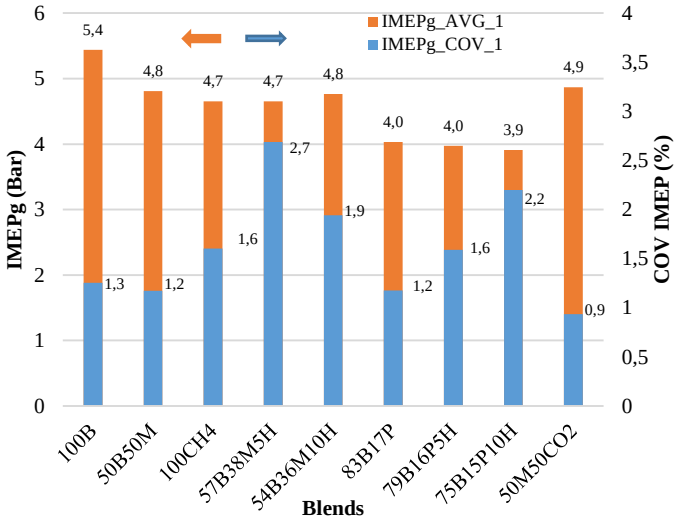

Figure 11 IMEP and COV IMEP. Base fuel: Methane

5.6.3.2 Experimental results for biogas with different equivalence ratios, base fuel: Methane

The purpose of varying the equivalence ratio is to find the best operating conditions for the engine by changing the amount of air in combustion. The intention of sweeping the equivalence ratio is to find the best conditions with the best fuel. Table 5 presents the global results for biogas runs with various equivalence ratios, using methane as a base fuel. Before the combustion chamber geometry change, the best fuel was purified biogas, and the equivalence ratio sweep found that the best performance occurred at an equivalence of 0.85. According with table 5, the best equivalence ratio was 0.9 after the geometry change, which results in higher output power with the highest generating efficiency, and has the highest exhaust temperature with low CO and CH_4 emissions. The peak pressure location was at less than 14 CAD degrees ATDC, the IMEP was the highest, and combustion duration was close to 15 CAD degrees. To reduce the equivalence ratio for lean combustion, the throttle valve % opening must be increased, which reduces the inlet pressure drop and increases the pressure and temperature at the end of the compression

stroke, increasing knocking tendency in spite of the increase in the inert gasses content of the mixture. The net effect leads to a reduced output power in order to be close the knocking threshold, consequently reducing the generating efficiency because of the comparatively higher heat losses. A fast combustion process, combined with a high CR and high turbulence intensity, results in a short combustion duration, which reduces the heat losses to the walls and achieves higher generating efficiency.

Table 5 Global result for biogas tests at various equivalence ratios. Base fuel: Methane

Dosados	Output power (kW)	Generating efficiency (%)	ST CAD	Exhaust temperature ºC	CH4 (%)	CO (ppm)	Throttle in percentage (ETVO)
100B Phi 0.95	8,5	27,95%	7	515	0,3	2850	72
100B Phi 0.9	8,6	28,20%	7	520	0,2	1227	75
100B Phi 0.85	8,4	27,53%	8	510	0,2	1086	78
100B Phi 0.8	7	25,38%	8	490	0,3	1034	90
100B Phi 0.7	7,4	26,83%	9	460	0,2	861	100

Dosados	CAD_PMAX	CAD50	CAD90	COMB_DUR	IMEPg_AVG	IMEPg_COV	KNOCK_PEAK
100B Phi 0.95	14,30	10,30	15,30	15,55	5,38	3,24	0,31
100B Phi 0.9	13,86	9,15	14,84	15,34	5,44	1,25	0,22
100B Phi 0.85	15,63	11,61	17,82	15,60	5,49	1,04	0,27
100B Phi 0.8	12,48	7,85	12,98	16,55	4,93	2,42	0,43
100B Phi 0.7	12,80	8,90	15,30	17,94	4,86	2,78	0,31

5.6.3.4 Characteristics of the flame front

Characteristics of the flame front are presented in Table 6. The ideal turbulent flame front is a flame front that burns at high pressure and high turbulence intensity using a fuel with high MN, low laminar flame speed and low flame temperature. For blends with low MN and low output power knocking occurred at low pressure, high turbulence intensity and high turbulent flame speed. For blends with high MN and high output power, knocking occurred at high pressure, high turbulence intensity, and high turbulent flame speed, even the low laminar flame speed of biogas.

Table 6 Characteristics of the flame front

Characteristics	Low MN	Medium MN	High MN
Pressure	Low	Medium	High
Turbulence intensity	High	High	High
Laminar flame speed	High	Medium	Low
Adiabatic flame temperature	High	Medium	Low

5.6.3.3 Comparisons between fuel properties and knocking tendency

In Figures 12 and 13, blends are arranged from left to right in decreasing maximum output power, i.e. from biogas with the highest knocking resistance to propane with the highest knocking tendency. The main blend properties used in this research were: Methane number, laminar flame speed, energy density, low Wobbe Index, and adiabatic flame temperature. This section looks at the relation between these properties and knocking. Figure 12a presents a comparison between methane number and output power; the output power was measured close to the knocking threshold in biogas SI engine, while the MN was measured in a CFR engine as described in [6]. There is a clear relation between output power and MN. This confirms that the biogas SI engine is a research engine similar to the CFR engine, but with a few differences. The biogas SI engine could measure the knocking tendency simultaneously while producing electric power at 60 Hz. Furthermore, the CFR engine could increase the CR until the knocking threshold to determine the critical CR, while the biogas SI engine could increase the output power until reaching the knocking threshold and the maximum output power, with similar tendencies in results.

Figure 12b presents a comparison between methane number and energy density. Blends with high energy density have low MN and get low output power. Blends with low energy density obtained higher output power, limited by the knocking threshold. Biogas required suitable conditions of high pressure and

turbulence to get the highest output power. The resulting relationship between output power and MN enables the measurement at the knocking threshold for each blend to predict which fuel has the greatest output power potential in an SI engine limited by knocking. The test results indicate that biogas can produce higher output power because of their high knocking resistance. Biogas have the lowest energy density, requiring less air to be burned. The best fuels are: Biogas, purified biogas, poor biogas, methane, blends of biogas with methane and hydrogen, blends of biogas with propane and hydrogen, and finally propane. Finally, the greater the flame front speed, the greater the knocking response. While natural gas is cleaner than propane and many others, biogas is an alternative fuel that can produce a higher output power than natural gas; biogas is cleaner than natural gas.

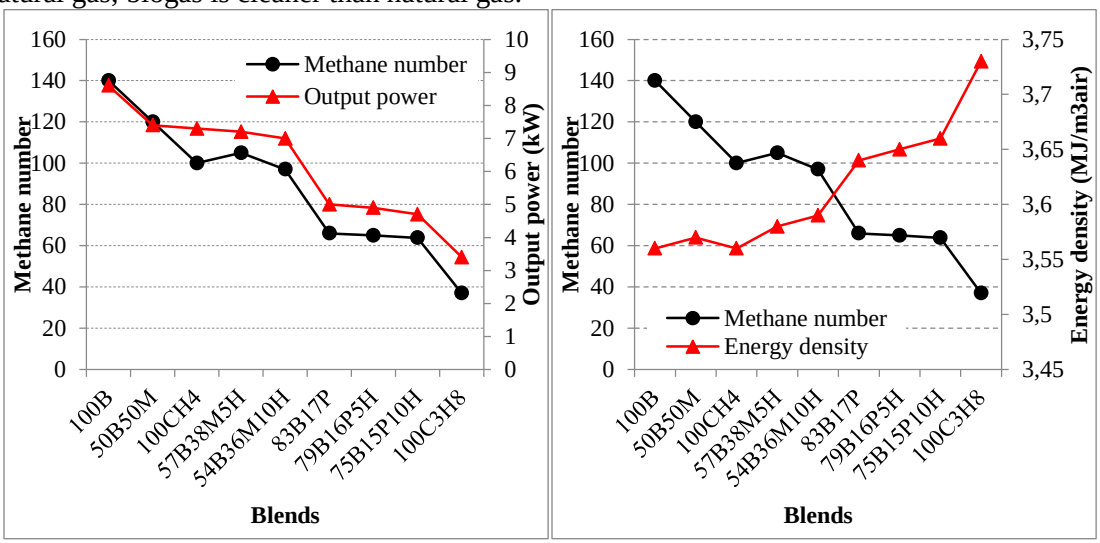

Figure 12 Methane number versus a) Output power and b) Energy density

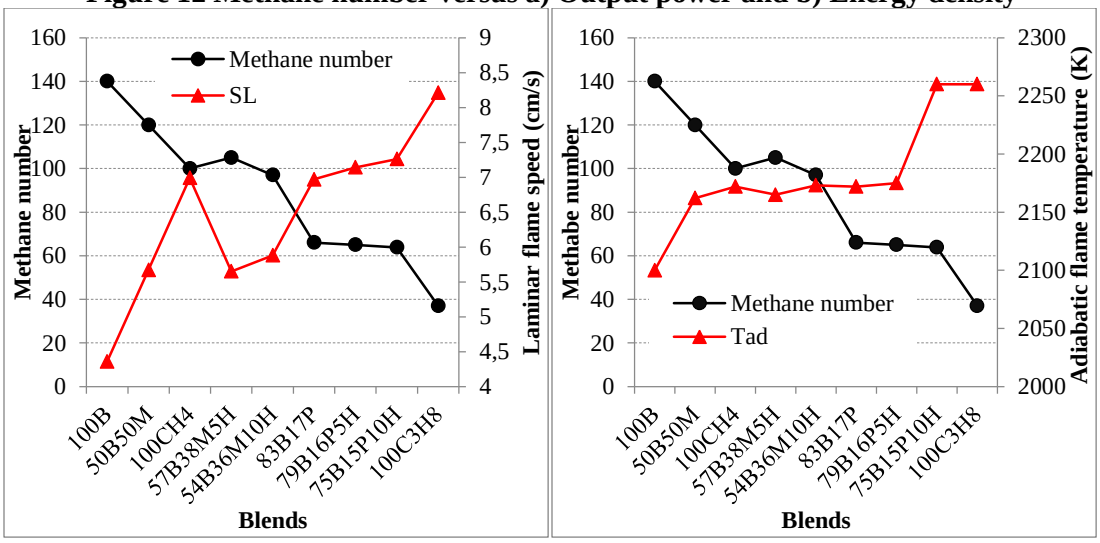

Figure 13 Methane number versus a) Laminar flame speed b) Adiabatic flame temperature

Figure 13a presents the comparison between methane number and laminar flame speed, revealing a similar tendency as reported in the CFR test [11]. Blends with high laminar flame speeds had low MN because of the high knocking tendency, leading them to have low maximum output power limited by the knocking threshold. Biogas with a low flame speed and a high MN obtained the highest maximum output power. Figure 13b presents a comparison between methane number and adiabatic flame temperature. Fuels that have a higher adiabatic flame temperature have a greater knocking tendency, resulting in less capacity to produce output power. Biogas have lower flame temperature than conventional fuels because of the

presence of carbon dioxide, resulting in increased resistance to knocking and thus greater capacity to produce power. Lower flame temperatures will result in lower NOx emissions.

5.6.4 Comments and conclusions

5.6.4.1 Comments

According to the results and the mentions in the introduction, knocking is a phenomenon whose occurrence depends on the combined effects related to physical properties, turbulence during flame front expansion, engine operating conditions, and combustion of the mixture. Knocking could be as quantitative measure of the disorder between mixture properties and engine operating conditions. To achieve the maximum output power in SI engines, with respect to the ideal combination, better settings will result in higher output powers. In other words, knocking is a natural limit of the maximum output power in SI engines measured with the knocking threshold. Knocking intensity depends on the end gas properties and the physical conditions in the combustion chamber after the flame front formation. Knock intensity also depends on the turbulent flame front characteristics; these conditions establish the probability and intensity of knocking. According to the test results, under extreme operating conditions of high pressure, temperature, and turbulence, biogas serves as the best blend for an SI engine with knocking as a limiting phenomenon. It is no the conventional way to evaluated the maximum output power of a SI engine, but knocking is natural response, better than use the throttle, as limit to maximum output power. Conventional SI engine are limited in the quantity of air, to the biogas SI engine the limit is fuel mass injection and knocking occurrence, partially throttle guarantee the air required for the fuel injected.

According to this study, biogas is not a poor fuel, but rather required specific extreme conditions to be used, could be better than the conventional fuels, usually recognized for their high energetic quality. Biogas could be more powerful and efficient than conventional fuels, but require modified engines to take advantage of their unique properties. It is suggested that there is a relationship between knocking and system entropy after flame front formation; knocking appears as a proportional response to the system disorder. The combined high compression ratio and high turbulence intensity converted the engine into a high knocking tendency engine, e.g. in additional testing, propane (MN 36.5) was used, producing only 3.4 kW as limited by the knocking threshold. This knocking occurred at lower pressure and temperature but higher turbulence intensity. Biogas SI engine with high compression ratio and high turbulence intensity can be considered as a low entropy engine, better mixture properties and engine operating conditions will result in better output power results. In this research, engine operating conditions and biogas properties have good balance with the results, resulting in high output power operation; according to this, entropy could even measure the disorder in a fuel's nature, like biogas chemical composition. Biogas formation has nature of lower entropy than conventional fuels. Entropy values in a SI engine depend on the end gas properties and conditions inside cylinder after the flame front formation. Systems with high entropy will experience the knocking threshold at lower output powers. Systems with low entropy will get the knocking threshold at higher output powers. Knocking and entropy are additive in the system after the ST, as mentioned in the introduction, knocking depends on several factors. Knocking is the nature response of the entropy system.

Finally, the purpose of this research was to increase the turbulent flame speed in order to reduce combustion duration and diminish the knocking probability. However, according to the test results, greater turbulent flame speed, greater knocking intensity, observed for all blends, forcing to reduce output power in order to be under the knocking threshold. The only exception was biogas, which obtained a higher output power after the combustion chamber modification. Purified biogas was the best blend before the change in the combustion chamber, with a maximum output power of 8.66 kW. With the increase in the turbulence intensity at the end of the compression stroke and during combustion, it was expected that output power could be increased a bit after chamber modification, but the increase in knock tendency limited the output power to 7.4 kW. The maximum output power before and after the change in combustion chamber geometry did not surpass 8.7 kW, or 8.75% higher than the original diesel operation, which is apparently the output power limit of the engine. The results of knocking measurements for different fuels indicate that, if the purpose is to produce the maximum output power, the fuels used should

have 1. Low laminar flame speed. It is better to use high turbulence intensity at the end of the compression stroke and during the combustion process to get high turbulent flame speed 2. Low energy density. The best fuels require less air for combustion 3. Low adiabatic flame temperature. Lower combustion temperatures will result in lower NOx emissions. Fuels with these characteristics achieve greater output powers and efficiencies in a high CR SI engine. Ideal turbulent flame front is a flame front that burns at high pressure and high turbulence, using a fuel with low laminar flame speed and low flame temperature.
According to the results and final ideas of this study, knocking appears to be as a response of nature which suggests that, since internal combustion engines are necessary for the modern lifestyle, biogas is preferable to petroleum-based fuels, with neutral greenhouse effects and that could get higher output power with high generating efficiency. In this case generating electricity in an low capacity biogas SI engine, but could evolve to different power levels and automation. Biogas not requires purification or enrichment, it could works well in extreme conditions of pressure, temperature and turbulence. Biogas has good knocking resistance. The low laminar flame speed is compensated with high turbulence intensity, modifying the chamber design to solve this inconvenience. Thus biogas is converted into a fuel with the highest capacity to produce output power under extreme conditions of pressure, temperature, and turbulence. This result invites the use of organic waste to produce biogas, as is the case in a small municipality in Colombia, El Carmen de Viboral, hometown of the author. For real changes, every town and every city should have systems to separate and recollect organic waste at the place of origin, enabling each individual to affect change. Each community should have biogas generation systems, reducing some of the impact of humanity on earth. The work would not be easy, but the continuous commitment will allow a reduction in the disorder of our system; we are thermodynamics beings, and thermodynamics tells us that work can lead us to a life of low entropy, even though we must to invest more effort that the reward we can achieve. Knocking tells us that we have been doing it wrong, that biogas can be better and more powerful than conventional fuels, and that it is better to use the fuels that require less air for the combustion, a beautiful and clear response from nature.

Entropy is quantum mechanical concept that measures the general disorder of a physical system with quantitative precision, similar with knocking as a measure of the disorder system, the system include the walls, the flame front and the end gas. Based on test results some ideas were presented regarding a relationship between knocking and entropy, suggesting that knocking is a quantum mechanical phenomenon response than limits the maximum output power of SI engines. Knocking could be seen as a measure of the disorder and randomness of turbulent flame front formation and its interaction with the end gas properties, establishing the maximum output power. The universe is governed by the principles of quantum mechanics with a fantastic precision. To analyze the limit phenomena of nature could permit read the message; in this case the phenomenon of nature read was the knocking threshold to 2 SI engines.

5.6.4.2 Conclusions

This research attempted to find the best configuration for a diesel engine converted to SI, namely a biogas SI engine with a high CR to get high output power and generating efficiency. The combustion chamber geometry was modified to increase the turbulence intensity at the end of the compression stroke to increase the turbulent flame speed. Biogas was blended with methane and propane and hydrogen additions, with the intention to improve combustion properties such as laminar flame speed and energy density. An equivalence ratio of 0.9 was selected and a sweep of the equivalence ratio was performed with biogas. All the runs were at the knocking threshold. The main conclusions from this research are:

- As a result of the direct relationship between output power and MN, the measurement at the knocking threshold for each blend allows prediction of which fuels have greater capacity to produce output power in an SI engine limited by knocking. Fuels that can produce higher output power are biogas with high MN because of their higher knocking resistance. These fuels have low energy density and low adiabatic flame temperature, resulting than the best fuel condition are using few air quantity and low flame temperatures to the combustion process. The ideal turbulent flame front burns at high pressure and high turbulence intensity using a fuel with high knocking resistence, low laminar flame speed and low flame temperature.

- In order from highest to lowest, the fuels than can generate the most power were: Biogas, purified biogas, poor biogas, methane, blends of biogas with methane and hydrogen, blends of biogas with propane and hydrogen, and finally propane. The greater flame front speed, the greater the knocking response. Alternative fuels can produce higher output power than methane and diesel.
- The biogas SI engine is a research engine similar to the CFR engine, but with the difference that the biogas SI engine could measure the knocking tendency while simultaneously producing electric power at 60 Hz. Biogas SI engine could increase the output power until the knocking threshold to get the maximum output power.
- Combustion duration in the biogas SI engine was shorter than conventional SI engines due to the high CR and high turbulence intensity at the end of the compression stroke. For biogas the combustion duration was only 15.3 CAD degrees, measured between 5-90% mass burned. Biogas had the best peak pressure and location. Biogas get the highest pressure at the end of the compression stroke, conditions to obtain the highest output power and generating efficiency.
- After the change in the combustion chamber geometry, biogas obtained the highest output power (8.6 kW) and high generating efficiency (28.2%), both higher than the original diesel engine. Biogas was the only blend than could take advantage of the engine's final conditions: 1. High CR to find high generating efficiency 2. High turbulence intensity to increase turbulent flame speed.
- Purified biogas was the best blend before the change in the combustion chamber. The maximum output power before or after the change in combustion chamber geometry not surpassed 8.7 kW, which apparently is the output power limit of the engine. Poor biogas obtained similar output power and generating efficiency values than pure methane.
- The SI engine used in the research was very sensitive to changes in chemical composition of the natural gas used to simulate biogas, even small changes in chemical composition by the additions of propane and ethane resulting in higher knocking tendency, forcing a reduction in maximum output power while remaining under the knocking threshold. Biogas SI engine is a high knocking tendency engine and biogas is the best fuel for this engine operational conditions.
- According to the test, higher laminar and turbulent flame speed will result in higher knocking tendency. Fuels with a low MN and high laminar flame speed are more prone to knock.

References

1. Bond T. and Templeton M.R., History and future of domestic biogas plants in the developing world. Energy for Sustainable Development, 2011. 15(4): p. 347-354.
2. Patel, S. *et al*. Biogas potential on Long Island, New York: A quantification study. Journal of Renewable Sustainable Energy 3, 043118, 2011.
3. Huang J. and Crookes R.J. Assessment of simulated biogas as a fuel for the spark ignition engine. Fuel, 1998. 77(15): p. 1793-1801.
4. Jeong C. *et al*. Generating efficiency and emissions of a spark-ignition gas engine generator fuelled with biogas–hydrogen blends. International Journal of Hydrogen Energy, 2009. 34(23): p. 9620-9627.
5. Gómez Montoya J.P. *et al*. Experimental study of spark ignition engine performance and emissions in a high compression ratio engine using biogas and methane mixtures without knock occurrence. Thermal Science: Year 2015, Vol. 19, No. 6, pp. 1919-1930. DOI 10.2298/TSCI140829119G, 2015.
6. Gómez Montoya J.P., Amell A.A. and Olsen D.B. Prediction and measurement of the critical compression ratio and methane number for blends of biogas with methane, propane and hydrogen. Fuel, 2016. 186: p. 168-175.
7. Porpatham E., Ramesh A. and Nagalingam B. Investigation on the effect of concentration of methane in biogas when used as a fuel for a spark ignition engine. Fuel, 2008. 87(8–9): p. 1651-1659.
8. Porpatham E., Ramesh A. and Nagalingam B. Effect of compression ratio on the performance and combustion of a biogas fuelled spark ignition engine. Fuel, 2012. 95(0): p. 247-256.
9. Heywood J.B. Internal Combustion Engines Fundamentals, ed. M.G. Hill. 1988.
10. Heywood J.B. and Tagalian J., Flame Initiation in a Spark-Ignition Engine. Combustion and Flame 64:243-246, 1986.
11. Arunachalam A. and Olsen D.B. Experimental evaluation of knock characteristics of producer gas. Biomass and Bioenergy, 2012. 37(0): p. 169-176.
12. Karim G.A. The onset of knock in gas fueled spark ignition engines prediction and experiment Journal of KONES Powertrain and Transport, Vol.14, No. 4, 2007.
13. Karim, G.A. Autoignition and Knock in Engines Fueled with Hydrogen and Hydrogen Supplemented Gaseous Fuel Mixtures, U.C. Mechanical Engineering, Editor.
14. Diaz G.A. and Martinez L.C., Knocking In Turbocharged Gas Spark Ignition Internal Combustion Engine For Stationary Application. Proceedings of ASME 2013. International Mechanical Engineering Congress & Exposition.
15. Shu, G. *et al.* Analysis of onset and severity of knock in SI engine based on in-cylinder pressure oscillations. Applied Thermal Engineering, 2013. 51(1–2): p. 1297-1306.
16. Zhen X. et al. The engine knock analysis – An overview. Applied Energy, 2012. 92(0): p. 628-636.
17. Law C.K. Combustion physics. Book ed. C.U.Press. 2006.
18. Juan Pablo Gómez Montoya. Doctoral thesis. Section 5.

6 General conclusions and future researches

6.1 General conclusions.

This research presents the experimental and numerical simulation results for an SI engine with high compression ratio, as well as CFR engine results for the methane number and critical compression ratio. Different fuels were used: diesel, natural gas, propane, biogas, and blends of biogas with methane or propane and hydrogen additions. The research aimed to find the best operating conditions for biogas as a main fuel in the SI engine. Thus the engine had a high CR and the combustion chamber geometry was modified to increase the turbulence intensity at the end of the compression stroke and during combustion. According to the CFD simulation results, the original diesel combustion chamber reached a turbulent intensity of 11.63 m/s at TDC. A cylindrical geometry modification resulted in the highest turbulence intensity of 14.5 m/s at TDC. This geometry was the best of 13 simulated geometries. This research also performed a repeatability analysis of the knocking effect on the operation and performance of the SI engine. Different strategies were implemented to improve the generating efficiency of the SI engine compared to the original diesel engine. The strategies used were: Transforming the diesel engine into an SI engine as biogas SI engine; using biogas as a main fuel to increase knocking resistance of the blends; blending biogas with natural gas or propane and additions of hydrogen; using ST for optimum generating efficiency close to the knocking threshold, which was defined as a knock peak pressure between 0.3 and 0.5 bars on average over 200 cycles. The COV of IMEP was lower than 4% for all the tests. The engine operated with two lean equivalence ratios 0.7 and 0.9. Fuels were injected at a pressure of 2 bars. A deep analysis related to the knocking is presented throughout the thesis.

6.1.1 Engine behavior before the change of the combustion chamber geometry

6.1.1.1 Output power and generating efficiency

- Using natural gas, 50B50M and blends 57B38M5H and 54B36M10H, with a fixed equivalence ratio of 0.9, the increased average of the output power was 7.5%, compared to the original diesel engine, under conditions of stable combustion and low CO, NOx, and CH_4 emissions. For biogas it was found that the output power loss with respect to the original diesel engine was 6.2%. Biogas blends with propane and hydrogen allowed for lower increases of output power compared to natural gas and blends 50B50M, 57B38M5H, and 54B36M10H. Because of the effect of propane and hydrogen, the mixtures are more sensitive to knocking. However, the power decrease with respect to the diesel was not considerable.
- All of the tested blends achieved generating efficiencies greater than or equal to the original diesel engine's generating efficiency of 28%. The blends that showed the highest generating efficiency, of approximately 30%, were natural gas, 83B17P, 50B50M, 57B38M5H, and 75B15P10H.

6.1.1.2 Specific fuel consumption and pressure inside the combustion chamber

- Blend 50B50M presented the lowest SFC. However, it was greater than the SFCs of diesel and natural gas, due to the presence of the carbon dioxide in the fuel. Blends of biogas, methane, and hydrogen were compared to blends of biogas, propane, and hydrogen. The firsts have lower SFCs, due to greater knock resistance, which allowed for greater output power generation under critical knocking conditions.
- The blend that achieved the highest peak pressure was 50B50M, due to its high output power and high knocking resistance. The blends of biogas with propane and hydrogen had the lowest peak pressures due to their high knocking sensitivity, which forces the output power reduction to be below the knocking threshold.

6.1.1.3 Heat release rate and spark timing

- Blends 50B50M, 54B36M10H, and 100CH4 had the highest heat release rates, while blends 100B, 83B17P, and 79B16P5H, had the lowest heat release rates. The determining factor is the pressure at the end of the compression stroke, which is limited by the knocking occurrence.
- Spark timing for biogas (5-13 CAD), 50B50M (4-9 CAD), and 57B38M5H (3-6 CAD) had the greatest range of CAD degrees over which combustion was knocking free. Fuels with the best combustion phasing were 100B, 50B50M, and 57M38M5H, the peak pressure ideally occurring between 12 and 17 CAD. Fuels that contained propane required delayed ST in order to avoid knocking, resulting in peak pressures occurring after 17 CAD ATDC.

6.1.1.4 Regarding the impact of opening and closing the throttle valve

- Reducing the equivalence ratio by opening the throttle valve, with the purpose of guarantee greater air intake, increases the pressure in the cylinder. This leads to two competing effects; the higher opening results in lower pressure drop at the intake stroke and thus more mass in the cylinder. However, due to the higher pressure at the end of the compression stroke, the knocking tendency of the engine is increased, forcing to reduce the output power to keep at the knocking threshold.

6.1.1.5 Knocking threshold to measure normal engine operation

- A knock peak pressure between 0.3 and 0.5 bar, on average over 200 cycles, presented an adequate definition as the maximum knocking free operation condition. The appropriate ST for maximum generating efficiency ensures ideal engine operation close to the knocking threshold for all blends and equivalence ratios. Also the COV IMEP was lower than 4% for all the tests.

6.1.1.6 Output power variation with the change in the equivalence ratio

- The change of the equivalence ratio from 0.9 to 0.7 reduced the output power and the generating efficiency of all blends, due to the increased knocking tendency. Blends of biogas with propane and hydrogen had high output power derating. Biogas had the greatest output power losses, at about 38%. 50B50M and blends of biogas with methane and hydrogen lost 7% of their output power, but improved CO and NO_X emissions.
- The decrease of the equivalence ratio from 0.9 to 0.7 generates apparently contradictory results, since it is expected that the knocking tendency will be reduced for the leaner mixture. However, due to the configuration of the diesel engine to operate in SI with a throttle valve, two phenomena occur as the equivalence ratio is decreased, ultimately increasing the knocking tendency: The inlet pressure is increased and more air enters the cylinder. The combined effect of the two phenomena is the increase of the pressures at the end of the compression stroke and during combustion. This increases the end gas temperature, leading to a greater knocking tendency. To compensate, the output power of the engine must be reduced in order to operate below the knocking threshold.

6.1.2 The behavior of the engine after the change of the combustion chamber geometry

6.1.2.1 Generating efficiency and output power

- As a result of the change in combustion chamber geometry, the combined effect of a high CR and higher turbulence intensity results in an increased knocking tendency for all the blends, except for biogas, making the engine more prone to knock with respect to the original geometry of the piston. Therefore, output power derating and lower generating efficiency occurred for all blends due to the geometry change of the piston. The blends of biogas with propane and hydrogen were more sensitive to this trend and experienced greater reductions in generating efficiency and output power. With the change of geometry the blends that experienced least reduction of output power and generating efficiency were 100B and 50B50M, and the greatest reduction was mixture 75B15P10H.
- After the combustion chamber geometry change, due to the increase in turbulence intensity and consequently high turbulent flame speeds, the knocking tendency of the engine was increased drastically, characterizing the engine as highly sensitive to knocking. As a result, all studied blends had a reduction in maximum output power, except for biogas which could exceed the 8 kW power output of the original diesel engine. Biogas reached 8.6 kW, which is comparable to the output power of the other blends before the change in piston geometry. Under extreme conditions of pressure, temperature, and turbulence, biogas operates better than fuels such as natural gas, enriched biogas, or blends of biogas with methane or propane, with hydrogen additions. The maximum output power for biogas before the piston change was 7.5 kW, limited by its low laminar flame speed and the low energy density. A delayed ST was required to avoid knocking for all blends after the change of geometry and consequent increase of the turbulence intensity.

6.1.2.2 Behavior of the throttle valve opening and output power with increasing turbulence intensity

- After the piston geometry change, although with lower output power, the throttle valve opening percentage was decreased by 25% on average.
- After the geometry change, switching the equivalence ratio from 0.9 to 0.7 reduced the output power and generating efficiency for all tests due to the increase in knocking tendency, which necessarily reduces the

output power and the ST advance in order to avoid the knocking threshold. This change with equivalence ratio was more severe with the modified geometry than that which occurred with the original piston geometry.

6.1.2.3 Behavior of biogas at a compression ratio of 15.5:1 and high turbulence intensity as a result of the piston geometry change

- Under extreme conditions of pressure, temperature, and turbulence, biogas worked better than blends such as natural gas, enriched biogas, or mixtures of biogas with methane or propane, with hydrogen additions. This is due to the high knocking resistance of biogas, which is measured with a high methane number. Furthermore, the low laminar flame speed of biogas proves to be beneficial with the high turbulence intensity. Biogas has typically been considered a poor fuel, but according to the results of this research, under extreme conditions of pressure, temperature, and turbulence, biogas performs better than other gaseous fuels, which is undoubtedly a good result for alternative energies.

6.1.3 Critical compression ratio and methane number tests in a CFR engine

- The MN and the CCR were measured for twelve blends of biogas with $CH_4/C_3H_8/H_2$ in a CFR engine. Blends of biogas with methane and hydrogen had a relatively high MN, close to 100. Blends of biogas with propane and hydrogen had an MN close to 65. A correlation between the MN and CCR was presented utilizing data from current and past tests.
- Comparing simulations in CHEMKIN of the IC engine module with the measurements of the CFR F2 engine constructed at CSU, it was concluded that USCII was the best mechanism for simulating the CCR, and San Diego was the best mechanism for simulating the MN. For almost all blends that include propane, the Butane mechanism was the best for predicting the CCR and MN. It was not possible to find an optimal mechanism for simulating the CCR and MN for all gaseous blends.

6.1.4 Relation between CFR engine and biogas SI engine.

- Biogas SI engine is a research engine similar to the CFR engine, but with the difference that the biogas SI engine could measure the knocking tendency while simultaneously producing electric power at 60 Hz. Biogas SI engine could increase the output power until the knocking threshold to get the maximum output power.

6.2 Future research

- Determine the optimum engine operation conditions for poor biogas, using a piston geometry producing greater turbulence intensity or a higher compression ratio.
- Test different fuels, with methane numbers between 0 and 140, to get an accurate map of the knocking tendency for all gaseous fuels.
- Conduct similar research with larger power scale engines; 100 kW must be the next aim using biogas, including from real biodigesters.
- Study durability and profitability of the SI biogas engine.
- Measure the turbulent flame speed for these same blends at close to knocking threshold, to determine if there is any constant that relates pressure, temperature, and turbulent flame speed at the knocking threshold.

Acknowledgements

I would like to acknowledge the support granted by:

1. My family and my friends.
2. GASURE group, Mechanical Engineering Department and University of Antioquia.
3. Colombia and Colciencias by Doctoral Scholarship 2012-2016.
4. Engines & Energy Conversion Laboratory, Colorado State University.
5. University of Antioquia, through the program CODI 2012-2013, IP: 71603452.